# GEOPHYSICAL ANALYSIS OF COLD SPRINGS AND LEMMON VALLEYS, WASHOE COUNTY, NEVADA

By Michael C. Widmer

---

Washoe County Department of Water Resources

October 31, 2000

# GEOPHYSICAL ANALYSIS OF COLD SPRINGS AND LEMMON VALLEYS, WASHOE COUNTY, NEVADA

By Michael C. Widmer

---

Washoe County Department of Water Resources

October 31, 2000

Copies of this report can be obtained from:

Washoe County
Department of Water Resources
Resource Planning & Management Division
4930 Energy Way
Reno, Nevada 89502

Department of
Water Resources

View north from Peavine Mountain to Cold Springs Valley. White Lake playa in foreground and Peterson Range in mid-ground.

View north from Peavine Mountain to Lemmon Valley. Silver Lake and Lemmon Lake playas are s
mid-ground with Hungry Hills in background. Note possible fault structures at right in foregrou

# TABLE OF CONTENTS

## LIST OF TABLES AND FIGURES

Figures are located in back of text

# INTRODUCTION

Washoe County is currently conducting water resources investigations in Cold Springs Valley and Lemmon Valley (see Figure 1). Both of these investigations will result in the development of separate groundwater numerical models. These models provide conceptual understanding of the occurrence and movement of groundwater primarily in the alluvial aquifers. Therefore it is important that the subsurface alluvium-bedrock configuration of these valleys are understood and delineated. Geophysical methods can provide an accurate image of the subsurface geologic structure. These methods include seismic reflection and refraction, magnetic surveys, and gravity surveys. Seismic methods are quire costly and impractical in urbanized areas such as Lemmon and Cold Springs valleys. Gravity and magnetic surveys were chosen for this investigation because of the relative ease in collecting the data as well as the reasonable cost of acquiring the data. Washoe County contracted an airborne geophysical survey (DIGHEM, 1996) to map the total magnetic field and electrical resistivity response of these basins. Washoe County also contracted a land based gravity survey (Carpenter, 1997 and 1998). Data from the Carpenter survey was combined with data from a 1979 USGS gravity survey conducted in Lemmon Valley (Schaefer and Maurer, 1981).

Density is not everywhere constant in the earth and it is because of this fact that the gravitational potential is not everywhere constant, even at the same elevation or distance. The anomalous gravitational force exerted on a unit mass by the earth at any distance can be determined from gravimeter measurements. If one were then to map these values they could contour points of gravitational attraction which would describe the "gravitational field" within the measured space. The spacing between contours on this map would represent the gradient of the gravitational field and reveal lateral changes in bulk geologic density within the study area. From gravity anomaly maps inferences can be made about the differences in geology especially where the gravity gradients are large. Within this study area, large gradients are indicative of bedrock-alluvial contacts where faulting has down-dropped the alluvial basins relative to the mountain ranges. Magnetic anomalies are similar to gravity anomalies in that the intensity of magnetization is dependent upon the magnetic susceptibility of a rock body where susceptibility is analogous to gravity density. In a simple case if a magnetic profile traverses across thick, unconsolidated sediments to a shallow magmatic dike and then back to unconsolidated sediments, a magnetic anomaly will be observed.

The interpretation of the total magnetic field and the gravitational field (sometimes referred to as potential fields modeling) can be used to locate the subsurface alluvium-bedrock interface and its high angle contacts. This is done through a forward modeling process that involves constructing geologic cross sections, evaluation of their calculated magnetic and gravity responses, and comparison to the actual measured data. The modeling of magnetic and gravity responses is however, non-unique as two or more differing geologic models can describe the measured potential fields data. In order to constrain the geologic models, surface data from geologic maps and subsurface data from water well drilling logs is used to guide the potential fields modeling. The Nevada Bureau of Mines and Geology published regional mapping of Washoe County (Bonham, 1969) that include these valleys. Detailed geologic maps of Lemmon Valley and Cold Springs Valley are published in a series of four quadrangle maps (Bonham and Bingler, 1973;

Soeller and Nielsen, 1980; Cordy, 1985; Bell and Garside, 1987). These maps provided the main constraint on potential fields modeling.

Electrical resistivity mapping takes advantage of earth materials as natural conductors or resistors of electrical current. Clay and saline water are two materials that are very conductive of current. Clay lithology is a good conductor because clay particles have loosely bound charges and act as dipoles of electric charge. These particles can also align themselves magnetically during the sedimentation process. Water is conductive because of the concentration of ionic species in the water. The more saline a water, the greater its conductivity. In direct current measurements a common type of earth resistivity measurement involves a four-electrode surface array or dipole-dipole array. One pair of electrodes introduces current into the earth and a second electrode pair measures the voltage potential due to that current. Resistivity is then calculated according to Ohm's Law, or resistivity = voltage x current, and is reported in units of ohm meters. Conductivity is simply the inverse of resistivity. In airborne resistivity mapping, frequency domain electromagnetic (FDEM) induction methods are used. This method is based in Faraday's Law and Ohm's Law and generally accomplishes the same result using magnetically induced electric fields. These fields are generated using alternating current in cable loops or coils as opposed to direct current electrodes. The FDEM method employs different frequencies which have the effect of sampling more of the earth, in a vertical sense, as the frequency is decreased. The term "skin depth" is used to describe the depth at which the electromagnetic (EM) energy is attenuated to 37% and is a function of the earth's resistivity and the transmitter frequency. Seventy-five percent of one skin depth is conservatively estimated in this report as the depth of investigation.

Resistivity is used to qualitatively map lithology and areas of poor quality groundwater. Saturated clay can have a resistivity of 10 ohm meters. The mixture of relatively high total dissolved solids (TDS) water in a clayey lithology will have a resistivity much less than 10 ohm meters. Rock formations will have resistivities that exceed 200 ohm meters. Personal experience in Washoe County has shown that resistivities of saturated sands and gravels are approximately 100 ohm meters, silty sands range from 40 to 60 ohm meters and clayey silts and sands are often less than 30 ohm meters. Resistivity mapping at multiple frequencies provides a proven means of mapping and delineating alluvial deposits to depths of up to 100 meters (330 feet).

**Acknowledgements**
The author would like to acknowledge Dr. Gary Oppliger of the Mackay School of Mines, University of Nevada, Reno. Dr. Oppliger tutored the author a sound theoretical and practical basis of knowledge in geophysical processing and analysis for which the author greatly appreciates. This report has been enhanced because of his participation and enthusiasm. The author also thanks Leonard Crowe Jr., Washoe County Water Resources Planning Manger, for his vision and support in the use of geophysical surveys for water resource investigations.

## GEOLOGIC SUMMARY

Plate 1 is a topographic map of the study area. The most prominent relief feature is Peavine Mountain, at 2,520 meters (8,266 feet) as the topographic high in the southern portion of the study area. Three north-trending mountain ridges, from west to east include: the Peterson

Mountains, the Granite Hills, and the Hungry Hills. An additional unnamed mountain in the southeastern portion of the study area separates Lemmon Valley from Sun Valley. The Granite Hills are a topographic and hydrographic divide between Cold Springs Valley and Lemmon Valley. Three topographic lows shown in Plate 1, from west to east, include White Lake (1,536 meters or 5,040 feet), Silver Lake (1,512 meters or 4,960 feet), and Lemmon Lake (1,500 meters or 4,920 feet) and are recognized as playas. When precipitation runoff collects in these playas, water depths are rarely greater than one meter (3-4 feet). Notable features of the topography are the apparent fault scarps forming steep slopes on the eastern sides of the Peterson Mountains, the Granite Hills and the southern Hungry Hills.

Plate 2 is a geologic map of Cold Springs Valley and Lemmon Valley comprised from the four quadrangle maps previously discussed. Generally the study area can be described with five geologic units (Table 1); Mesozoic metasediments and metavolcanics, Cretaceous granodiorite, Tertiary volcanics, Tertiary sediments, and Quaternary alluvium.

**Table 1.**
**Generalized geologic units.**

| | |
|---|---|
| Qal | Quaternary Alluvium |
| Ts | Tertiary Sediments |
| Tv | Tertiary Volcanics |
| Kgr | Cretaceous Granodiorite |
| Mzv | Mesozoic Metasediments And Metavolcanics |

Little is known of western Nevada's Paleozoic and Mesozoic geologic history. The oldest exposed rocks are the Mesozoic metavolcanics associated with the Peavine sequence. These metamorphosed rocks are primarily intermediate volcanic extrusives and detritus. They have been uplifted by Cretaceous granodiorite associated with the Sierra Nevada batholiths, dated at 90.7 million years (m.y.) (Bell and Garside, 1987). However, the uplift has only recently occurred within the last 2-3 m.y. (Schweickert, 1999). Tertiary (Miocene age) volcanics are comprised of andesite to rhyolite flows, intrusives, and ash flow tuff. They are associated with the Hartford Hill Formation, the Alta Formation, and the Kate Peak Formation which are mapped in other areas of Washoe County. These volcanics are mostly found in the southeastern portion of the study area. Tertiary sediments are comprised of the Hunter Creek sandstone and siltstone and appear to be the largest sedimentary unit. Quaternary alluvium is mapped primarily as alluvial fan deposits.

Little is also known of the geologic structure prior to the tectonic event known as the Sierra Nevada orogeny that occurred in the last 3-4 m.y. Normal faulting during this orogeny created north-south trending mountain ranges comprised of granodiorite and metavolcanic rocks with sediment and alluvial filled basins. Most fault structures appear to be oriented northeastsouthwest although east west oriented faults are mapped along the northeastern flanks of Peavine Mountain. One notable fault structure is the Airport Fault whose trace is found in central Lemmon Valley. It appears to originate in the southern Hungry Hills and strikes south toward Peavine Mountain. It is mapped as an east-dipping normal fault and has been interpreted as an impermeable barrier to ground water flow (Harrill, 1971).

## POTENTIAL FIELDS DATA

### Gravity Data

Gravity information was compiled from two sources. Washoe County contracted Tom Carpenter for a gravity survey during the period 1997 to 1999 in which 282 gravity stations were measured (Carpenter, 1997, 1998, 1999). Mr. Carpenter also conducted a bathymetric survey of White Lake, Lemmon Lake and on Silver Lake (playas in Cold Springs Valley, East Lemmon Valley and West Lemmon Valley, respectively) which included gravity readings. The data were collected using a LaCoste and Romberg Model G-230 gravimeter with a precision of 0.01 mGal. Positions were located by rapid static GPS survey methods using a WILD GPS – System 300 manufactured by Leica. The elevation accuracy is believed to be better than ±20cm. The International Gravity Reference Network base at the James G. Scrugham Engineering, Mines Building at the University of Nevada, Reno served as the local reference gravity value. The measured data were reduced to Complete Bouguer values.

In 1980, the USGS conducted a gravity survey in Lemmon Valley (Schaefer and Maurer, 1981) where 235 stations were occupied. This data was collected using a temperature controlled Worden gravimeter with a sensitivity of 0.1 mGal. The data were reduced to Complete Bouguer anomalies. This data set used estimated elevations from 7.5 minute topographic maps (elevation accuracy ±4 meters or ±0.75 mGals), but did contained two stations that were read at surveyed benchmarks. Mr. Carpenter re-occupied these benchmarks and recorded readings that differed from the USGS readings by –3.05 and –3.07 mGals. In order to merge the two data sets, a correction of +3.06 mGals was subtracted from the USGS set. Both data sets used slab densities of 2.67 g/cm$^3$.

### Magnetic Data

DIGHEM, Inc. was contracted by Washoe County to conduct the aeromagnetic geophysical survey (DIGHEM, 1996). Instrumentation was installed in an Aerospatiale AS350B turbine helicopter (Skydance Helicopters, Inc.) which flew at an average airspeed of 100 kph (62 mph) with a magnetometer bird height of 50 meters (165 feet) above ground level. The survey consisted of 352 kilometers of traverse line (219 miles) oriented at 90°/270° to geographic north with 667 meters (2000 feet) line spacing. The tie lines (27.4 kilometers or 17 miles) were oriented at 0°/180° to geographic north. The magnetic data was collected with a Picodas 3340 optically pumped cesium vapor magnetometer. The sampling rate was 10 per second with a sensitivity of 0.01nT. Navigation and positioning consisting of a Sercel NR 106 real-time differential global positioning system with <5 meter accuracy. A Scintrex MEP-710 cesium vapor magnetometer was operated at the survey base to record diurnal variations. The base station clock was synchronized with that of the airborne system to permit subsequent removal of diurnal drift. Data processing by DIGHEM, Inc. consisted of corrections for diurnal variations and leveling. Data processing by Washoe County consisted of reduction to pole and 100 meters of upward continuation (Geosoft, 1999).

**Potential Field Maps**

Figure 2 is a contoured grid of the Complete Bouguer Anomaly (CBA) gravity data and presented in color-shaded relief. Also plotted are the gravity stations. The gridding was accomplished with a minimum curvature routine (Geosoft, 1999). Three synthetic values were included in the data set in order to give a better representation at the southern end of the Granite Hills. Values were selected based upon other measurements atop the crest of the Granite Hills. The total range of gravity anomaly variation within the study area is 18.9 mGals and is common for basin and range structure adjacent to the eastern Sierra Nevada. In eastern and central Nevada, variations in gravity anomalies can be as high as 60 mGals in basins as deep as 3 kilometers (10,000 feet).

This Figure clearly shows where the low gravity anomalies (coded blue and ranging from -187.4 to –183.5 mGals) represent relatively deep alluvial basins. The Granite Hills, outlined by the mid-range gravity anomalies (coded as greenish-yellow and ranging from -176.0 to -174.0 mGals), separate the deep basins of Cold Springs and West Lemmon Valley. A difference of 12.1 mGals is seen from the Cold Springs Valley basin floor to the top of the Granite Hills and similarly a difference of 10.6 mGals is seen from the Lemmon Valley basin to the top of the Granite Hills. The basin of Cold Springs is deep, circular and approximately 10 $km^2$ (4 $mi^2$) in area and bounded by Peavine to the south and the Peterson Mountains to the north. The gravity data suggests a small subsurface ridge separating Cold Springs Valley from Long Valley to the west. The West Lemmon Valley basin is an elongated north trending basin that continues to the north. In East Lemmon Valley, a sub-basin is located east of the deeper basin of West Lemmon Valley. The ridge that separates this sub-basin from the deeper basin to the west is coincident with the Airport Fault. At the eastern end of the study area the higher anomalies (-174.0 to -169.5 mGals, coded yellow to orange) are associated with volcanic units.

Figure 3 shows the gravity anomaly contours overlying a digital elevation model (DEM) for the study area and helps to better define these basin structures. It is readily apparent that the low gravity anomalies are coincident with the lower topographic elevations and that the high gravity anomalies match well with the high topographic elevations. Compared to the mountains of large density (2.67 $g/cm^3$), the gravity lows represent relatively thick sequences of less dense sediment (2.07 $g/cm^3$) overlying "down-dropped basement" rock. The steep gravity gradients depict deep basin structure and match well with assumed normal fault structure. A steep gradient located between East and West Lemmon Valleys is coincident with the mapped Airport Fault. This feature is interpreted as a subsurface bedrock ridge that separates these two sub-basins.

Figure 4 is the total field magnetic map, reduced to pole and upward continued to 100 meters of the aeromagnetic data with the flight lines plotted (light gray). The gridding was accomplished using a minimum curvature routine (Geosoft, 1999). The southern area in magenta represents highly magnetic lithology (volcanics) whereas the areas in blue and green represent relatively nonmagnetic lithology (alluvium). The reddish colors represent both granodiorite and volcanic units. The range between high and low magnetic values is 644 nT (51,702 to 52,346 nT). The small dimension, but extremely low magnetic anomaly found in the center of the Figure is thought to be caused by a large warehouse complex.

This Figure is similar to the Complete Bouguer Anomaly map and shows that the alluvial basins are associated with magnetic lows (51,200 to 51,500 nT and color coded blue) and the mountain ranges are associated with magnetic highs (51,700 to 52,000nT and in light to dark yellow). The deeper basins in Cold Springs and West Lemmon Valley are less well defined relative to the gravity map, but still apparent, as are the previously mentioned smaller basins in East Lemmon Valley and Long Valley. The most striking magnetic anomalies are seen in the most southern and in the north central portions of the study area. These magnetic highs are coincident with mapped Mesozoic quartz monzonite in the north (Hungry Hills) and with Tertiary volcanics and Mesozoic metavolcanics (Peavine Sequence) in the south. Figure 5 is a digital elevation model overlain with the total field magnetic contours from Figure 4. Although not as clearly defined as the gravity anomalies, this map shows magnetic highs associated with the granodiorite and volcanic mountains and magnetic lows associated with the basin structure.

Figure 6a is digital elevation map overlain with the Complete Bouguer Anomaly contours from Figure 2. The lineaments were produced from the contour map and then overlain on the digital elevation map. The lineaments were drawn parallel to steep gradients or trends in an attempt to identify fault structure based upon density contrasts. Eleven lineaments (L1a through L11a) are noted in this Figure. Two sets of trends are seen. A north-northwest trend denoted by the seven lineaments L1a, L2a, L3a, L4a, L5a, L7a, and L11a. A north-northeast trend is denoted by the four lineaments L6a, L8a, L9a, and L10a. The DEM shows that these lineaments outline inferred horst-block relationships, mostly where major elevation changes occur.

Likewise Figure 6b is digital elevation map overlain with the total field magnetic anomaly contours from Figure 4. The lineaments were also produced from the contour map and then overlain on the digital elevation map and drawn parallel to steep gradients or trends in an attempt to identify fault structure based upon magnetic contrasts. Nine lineaments (L1b through L9b) are noted in this Figure. Three sets of trends are seen. A north-northwest trend denoted by the three lineaments L1b, L3b, and L7b. A north-northeast trend is denoted by the three lineaments L2b, L5b, and L6b. A east-west trend by the three lineaments L4b, L8b, and L9b. This Figure is not conclusive and only compares to Figure 6a with two sets of northward trending lineaments.

## GEOPHYSICAL MODELS

### Description of Units

Table 2 lists the major lithologic units found in the study area and their associated density range and magnetic susceptibility used in the modeling. Densities and magnetic susceptibilities were taken from similar rocks measured in the South Truckee Meadows, approximately 5 miles to the south (Skalbeck, 1998). The alluvial values of density are considered to be within the range of water saturated alluvium.

**Table 2**
**Listing of lithologic units, densities and magnetic susceptibilities**

| Lithology | Density ($g/cm^3$) | Susceptibility (dimensionless cgs) |
|---|---|---|
| Quaternary Alluvium | 2.07 | 0 |
| Tertiary Sediments | 2.17 | 0 |
| Tertiary Volcanics | 2.47 – 2.67 | 0.002-0.009 |
| Mesozoic Metasediments and Metavolcanics | 2.57 | 0.00002 |
| Cretaceous Granodiorite | 2.67 – 2.77 | 0.002 – 0.006 |

As mentioned previously, potential fields modeling is non-unique. By changing the density and/or susceptibility of lithologic units, the model thickness of these units will change and vice versa. The practice of the present modeling effort was to keep density and susceptibility estimates within a very tight range of values. No consideration was given to lithologic units of reversed magnetization because there was no direct evidence for these types of units although they probably exist and have been noted in the South Truckee Meadows (Skalbeck, 1998). The model separation of the Quaternary alluvium from the Tertiary sediments is somewhat arbitrary. The Quaternary unit is assumed to be a result of alluvial fan and lacustrine depositional environments, however the thickness is not known. The Tertiary sediments are assumed to be semi-consolidated to consolidated fine grained sediments, again the thickness is unknown. These units were modeled with the assumption that they had no magnetic susceptibility. Taken together they had influence on the gravity interpretation, but their thickness relative to each other could not be resolved.

The dominant rock units within the study area are Cretaceous granodiorite followed by Mesozoic volcanics. The Tertiary volcanics mostly crop out in the eastern and southeast portion of the study area. Here again, the relative thickness of these volcanic units are subjectively modeled in order to render best fits to the gridded magnetic and gravity data. Their physical properties are assumed to be constant but probably vary widely.

**Modeling Approach**

Potential fields modeling was accomplished using the software package GM-SYS™ (Northwest Geophysical Associates, 1996). The gravity and magnetic data were formatted for modeling using Oasis Montaj™ software (Geosoft, 1999). Coincident line data was needed for the magnetic, gravity, topographic elevation and magnetometer "bird" elevation data. Data sets for each were gridded and lines coincident to the aeromagnetic survey flight paths were generated. The elevation data came from surveyed gravity stations and topographic maps. The bird height elevation was recorded during the aeromagnetic survey. As a result, each line had the appropriate data at a minimum of 200 meter (656 feet) intervals.

Mapped surface geology was strictly honored as control for each model cross section. Where possible, lithologic data from water well drilling was also used in constraining the modeling effort. The observed and modeled gravity data were fit as closely as possible whereas the magnetic data was fit to a lesser degree. It should be re-emphasized that the purpose of the modeling was to configure a bedrock elevation model. Consequently, the results should be considered "best-fit" models where importance was placed, in descending order, mapped geology, gravity and then magnetic data.

**Results**

This section will discuss only seven of the modeled cross sections. All modeled lines are contained in the appendix (where derrick symbols represent the locations of mapped faults and well sites). Fifteen lines were modeled in Cold Springs Valley and twenty lines were modeled in Lemmon Valley. The discussion will start with northern cross sections and continue southward. Figure 4 shows the location and number of the aeromagnetic survey flight lines and consequent modeled cross-sections imposed.

The following figures illustrate the geologic cross sections based upon the gridded gravity data and observed magnetic data, which are also shown. The magnetic curve (top section) plots the observed data (dots) and the calculated (solid line) data based upon the modeled geologic cross section. The middle section is the gravity data, again the observed (dots) versus the calculated (line). The lower section is the modeled geologic section where lithologic symbols (Table 1) are shown. A distance scale is at the bottom and will be referred to below. In Lemmon Valley the Cretaceous granodiorite density and susceptibility have been modeled as varying slightly. This variation is noted with a different label, i.e. hard Kgr. Alteration zones and fractured areas have also been interpreted and are also noted.

<u>Line 20020</u>

Figure 7 shows the geologic model for the northern portion of the study area. At the most western edge of the Figure (the east side of the Peterson Mountains and distance 1,500m) a fault zone is modeled to account for a magnetic low. This fault is also indicated on the geologic map (Soeller and Nielsen, 1980). To the east of this fault structure is a basin (distance 1,500-3,000m) with maximum thickness of 75 meters (246 feet) and thins to the east and to the north (line 20010). The number of gravity measurements in this area (see Figure 2) is relatively sparse which results in poor definition of these sediments as well as topography. Moving east, the Granite Hills (distance 3,500-7,000m) are encountered and a thick Mesozoic unit is modeled. Further east, an alluvial basin (distance 7,000-11,000m) is estimated to have a maximum thickness of 466 meters (1,538 feet). A small alluvial basin (distance 13,500-15,000m) north of West Lemmon Valley and between the Hungry Hills is modeled with a maximum thickness of 60 meters (197 feet) and is probably mostly broken and decomposed granodiorite.

<u>Line 20050</u>

Figure 8 shows a geologic model that essentially duplicates line 20020. However, the Mesozoic metavolcanics east of Peterson Mountains (distance 1,500-3,000m) is substantially thicker. The sediments in the central portion of Cold Springs Valley thicken to 120 meters (394 feet). To the east in Lemmon Valley the sedimentary basin (distance 6,000-12,500m) has increased in depth and width. In the center of the West Lemmon Valley a graben feature (distance 9,000-10,500m) is mapped, but is not supported by the model. The thickest sediments are estimated at 450 metes (1,480 feet). At a distance of 13,000 meters the mapped airport fault is modeled as a mapped outcrop of granodiorite. To the east, the East Lemmon Valley basin (distance 13,000-16,000m) is shown that appears to extend beyond Lemmon Valley proper.

Line 20080
Figure 9 shows the geologic model further to the south and beneath the northern edge of the Cold Springs playa (White Lake and distance 500-3,500m). The basin sediments thicken dramatically to 600 meters (1,970 feet). At the western edge of this Figure an apparent ridge of Tertiary consolidated sediments (distance 500m) is shown. This particular configuration of consolidated sediments and Mesozoic volcanics is apparently caused by intrusive granodiorite (Kgr) and fault structure that is not fully understood. In Lemmon Valley both basins thicken with the West Lemmon Valley basin (distance 6,000-12,000m) at approximately 473 meters (1,550 feet) and the East Lemmon Valley basin (distance 12,000-16,000m) at 150 meters (490 feet) of sediment. The mapped Airport Fault (distance 12,000m) is not as well defined with respect to the granodiorite, located under approximately 106 meters (350 feet) of sediment.

Line 20100
Figure 10 shows the geologic model beneath the Cold Springs playa (distance 1,000-3,500m) representing the deepest section of the basin with 550 meters (1,800 feet) of sediments. At the western edge of Cold Springs (distance 500m), the model indicates that the Tertiary sediments thin, but become more laterally extensive. At the eastern edge of Cold Springs (distance 3,500m) an apparent dike and zone of altered granodiorite is modeled. The Tertiary volcanics are mapped in surface outcrop to the north (Line 20090). The sediments in West Lemmon Valley (distance 8,500m) thicken to 520 meters (1,700 feet) as compared to Line 20080 and thicken to 200 meters (656 feet) in East Lemmon Valley (distance 13,500m). The magnetic data at a distance of 9,000 meters is likely the result of cultural noise.

Line 20120
Figure 11 shows that the Cold Springs Valley basin sediments (distance 1,000-3,500m) thin (390 meters or 1,280 feet) as the slopes of Peavine Mountain are encountered. The Mesozoic volcanics become much more extensive. However, the thickness of this volcanic unit is uncertain, as the calculated magnetic anomaly is not well fitted to the observed data. In Lemmon Valley, the Airport Fault (distance ~15,000m) separating East from West Lemmon Valley is neither apparent in this modeled cross section nor mapped by Cordy (1985). The basin sediments thin to 435 meters (1,425 feet) in West Lemmon Valley (distance 6,500-10,000m) and remain about the same thickness at 200 meters (655 feet) in East Lemmon Valley (distance 11,500-14,500m).

Line 20150
Figure 12 shows the modeled cross section primarily in Lemmon Valley. The Tertiary dike (distance 3,500m) mapped by Soeller and Nielsen (1980) on the west side of the Granite Hills is modeled well to the magnetic data and is likely related to the contact between the granodiorite and the Mesozoic metavolcanics. The sedimentary basins thin in both West (distance 7,000-9,000m) and East Lemmon Valley (distance 9,000-13,000m) at 346 meters (1,135 feet) and 122 meters (400 feet) respectively. The Airport Fault appears to have no influence on basin structure.

Line 20180
Figure 13 is the most southern cross section discussed and is located on the northern slopes of Peavine Mountain. The sediments are 80 meters thick (260 feet). At the eastern edge (distance 9,500-12,000m) of the cross section, Golden Valley is modeled as a basin of mostly fracture granodiorite. The sediments and fractured rock appear to be at least 100 meters (328 feet) thick.

Configuration of Basin Bedrock
Figure 14 is a digital elevation map overlain with a shaded relief image of the modeled bedrock elevation (in meters above sea level) of these two valleys. The contour interval is 20 meters (66 feet). The locations of flight lines are also visible and labeled. This figure is similar to Figure 2, the Complete Bouguer Gravity Anomaly Map, and outlines the deep sedimentary basins in Cold Springs Valley (left edge of Figure) and West Lemmon Valley (center). These two basins are separated by the Granite Hills. Left of center in the Figure, East Lemmon Valley is shown as a lesser basin. Golden Valley (see also Figure 1) is modeled as an elongated, east west and shallow basin (lower right). Peavine Mountain is shown at the southern end of the study area (bottom).

In Cold Springs Valley the alluvial/bedrock surface has a base elevation of 1,040 meters above sea level (3,411 feet). The bedrock ridge separating Cold Springs Valley from Long Valley to the west is interpreted at an elevation of 1,320 meters (4,339 feet). A smaller basin north of the main basin also exists with a base elevation of 1,440 meters (4,723 feet). To the east, the north south trending basin of West Lemmon Valley has a bedrock elevation of approximately 1,020 meters (3,345 feet). Further east, the East Lemmon Valley basin's lowest bedrock elevation is 1,300 meters (4,264 feet). The sub-surface ridge between East and West Lemmon Valley basins has a consistent elevation in the central portion of the Figure. The gravity and magnetic data do not provide useful constraints on the location of the Airport Fault in this profile. Golden Valley's bedrock configuration is elongated in an east west orientation with a base elevation of 1,500 meters (4,920). At the bottom left of the Figure, Peavine Mountain rises to the south above 2,600 meters (8,530 feet).

## RESISTIVITY MAPPING

The DIGHEM electromagnetic system consisted of three coplanar coil configurations operating at 56,000 Herz, 7200 Herz and 900 Herz frequencies. A forth coil pair was configured as a coaxial and operated at 900 herz. In the towed bird, the coil separation was 8 meters (26 feet) for the 900 herz and 7200 Herz frequencies and 6.3 meters (21 feet) for the 56,000 Herz coil pair. The sampling rate was 10 per second with a sensitivity that ranged from 0.06 ppm (900 Hz) to 0.3 ppm (56,000 Hz). The bird elevation was at a nominal height of 30 meters (98 feet). In-phase and quadrature channels record the secondary fields from each transmitter-receiver coil-pair. Apparent resistivity is calculated using the pseudo-layer half space model (Fraser, 1978). The following maps have been generated using the Oasis Montaj™ (Geosoft, 1998) software package. These maps display the 900, 7200 and 56,000 Herz frequencies of apparent resistivity mapping (Figures 15, 16 and 17) over the Cold Springs Valley and Lemmon Valley areas. Figures 15b, 16b and 17b display these same apparent resistivities as color-coded with the depth of investigation contoured. For this report the depth of investigation is 75% of the skin depth as measured from land surface. Note that the depth of investigation is a maximum at the lowest EM frequency of 900 Hz that becomes sharply reduced (to as little as 25 meters or 82 feet) over the conductive playa lake deposits. Figure 15c, 16c and 17c display contoured apparent resistivity overlying digital elevation models of the study area.

**56,000 Herz Apparent Resistivity**
Figure 15a shows the apparent resistivity of the 56,000 Herz frequency mapped over the study area. The exposed bedrock areas of Peavine Mountain, Hungry Hills and Granite Hills show resistivities greater than 70 ohm meters (ohm meters). Most of the alluvial basins are mapped between 5 and 25 ohm meters. The playas are generally mapped at less than 10 ohm meters. In the center of the Figure are areas mapped at 20 to 50 ohm meters that correspond to alluvial areas within the basin. These anomalous resistive areas are not readily explained from the surface geology, but do correspond somewhat to areas under housing and commercial development. Also of note is the linear trend of low resistivity units that strike northwest southeast between Peavine Mountain and the Granite Hills. Figure 15b shows the depth of investigation of this frequency. It is shown that over the alluvial material the depth of investigation is between 5 and 10 meters (16 and 33 feet) whereas over hard rock terrain the depth of investigation is generally 20 to 40 meters (66 to 130 feet). Figure 15c shows the contoured apparent resistivity plotted on the DEM and clearly identifies the geographic locations of the resistivity. All three playas have shallow resistivities of 5 ohm meters. The highest resistivities correlate well with the hard rock terrain.

**7200 Herz Apparent Resistivity**
Figure 16a shows the apparent resistivity of the 7200 Herz frequency mapped over the study area. The same trends as in the 56,000 Hz map exist except for the units related to the residential and commercial development. This area now shows lower resistivity and is more comparable to the resistivities mapped laterally from this developed area. This Figure clearly outlines the playas of Cold Springs and Lemmon Valleys noted as 5-10 ohm meters units. In the north of Lemmon Valley, more resistive units of 30–50 ohm meters likely map relatively coarse grained alluvial fan material. Figure 16b shows the depth of investigation for the 7200 Hz frequency. In the alluvial terrain the depths are from 10 to 40 meters (33 to 130 feet). Figure 16c is the DEM overlain with the 7200 Hz resistivity. Again, the playas are well defined resistivity lows. The higher resistivities north of West Lemmon Valley correspond to coarser alluvial deposits. In Golden Valley, resistivities of 40 to 60 ohm meters probably represent coarse granitic alluvial deposits. In general the resistivities are larger than those found in the higher frequency apparent resistivity of Figure 15c indicating that coarser material or hard rock is encountered as the depth of investigation increases.

**900 Herz Apparent Resistivity**
Figure 17a shows the apparent resistivity of the 900 Herz frequency mapped over the study area. This Figure also duplicates Figure 16a. In northern Cold Springs Valley a sub-basin north of the playa (White Lake) is delineated and compares well with Figure 14. An apparent sub-surface hard rock unit is found (>200 ohm meters and of circular shape) south of West Lemmon Valley and north of Peavine Mountain (also shown in Figure 16a). In general, the resistive area of the alluvial deposits is the same in this Figure versus Figure 16a even though the depth of investigation is greater in this Figure. This supports the potential fields modeling interpretation

that the basin boundaries are very steep. A moderate resistive trend is seen along the southern portion of the mapped area from the lower right corner and traverses north-west to Cold Springs Valley (color-coded green with resistivities from 20 to 80 ohm meters) and is also seen in the other apparent resistivity maps. Figure 17b shows an increased depth of investigation that maps the coarse alluvial material north of Silver Lake (20 to 40 ohm meters and colored-coded blue) to depths of 60 to 100 meters (200 to 300 feet). Figure 17c is the DEM with the 900 Hz resistivity plotted as contours.

**Analysis**

A large electrical resistivity contrast exists between the alluvial deposits and the exposed rock lithology as shown in Figure 17a, and illustrates the depositional nature of the study area. The dominant features are low resistive playas in the central portions of both Lemmon and Cold Springs Valleys. Resistivities increase in the northern portion of Lemmon Valley indicating a higher energy depositional environment with coarser material. Generally, the detrital composition of these alluvial deposits can be inferred from the resistivity mapping where low resistivities indicate fine grained (silty to clayey) deposits. The apparent resistivity figures as a group indicate increasing resistivities with depth, which suggest a downward coarsening of the alluvial deposits. The hard rock lithologies are distinctly mapped by resistivities above 200 ohm meters (see Figure 17a).

The southeast-northwest trend of the mid-range resistivities that parallel Peavine Mountain is common to all frequencies and maybe fault related. This is supported by Figure 17b as these resistivities persist beyond the 100 meter (330 feet) depth of investigation. Fault gouge, especially from volcanic units coincident to this trend, would have a low electrical resistivity signature due to the formation of clays. The large circular resistivity high in the center of this trend is of interest because it may represent an intrusive body at or below 100 meters (330 feet). To the east of this trend the fractured and decomposed granodiorite is delineated as a resistivity low in Golden Valley. The coarsest sediments are mapped in the northern portion of Lemmon Valley, where resistivities of 30 to 50 ohm meters are found over approximately 20 $km^2$ (7.5 $mi^2$) to depths of at least 60 to 80 meters (200 to 260 feet). Depth to bedrock is estimated at 450 meters (1,500 feet) at the center of this area. This area is also undeveloped with respect to groundwater and represents a good target area for groundwater development or recharge.

## CONCLUSIONS

The magnetic and gravity data are complementary and consistent with the geology and topography. The gravity data displayed in Figure 3 defines basin structure where steep gravity gradients highlight the steep basin structure. The magnetic data also reflects topography and outlines basin structure in Figures 4 and 5.

Consistent geologic cross sections resulted from the modeling of the individual flight lines and associated gravity, in particular the individual basin's geometry. Some non-unique and therefore subjective contacts of hard rock lithologies were interpreted with respect to the metavolcanics and granodiorite as well as to the quaternary and tertiary sediments. However, the geologic models matched the potential fields data very well as shown in Figures 8 through 13. Figure 14 is the final basin configuration derived from the modeling of the potential fields data. It has defined relatively deep basin and sub-basin structures that appear to have formed from normal faulting typical of Nevada Basin and Range geology. The main basin structures are oriented north south and parallel the Granite Hills on either side. The Granite Hills correspond to a horst block in this type of faulting. Peavine Mountain terminates these basins on the south where a possible fault zone has been mapped by the 900 Hz apparent resistivity. A small sub-basin is modeled directly north of the Cold Springs basin and a larger sub-basin directly east of the West Lemmon Valley basin. The Golden Valley sub-basin is modeled as an east west, elongated valley that is relatively shallow. This sub-basin' alluvium is mostly comprised of fractured and/or decomposed granodiorite.

Actual fault locations are not well constrained by the current modeling. The major fault structures are associated with the steeply dipping horst blocks of the Granite Hills and the Hungry Hills. The Airport Fault appears to be defined by a shallow granodiorite block that extends south from Hungry Hills and forms the western edge of the East Lemmon Valley sub-basin. The fault scarp trace mapped by Cordy (1985) appears to represent a "rim" of granodiorite that frequently outcrops and is well displayed in Figure 2. The appendix contains geologic cross sections of lines 20050 to 20080 that attempt to delineate this "fault structure".

The dominant EM features are the low resistive units that map the playas in Lemmon and Cold Springs Valleys. The very low resistivity units found in the playas are indicative of the accumulation of clay size particles. The groundwater in these sediments does not necessarily contain a high concentration of dissolved solids. Throughout the valleys, the sediments are interpreted as fine grained, but coarsen to the north in West Lemmon Valley where the resistivity increases. The sediments mapped above 40 ohm meters in this area should be considered for possible groundwater recharge and recovery well sites.

## REFERENCES


Bell, J. and Garside, L., 1987. Geologic Map of the Verdi quadrangle. Nevada Bureau of Mines and Geology, University of Nevada-Reno. Map number 4Gg.

Bonham, Harold., 1969. Geology and mineral deposits of Washoe and Storey Counties, Nevada. Nevada Bureau of Mines and Geology, Mackay School of Mines, University of Nevada, Reno.

Bonham, Harold and E. Bingler, 1973 Geologic Map of the Reno quadrangle. Nevada Bureau of Mines and Geology, University of Nevada-Reno.

Carpenter, 1997, 1998. Gravity data acquisition and processing, West Lemmon Valley Project, Washoe County, Nevada. Consultant report prepared for Washoe County Department of Water Resources, Reno, Nevada

Carpenter, 1997. Gravity data acquisition and processing, Cold Springs Valley Project, Washoe County, Nevada. Consultant report prepared for Washoe County Department of Water Resources, Reno, Nevada

Carpenter, 1999. Letter Report to Washoe County Department of Water Resources, Reno, Nevada

Cordy, Gail E., 1985. Geologic Map of the Reno NE quadrangle. Nevada Bureau of Mines and Geology, University of Nevada-Reno. Map number 4Cg.

DIGHEM, 1996. Dighem$^V$ survey for Utility Division, Washoe County Public Works, Reno, Nevada. Consultant report prepared for Washoe County Public Works, Reno, Nevada.

Fraser, Douglas C., 1978. Resistivity mapping with an airborne multicoil electromagnetic system. Geophysics, vol. 43, p.144-172.

Geosoft, Inc.,1999. Oasis Montaj, data processing and analysis system for earth science applications, Version 4.3. Geosoft, Inc. Toronto, Ontario.

Harrill, James R., 1973. Evaluation of the Water Resources of Lemmon Valley, Washoe County, Nevada, with Emphasis on Effects of Ground-Water Development to 1971. USGS Water Resources Bulletin No. 42.

Northwest Geophysical Associates, 1996. GM-SYS, Gravity and Magnetics Modeling for Windows. Version 4.00. Northwest Geophysical Associates, Corvallis, Oregon.

Schaefer and Maurer, 1981. Geophysical reconnaissance of Lemmon Valley, Washoe County, Nevada. USGS Open File Report 80-1123

Schweickert, Richard, 1999. Personal communication. Department of Geological Sciences, Mackay School of Mines, University of Nevada, Reno.

Skalbeck, John D., 1998. Measurement of Physical and Paleomagnetic Properties from Rocks in the Steamboat Hills and Carson Range, Washoe County, Nevada. Unpublished report prepared for Washoe County Department of Water Resources, Reno, Nevada.

Soeller, S.A. and Nielsen, R. L., 1980 Geologic Map of the Reno NW quadrangle. Nevada Bureau of Mines and Geology, University of Nevada-Reno. Map number 4Dg.

Widmer, Michael C., 2000. Potential Fields and Electromagnetic Interpretation. Unpublished report prepared for Washoe County Department of Water Resources, Washoe County, Reno, Nevada

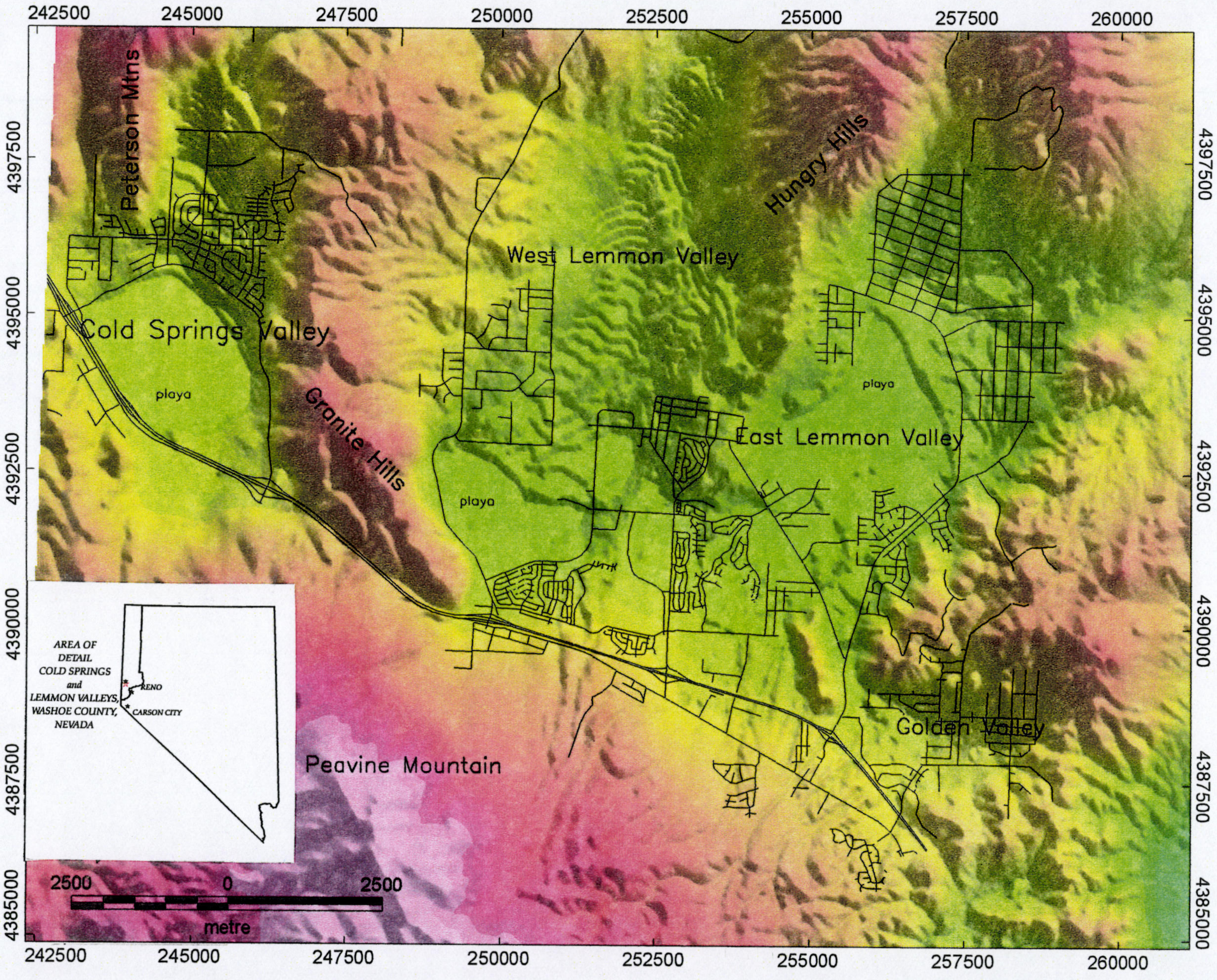


Figure 1. Location map of Cold Springs and Lemmon Valleys

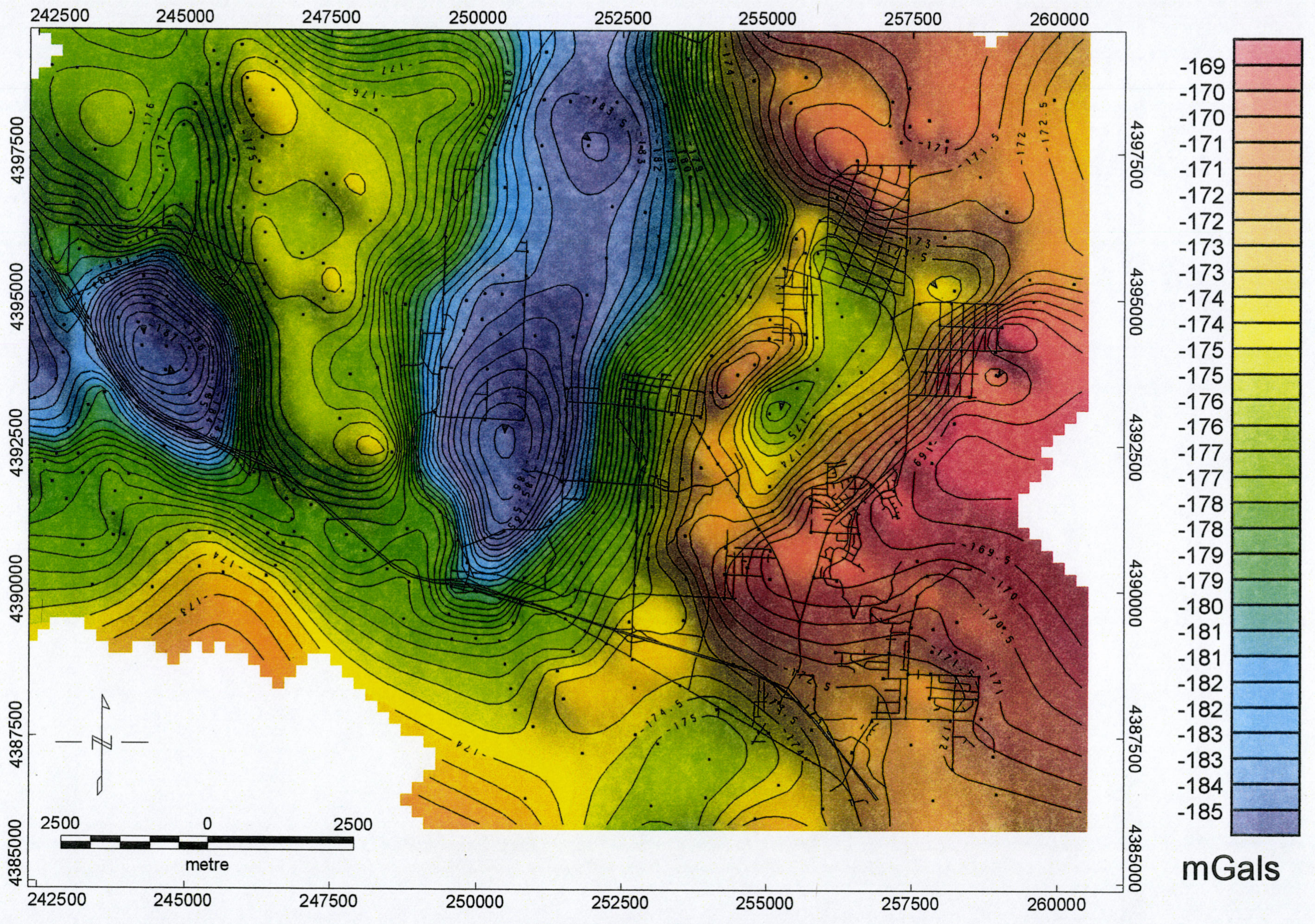


Figure 2. Complete Bouguer Gravity Anomaly Map of Cold Springs and Lemmon Valleys. Contour interval is 0.5 mGals, slab density is 2.67 g/cc. Gravity stations are located by dots and major roads are plotted.

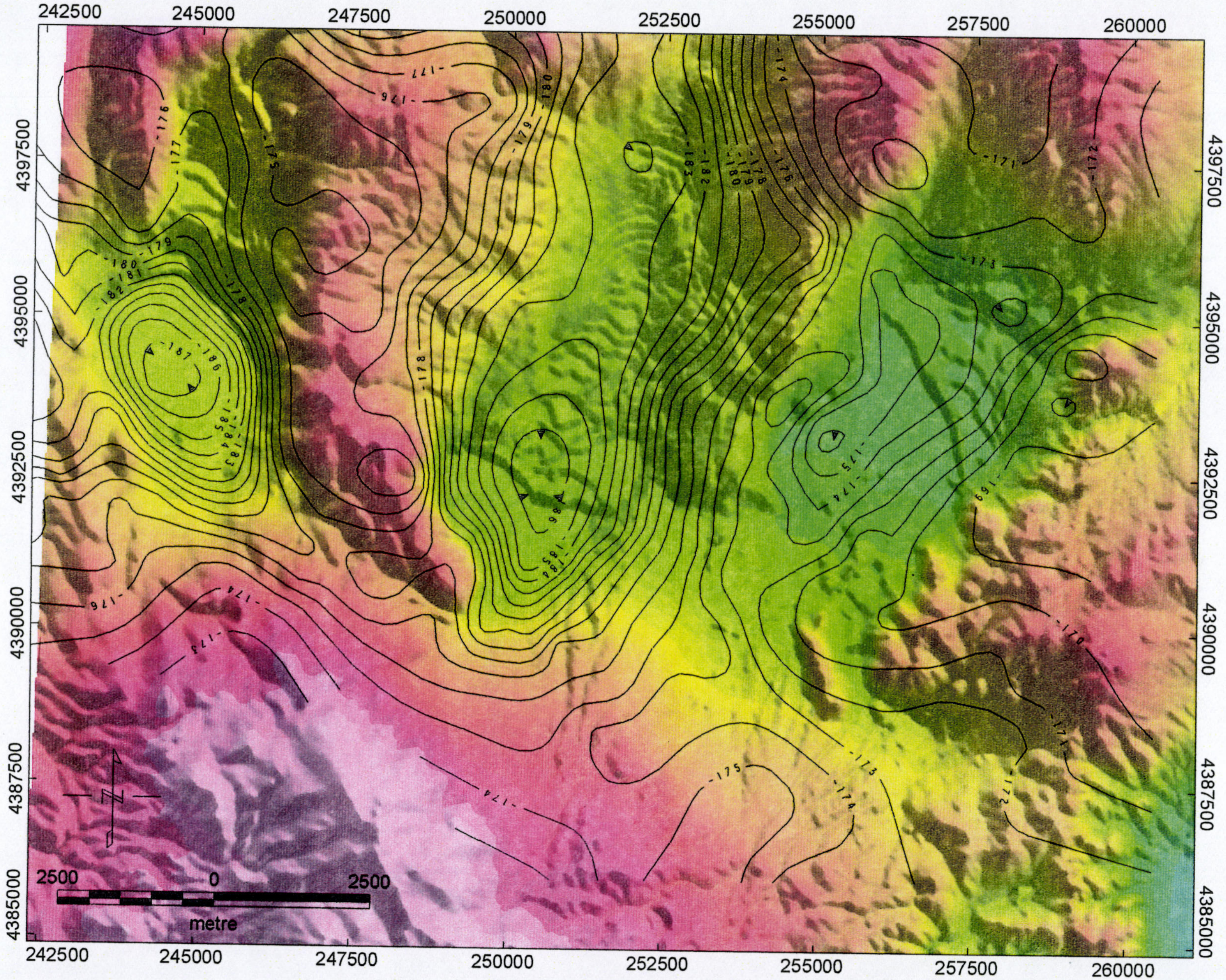


Figure 3. Digital Elevation Map with gravity anomalies

Cotour interval is 1.0 mGals

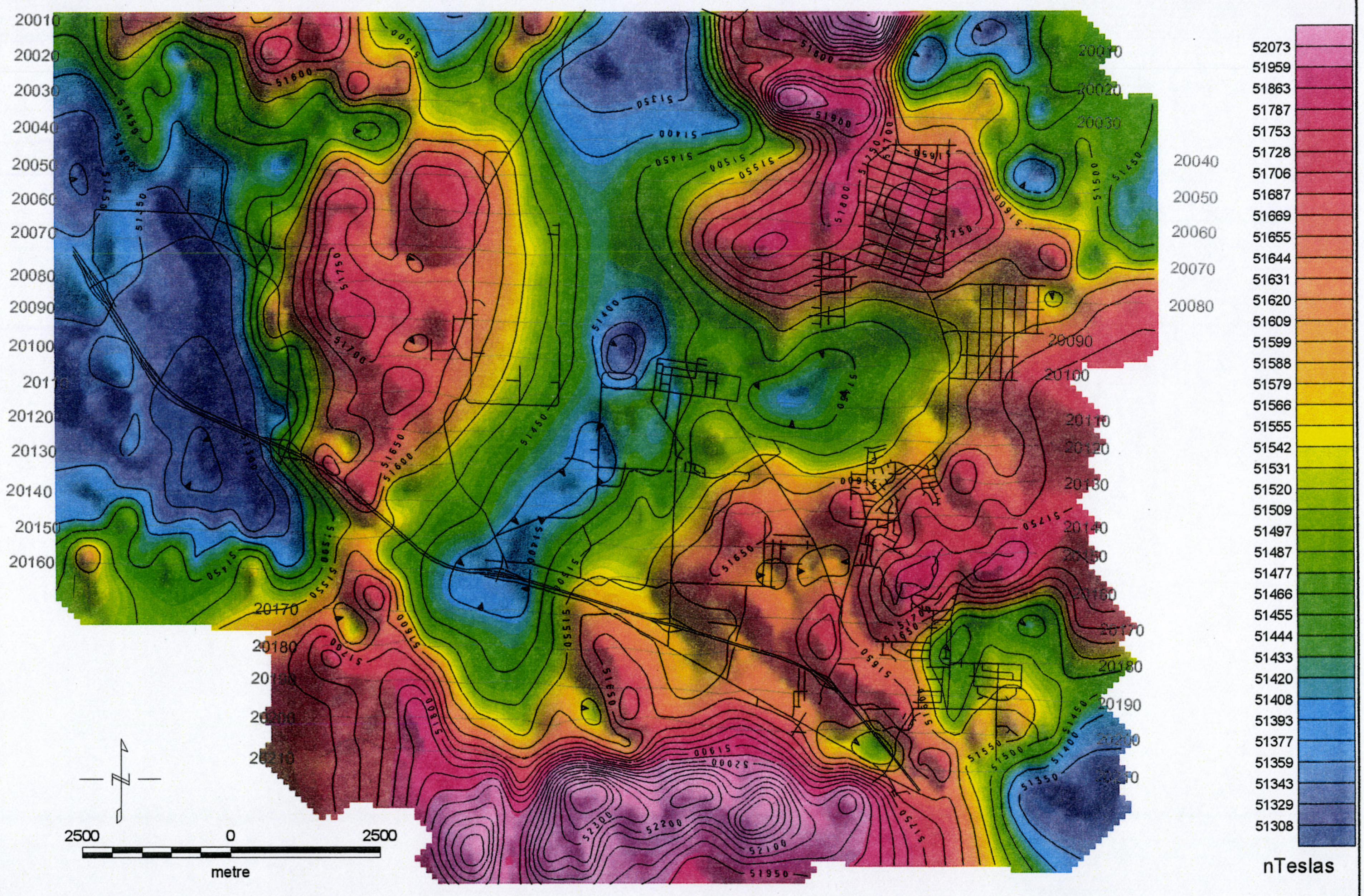


Figure 4. Total field magnetic map, reduced to pole and upward continued 100m.
Contour interval is 20 nTeslas. Roads and flight lines are plotted for reference.

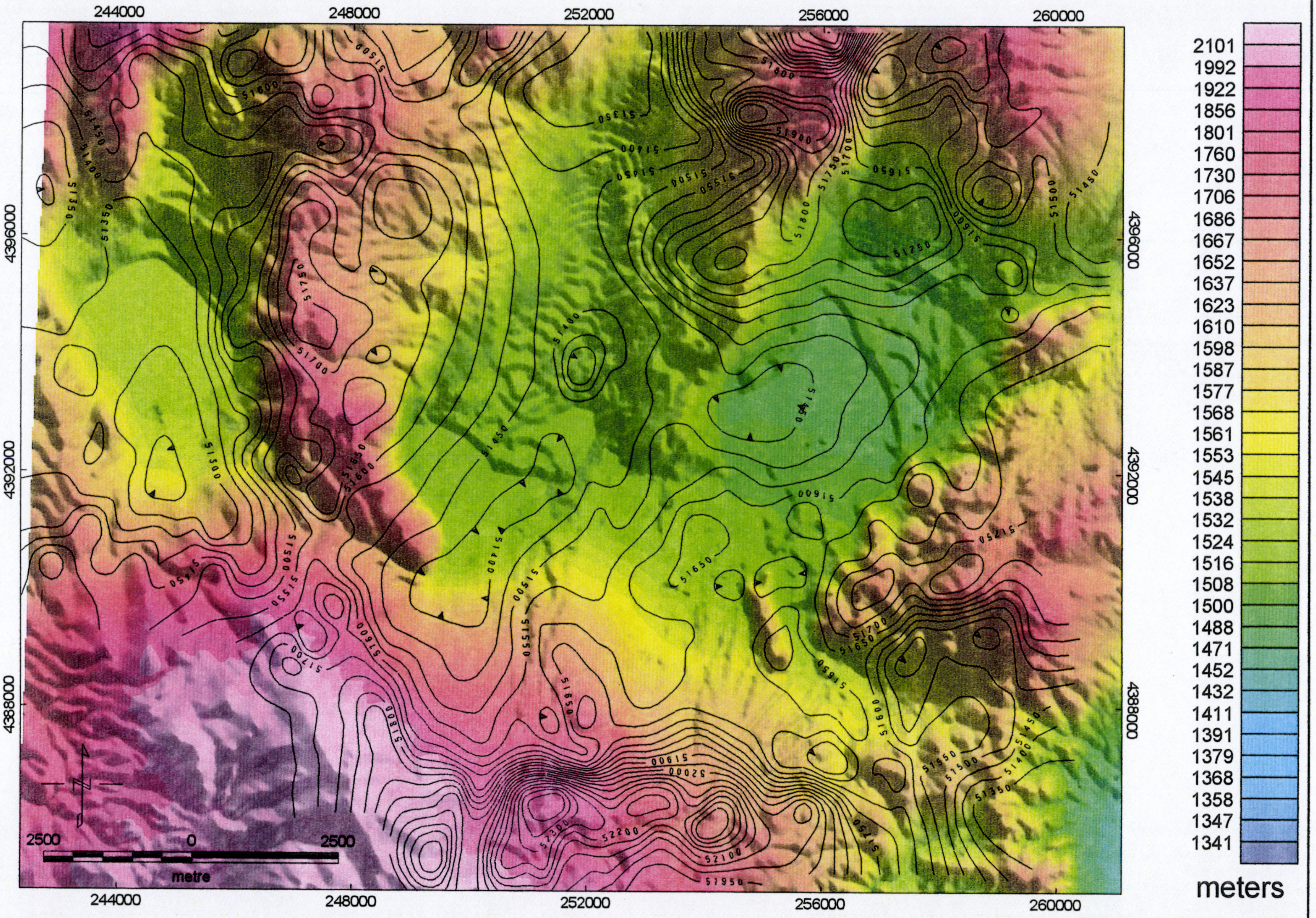


Figure 5. Digital elevation map overlain with total field magnetic contours from Figure 4.

Contour interval is 50 nTeslas.

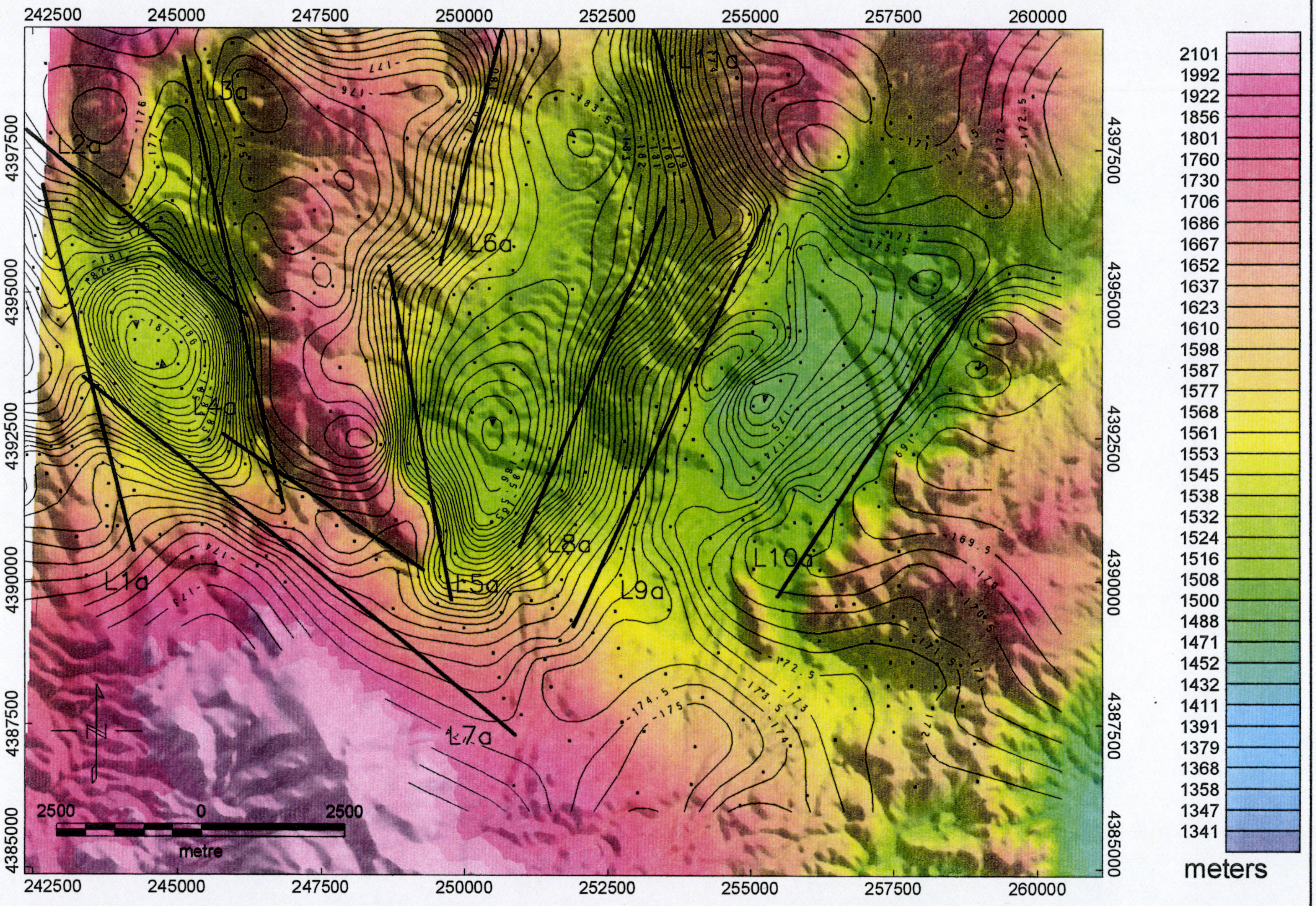


Figure 6a. Digital elevation map overlain with Complete Bouguer Anomaly contours from Figure 2 with lineaments L1a to L11a. Contour interval is 0.5 mGals.

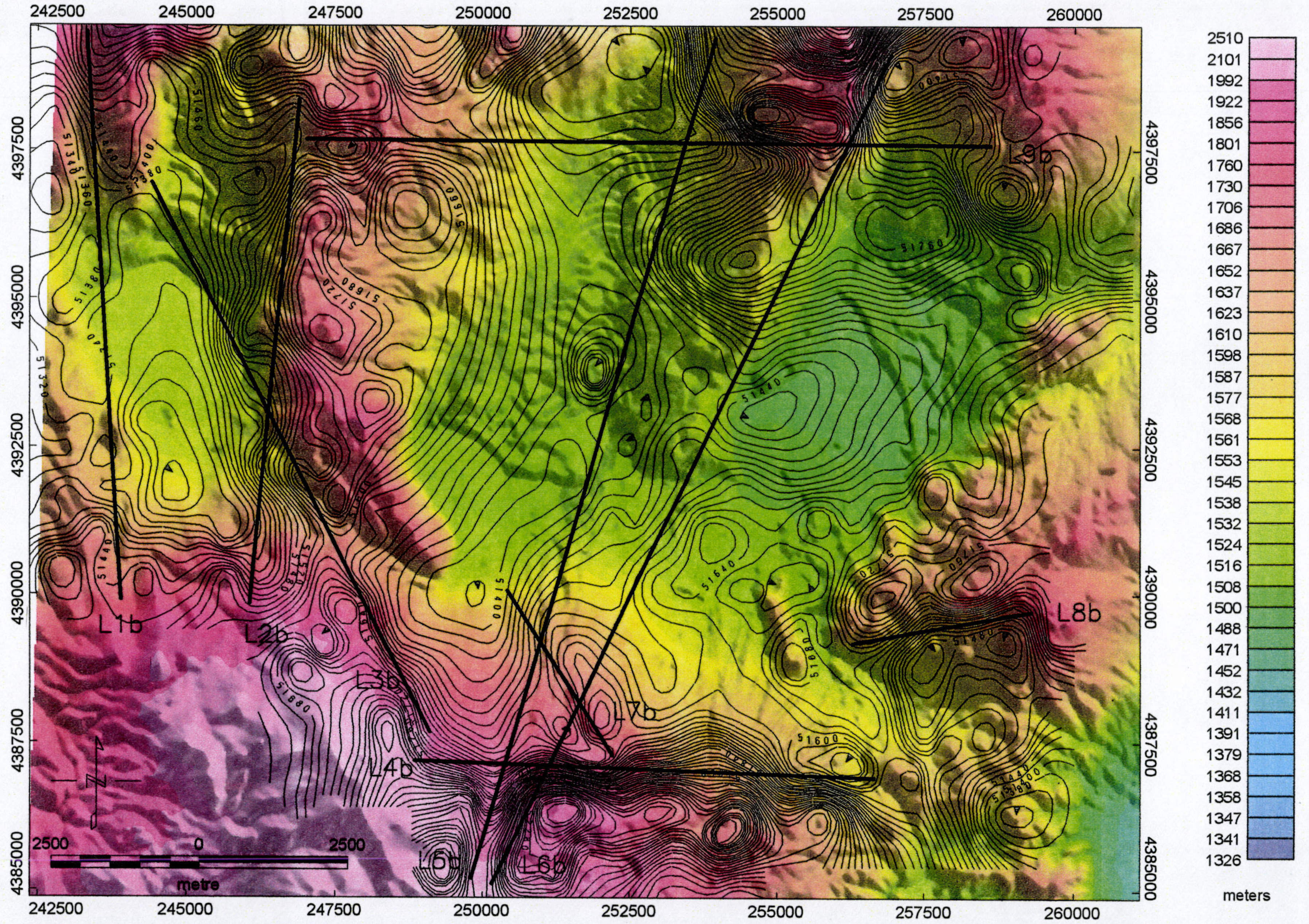


Figure 6b. Digital elevation map overlain with reduced to pole magnetic anomaly contours from Figure 4 with lineaments L1b to L11b. Contour interval is 20 nTeslas.

Figure 7. Geologic Model of Line 20020 in Cold and Lemmon Valleys

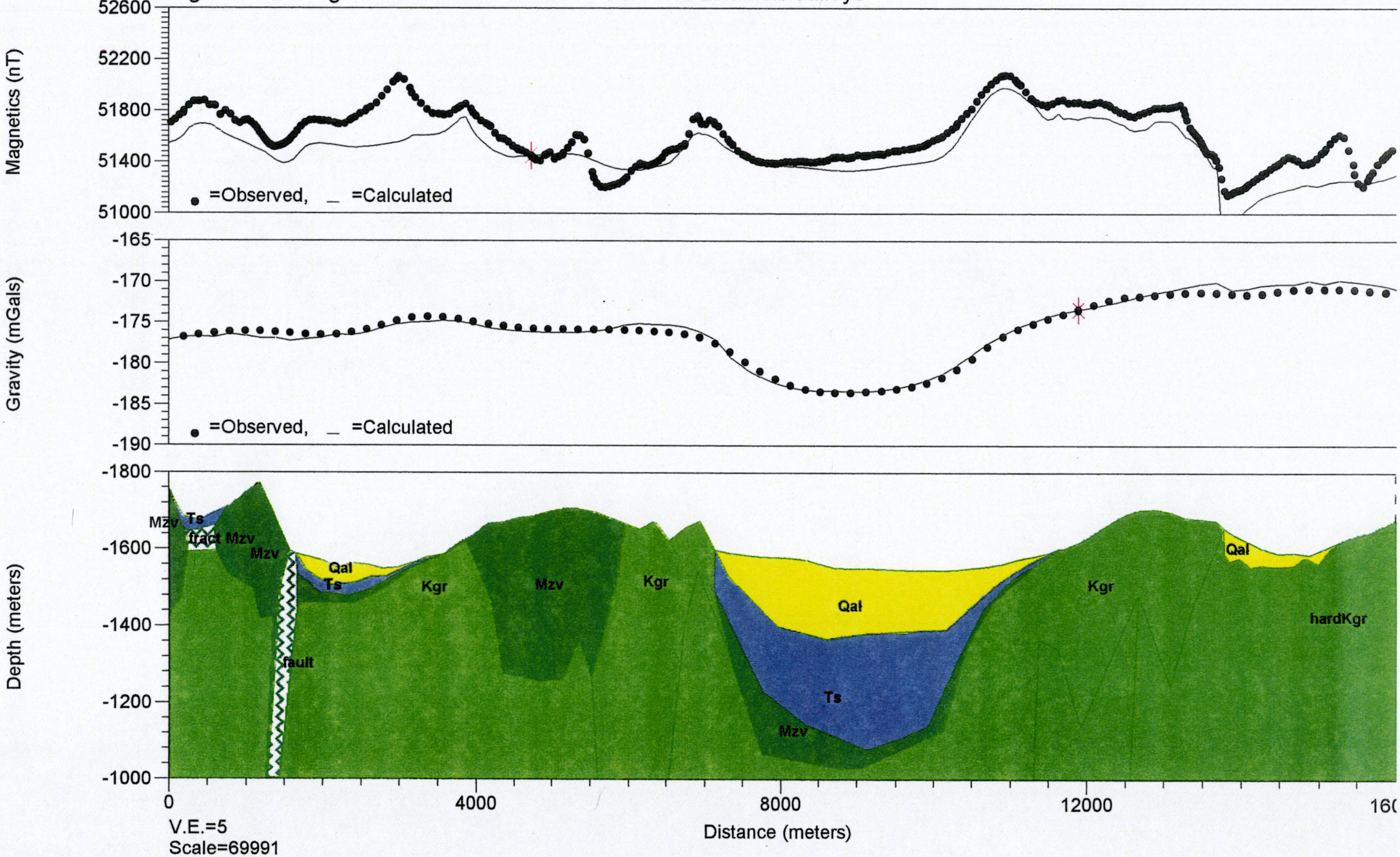

Figure 8. Geologic Model of Line 20050 in Cold and Lemmon Valleys

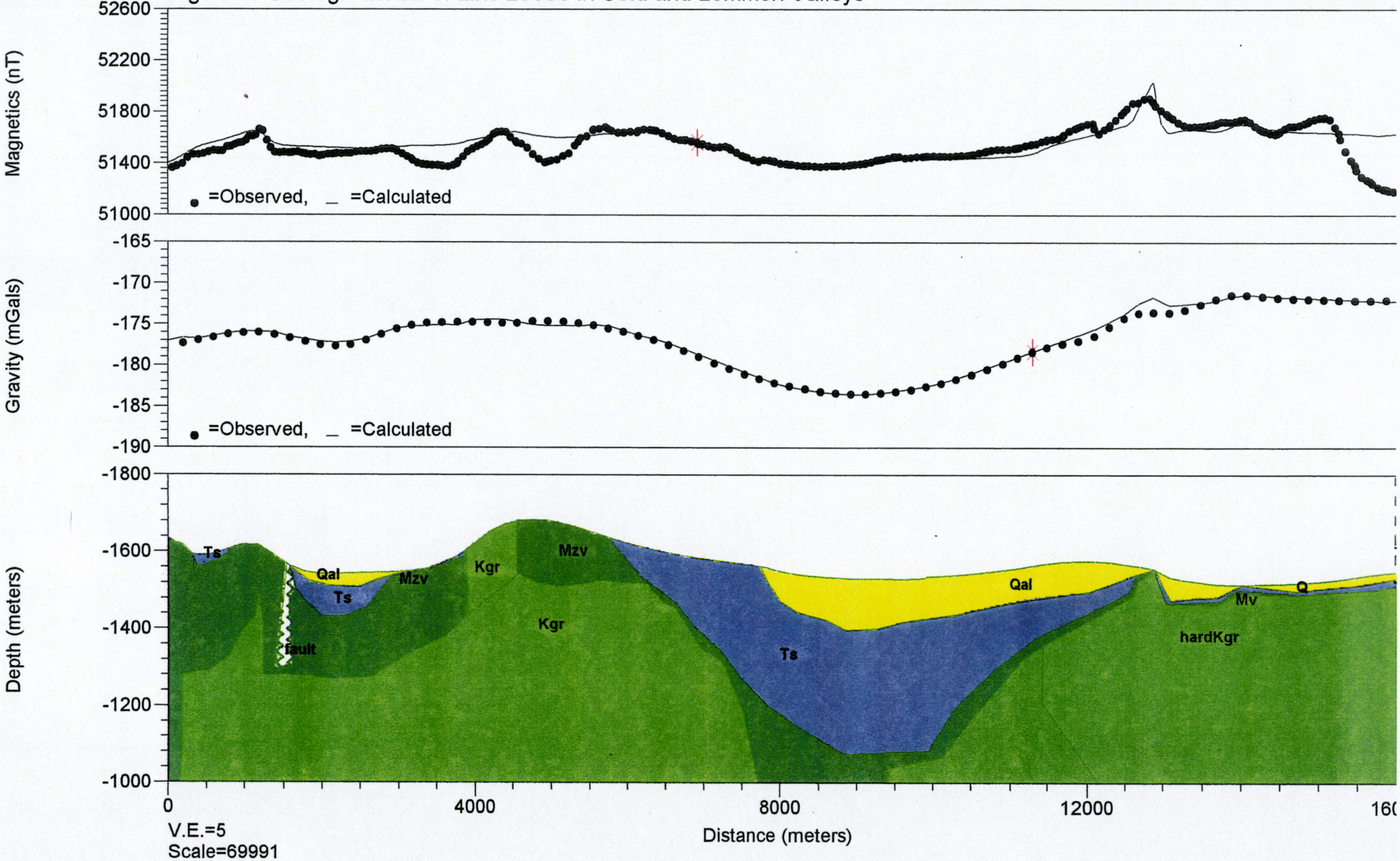

Figure 9. Geologic Model of Line 20080 in Cold and Lemmon Valleys

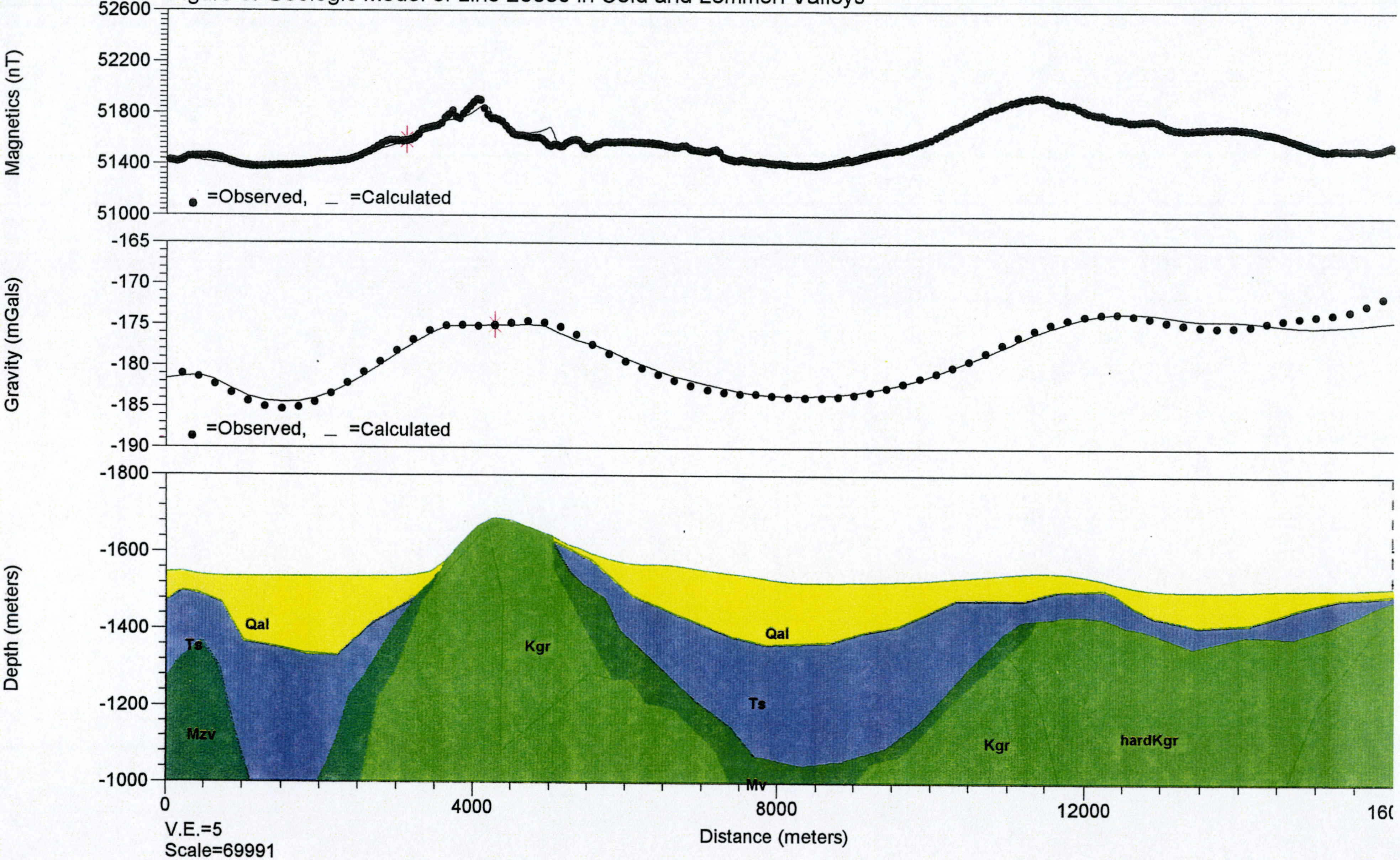

Figure 10. Geologic Model of Line 20100 in Cold and Lemmon Valleys

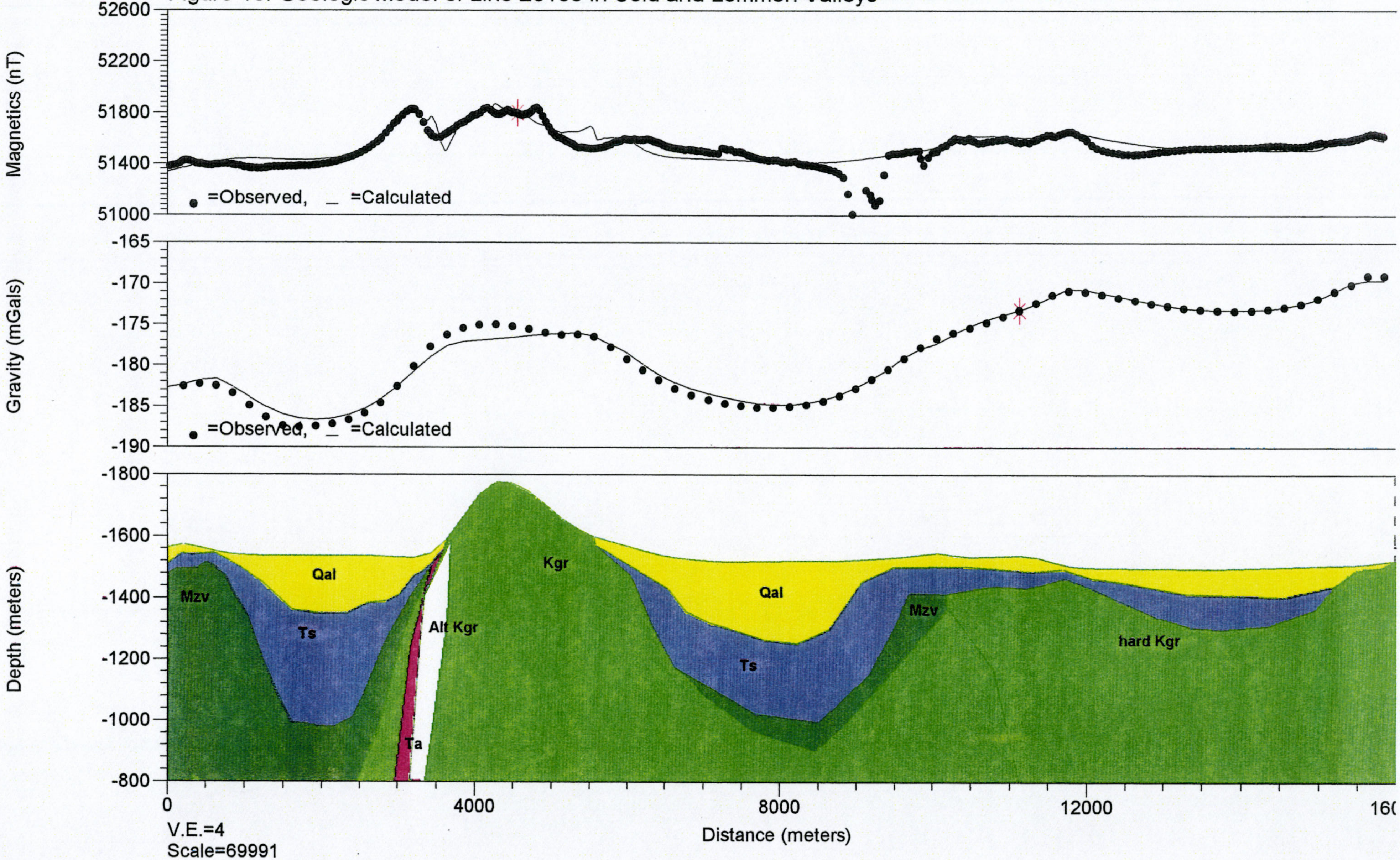

Figure 11. Geologic Model of Line 20120 in Cold and Lemmon Valleys

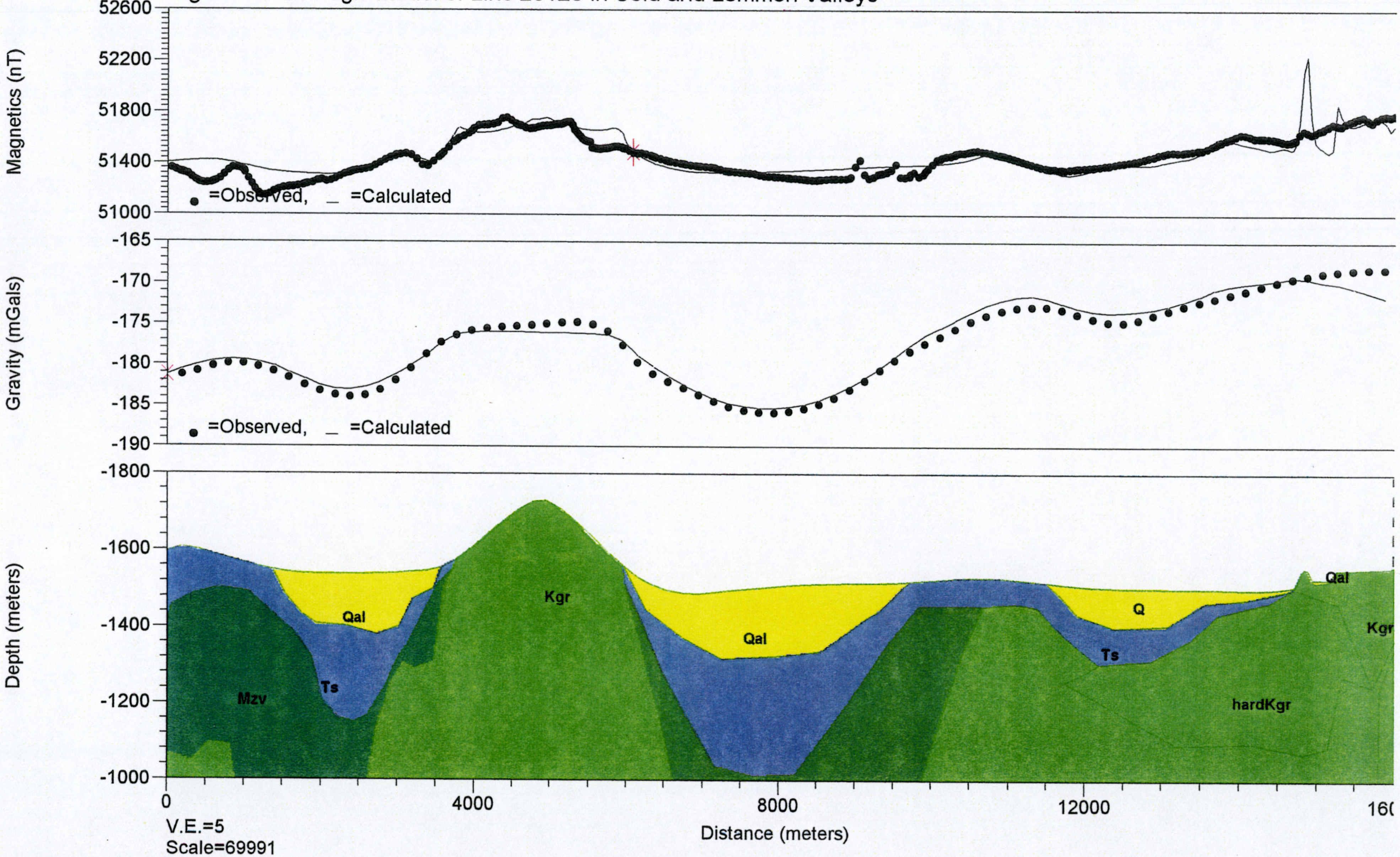

Figure 12. Geologic Model of Line 20150 in Cold and Lemmon Valleys

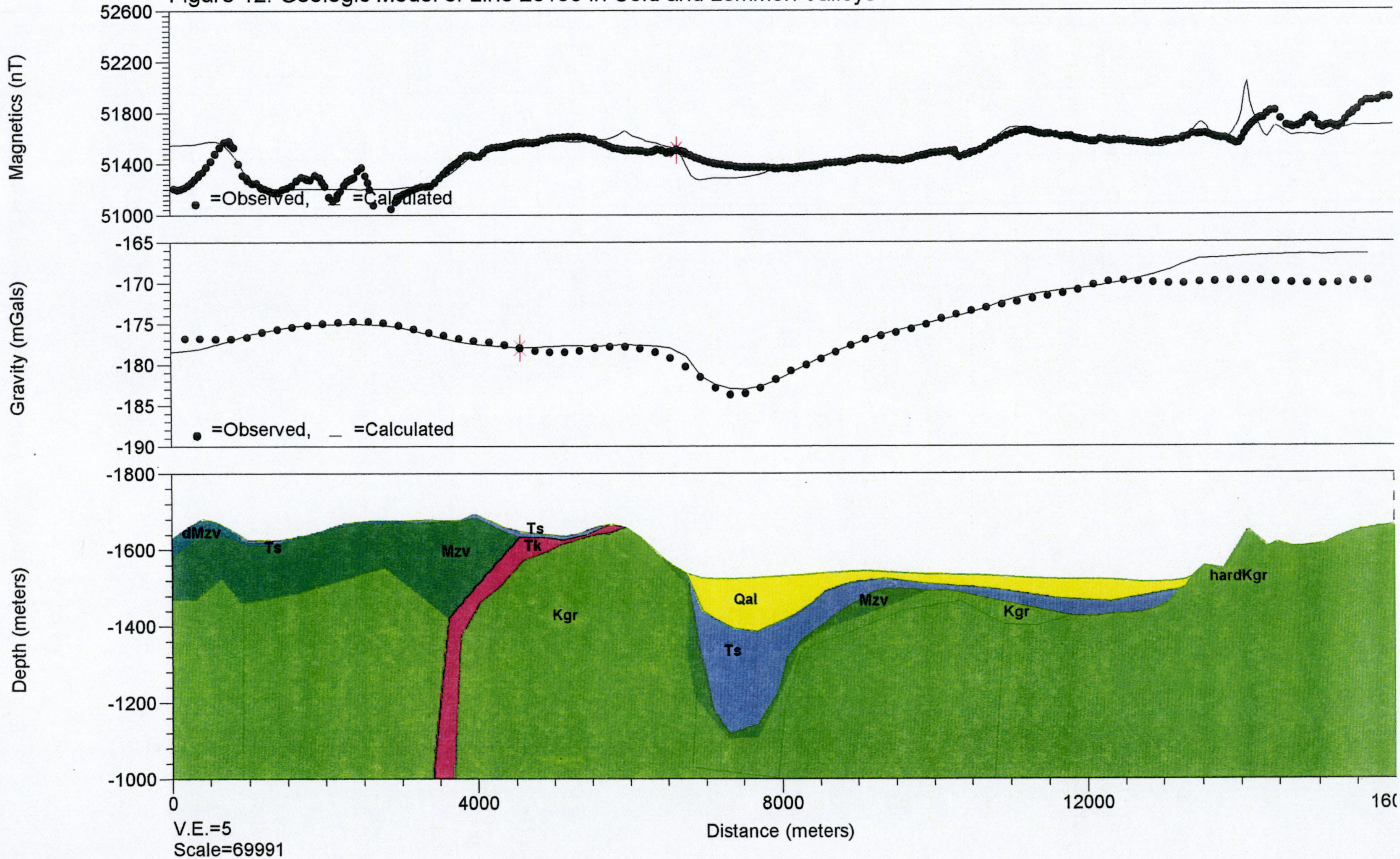

Figure 13. Geologic Model of Line 20180 in Cold and Lemmon Valleys

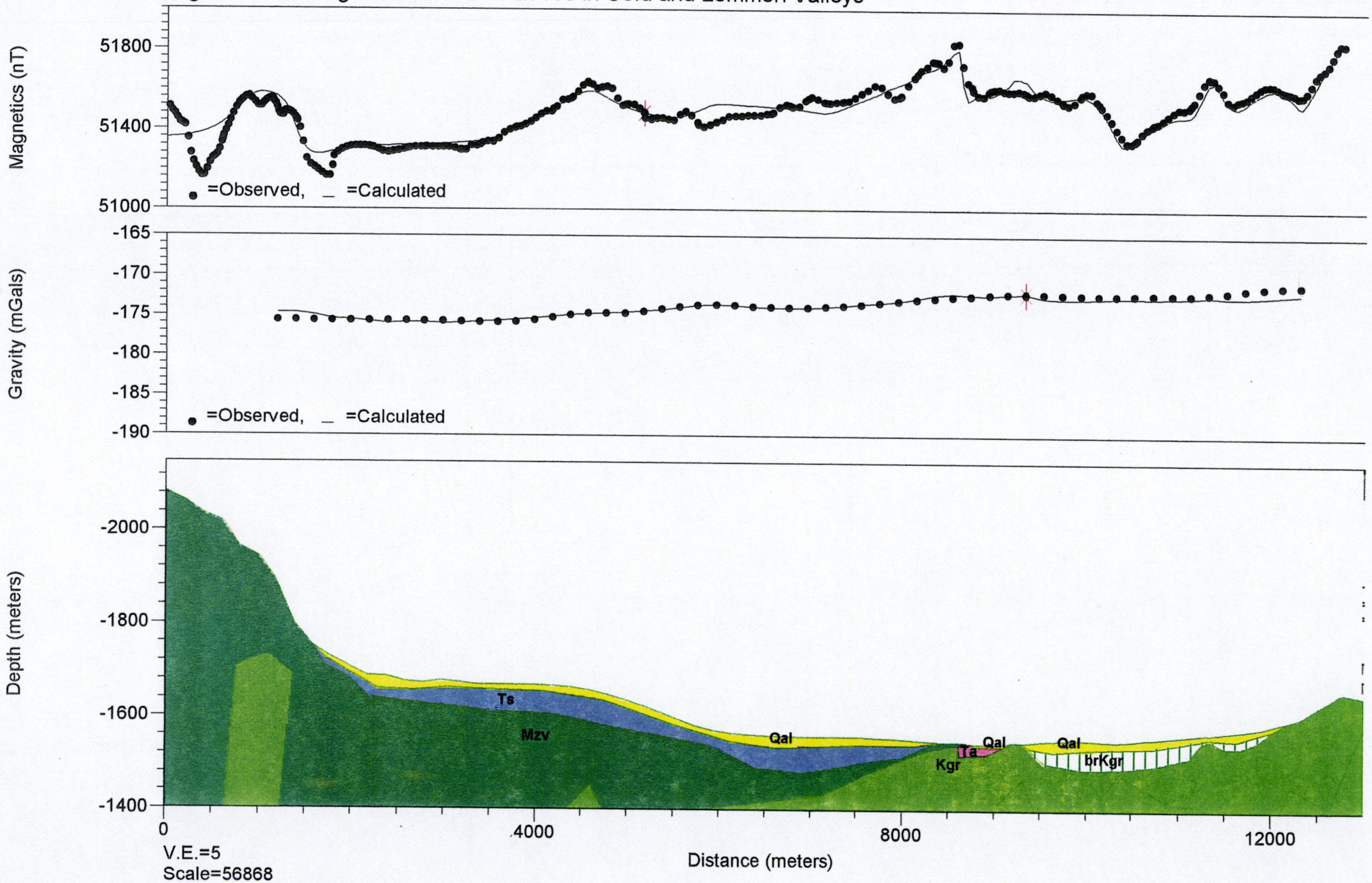

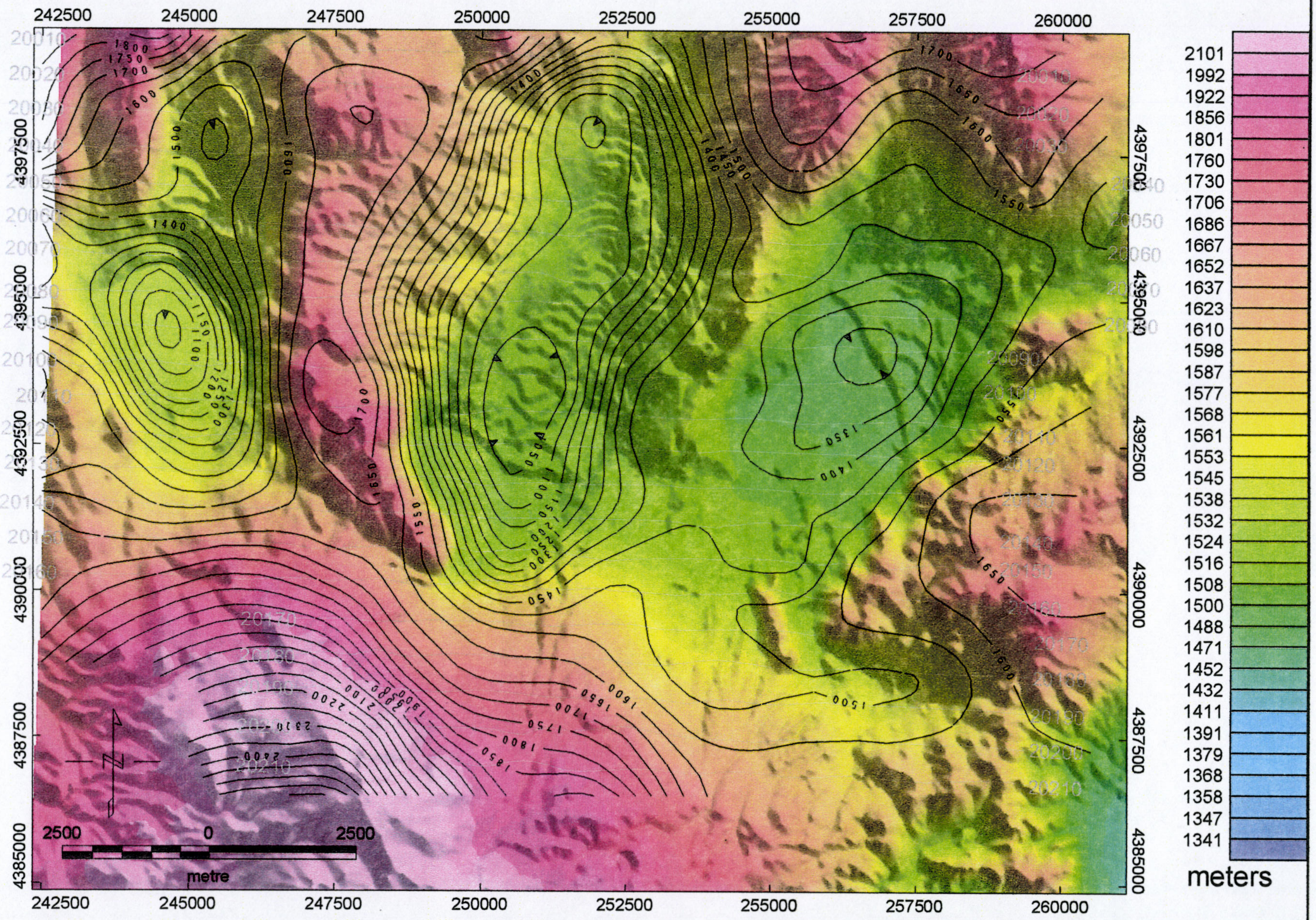


Figure 14. Digital elevation map overlain with bedrock elevations.

Contour intervals are 50 meters. Modeled lines 20010 to 20210 are faintly plotted.

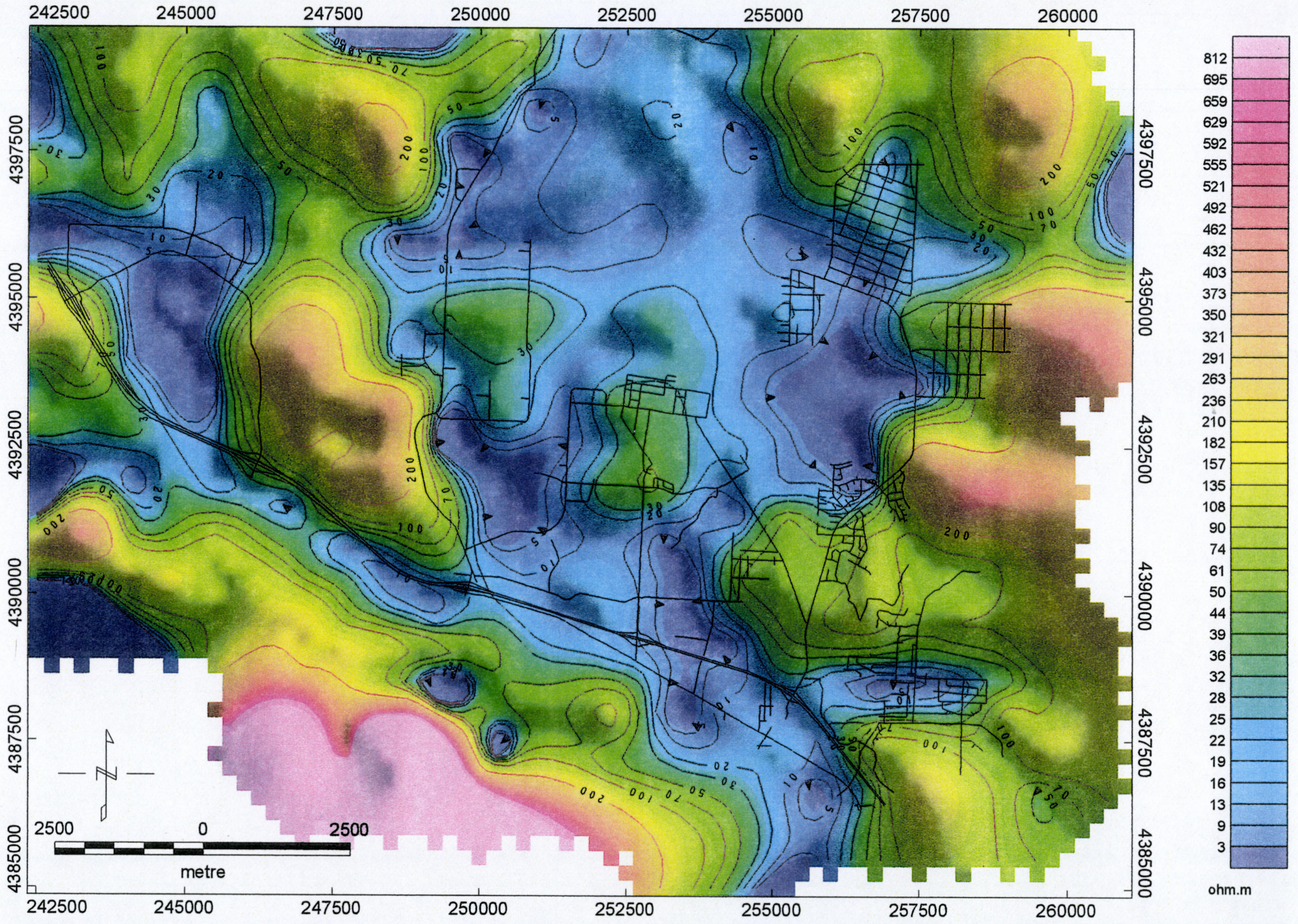


Figure 15a. 56,000 Hz apparent resistivity map with reference roads.

Contour intervals are bracketed from 5 to 200 meters.

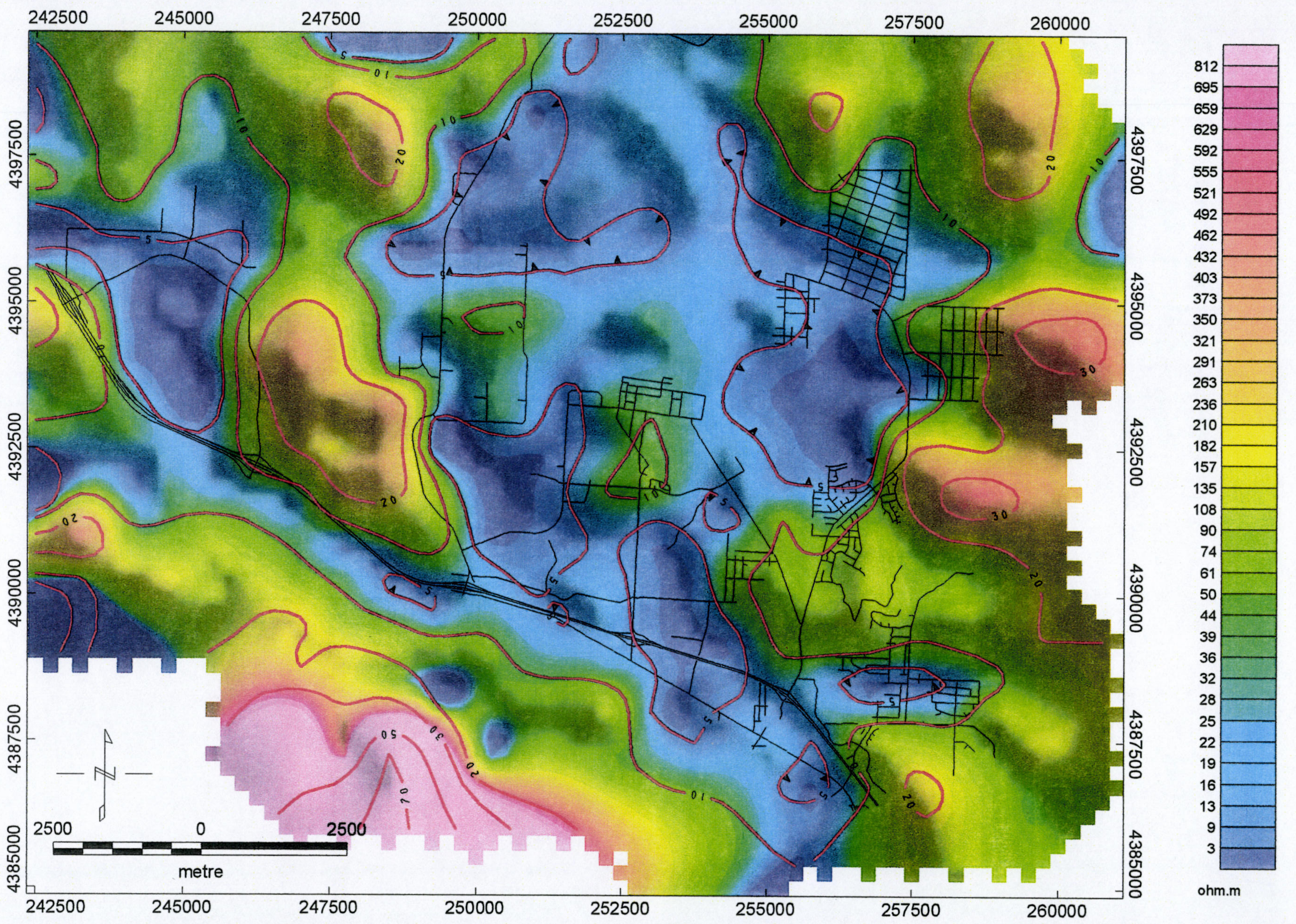


Figure 15b. 56,000 Hz apparent resistivity map with depth of investigation plotted (75% of one skin depth). Contour intervals are bracketed from 5 to 200 meters. Roads are shown for reference.

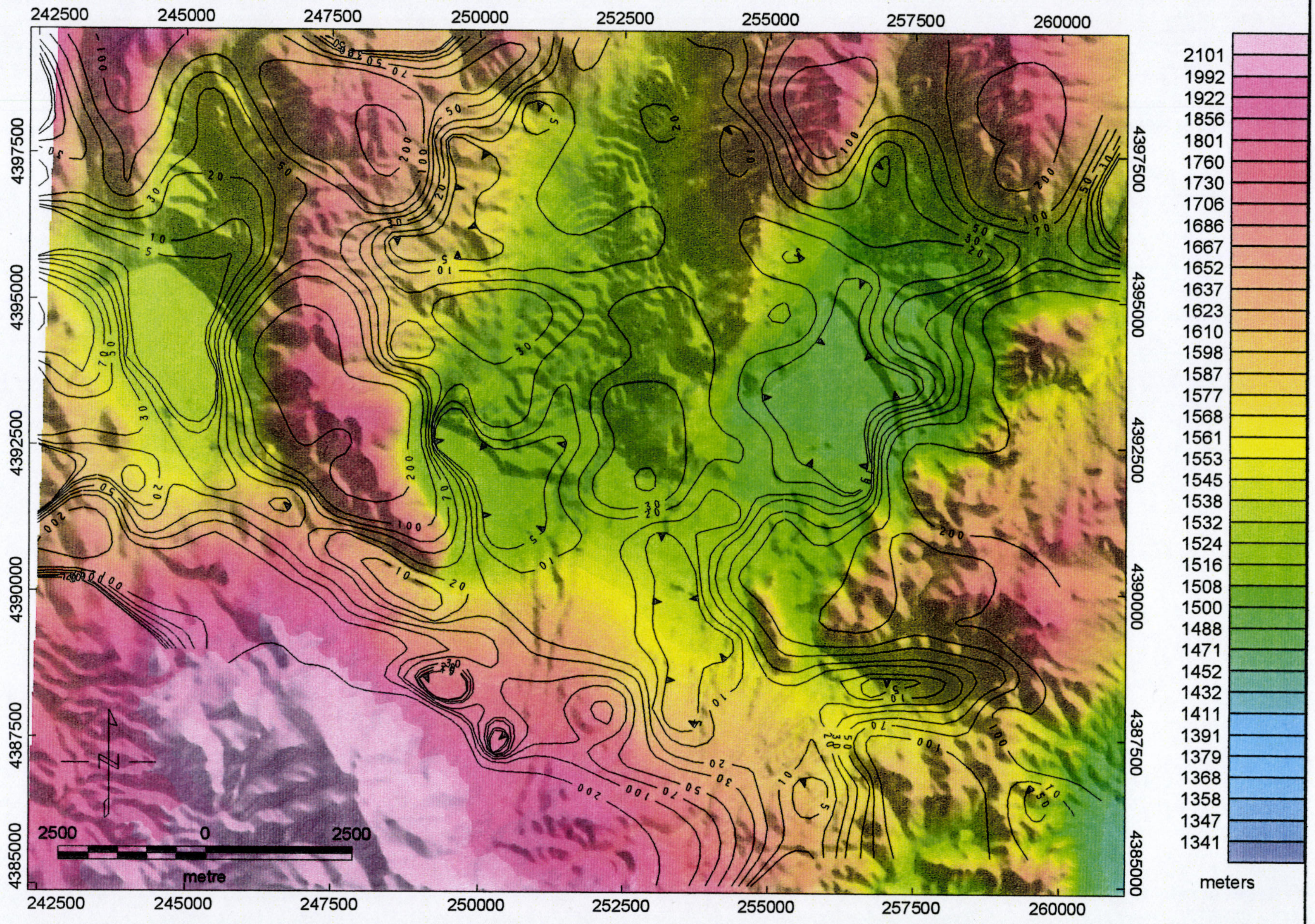


Figure 15c. Digital elevation map overlain with 56,000 Hz apparent resistivity.

Contour intervals are bracketed from 5 to 200 ohm.m.

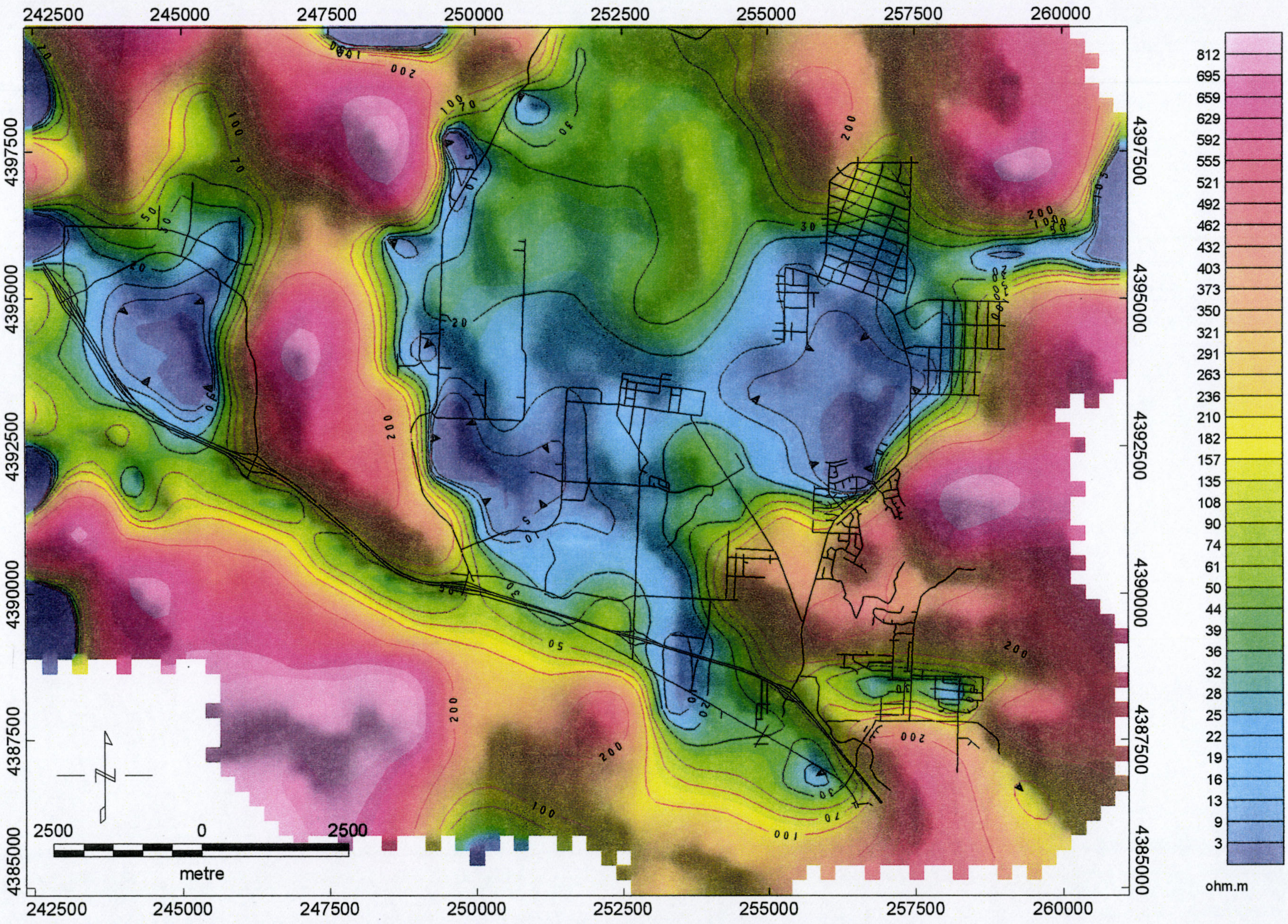


Figure 16a. 7,200 Hz apparent resistivity map with reference roads.

Contour intervals are bracketed from 5 to 200 meters.

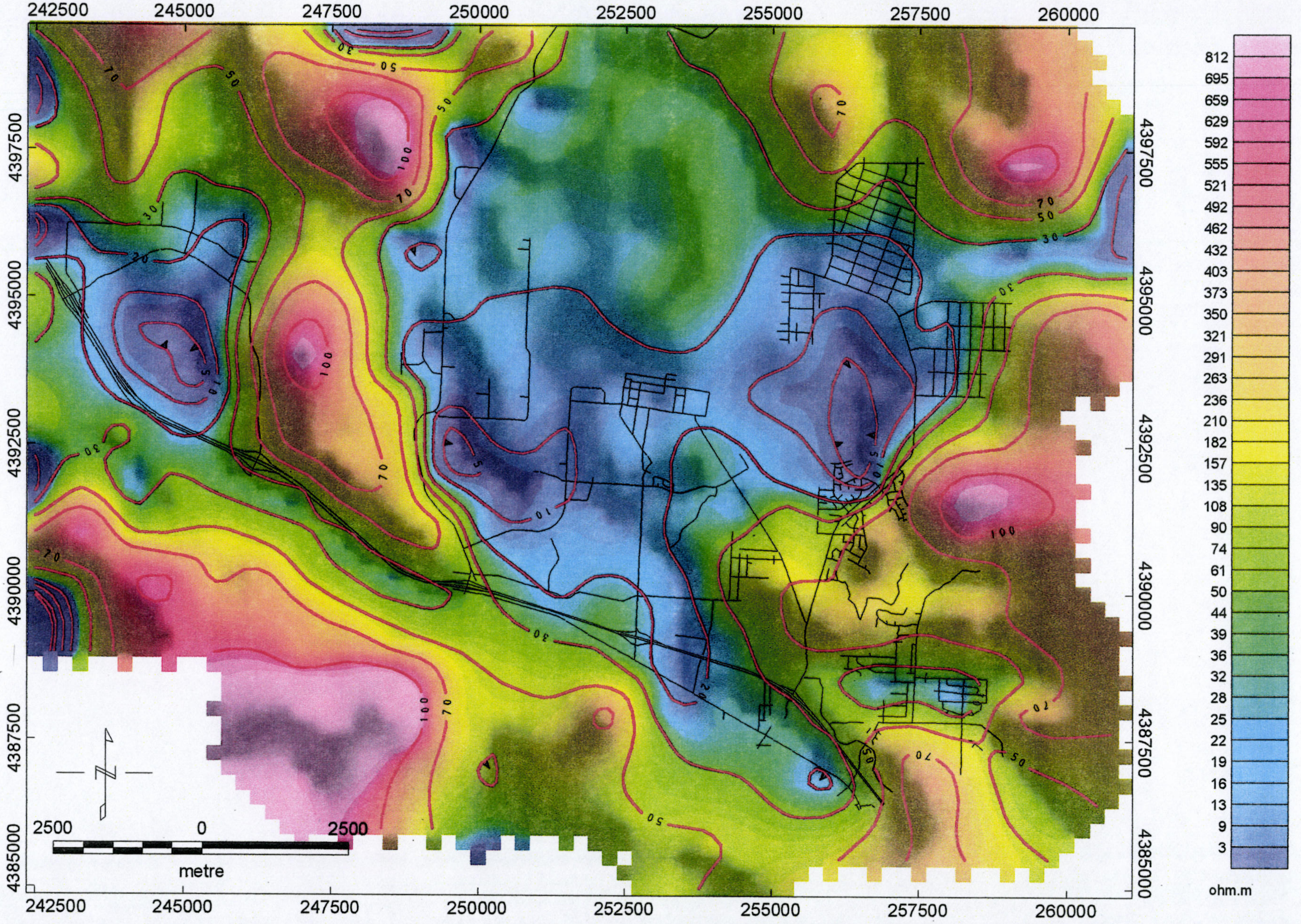


Figure 16b. 7200 Hz apparent resistivity map with depth of investigation plotted (75% of one skin depth). Contour intervals are bracketed from 5 to 200 meters. Roads are shown for reference.

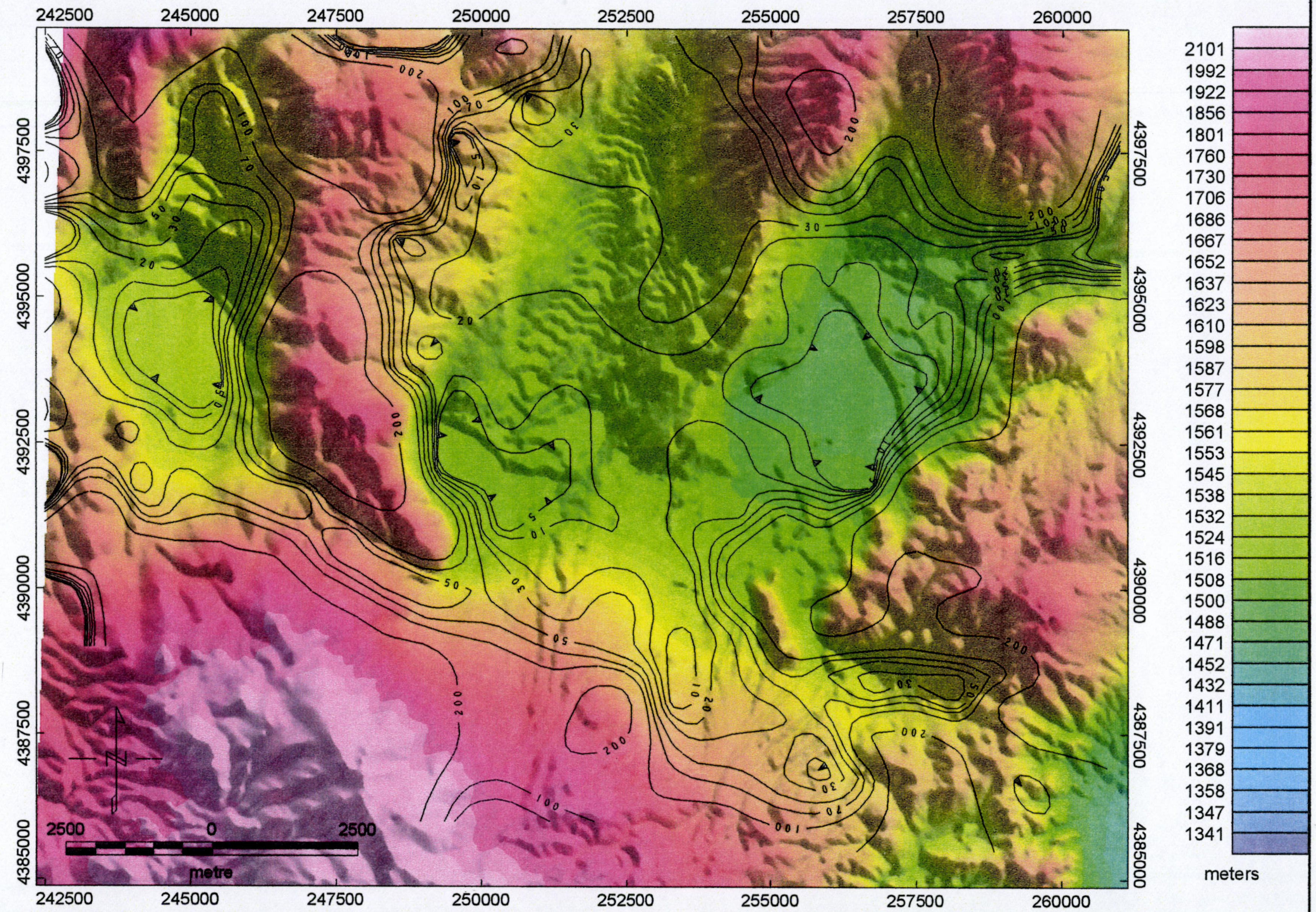


Figure 16c. Digital elevation map overlain with 7200 Hz apparent resistivity.

Contour intervals are bracketed from 5 to 200 ohm.m.

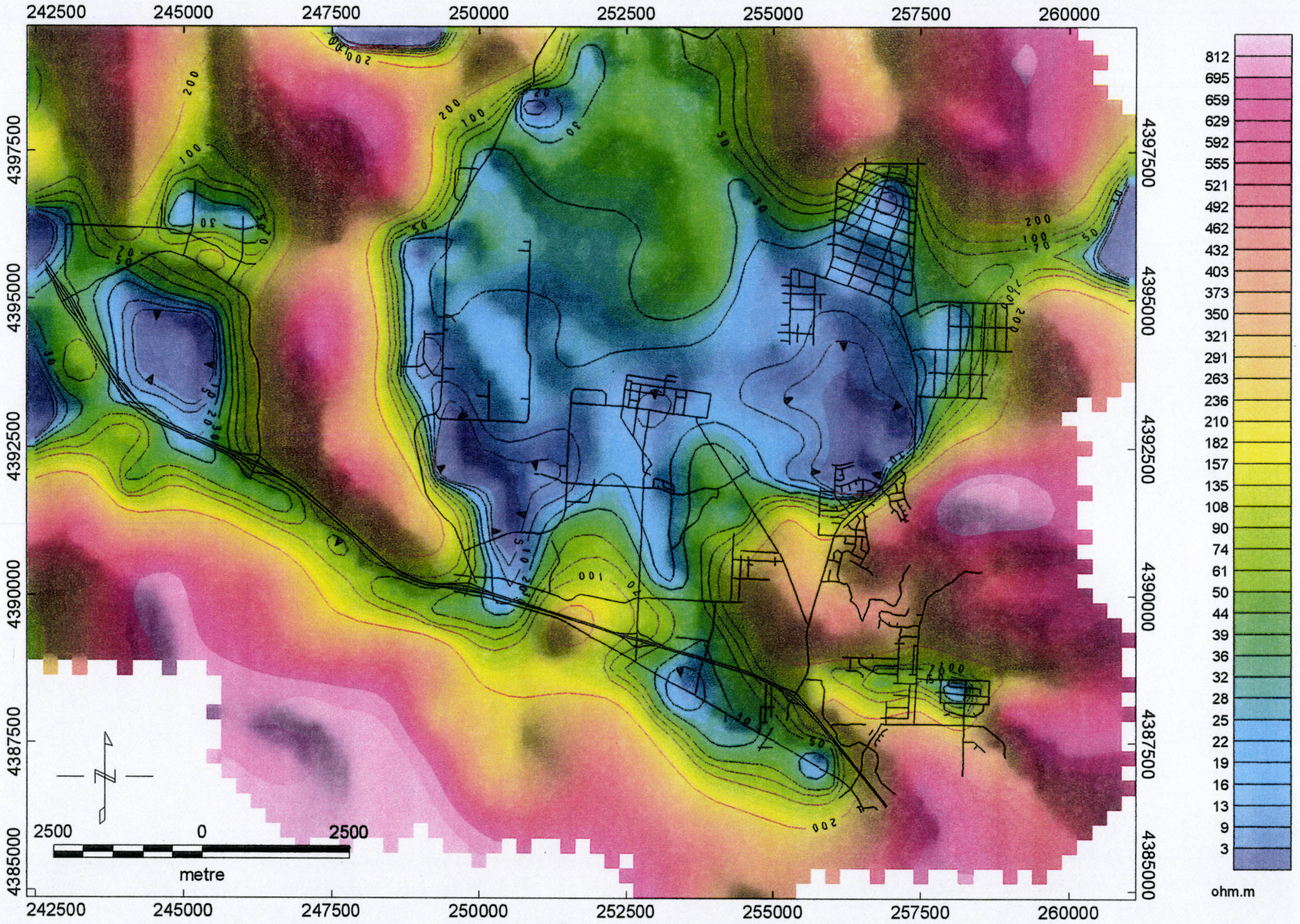


Figure 17a. 900 Hz apparent resistivity map with reference roads.

Contour intervals are bracketed from 5 to 200 meters.

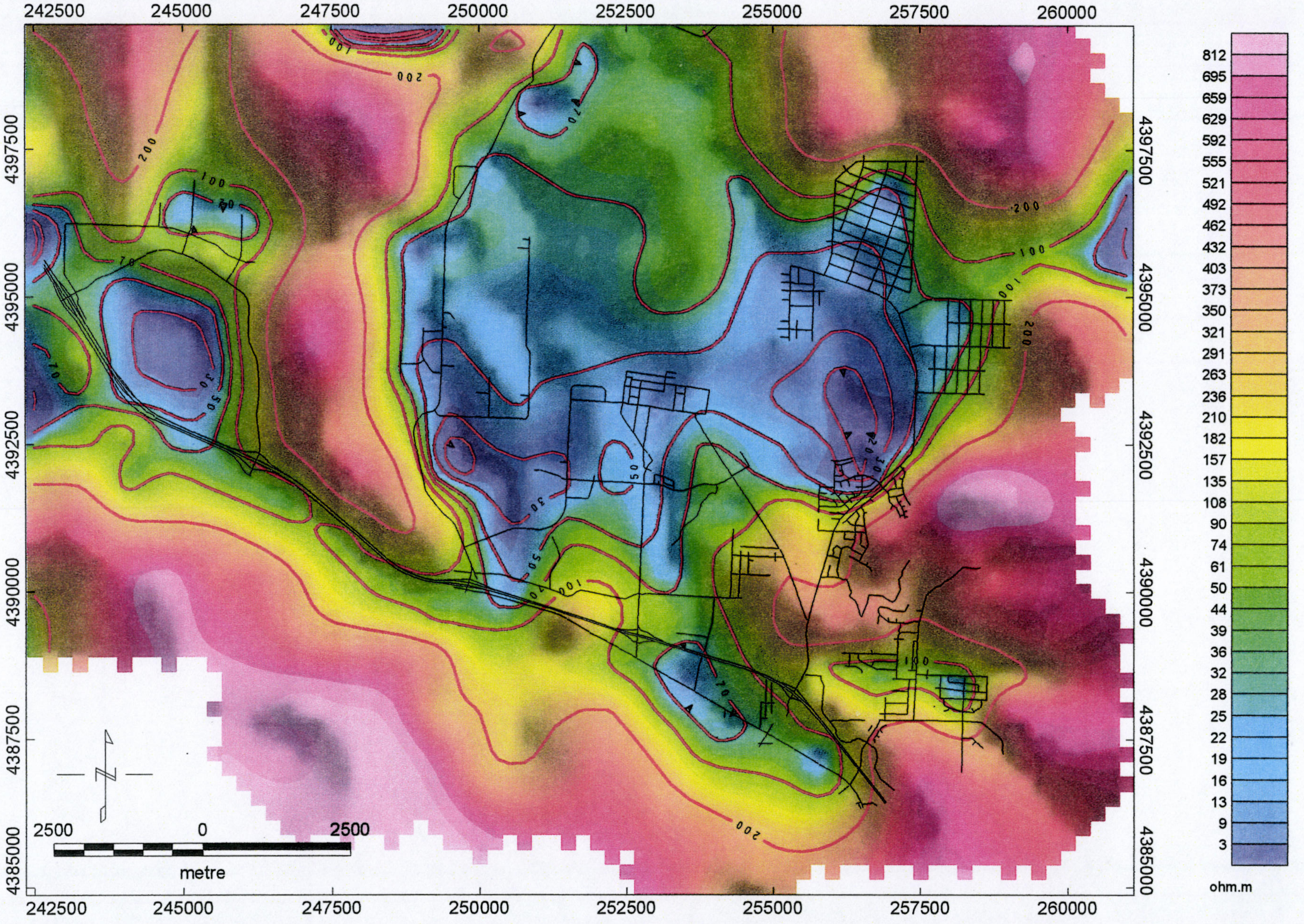


Figure 17b. 900 Hz apparent resistivity map with depth of investigation plotted (75% of one skin depth).

Contour intervals are bracketed from 5 to 200 meters. Roads are shown for reference.

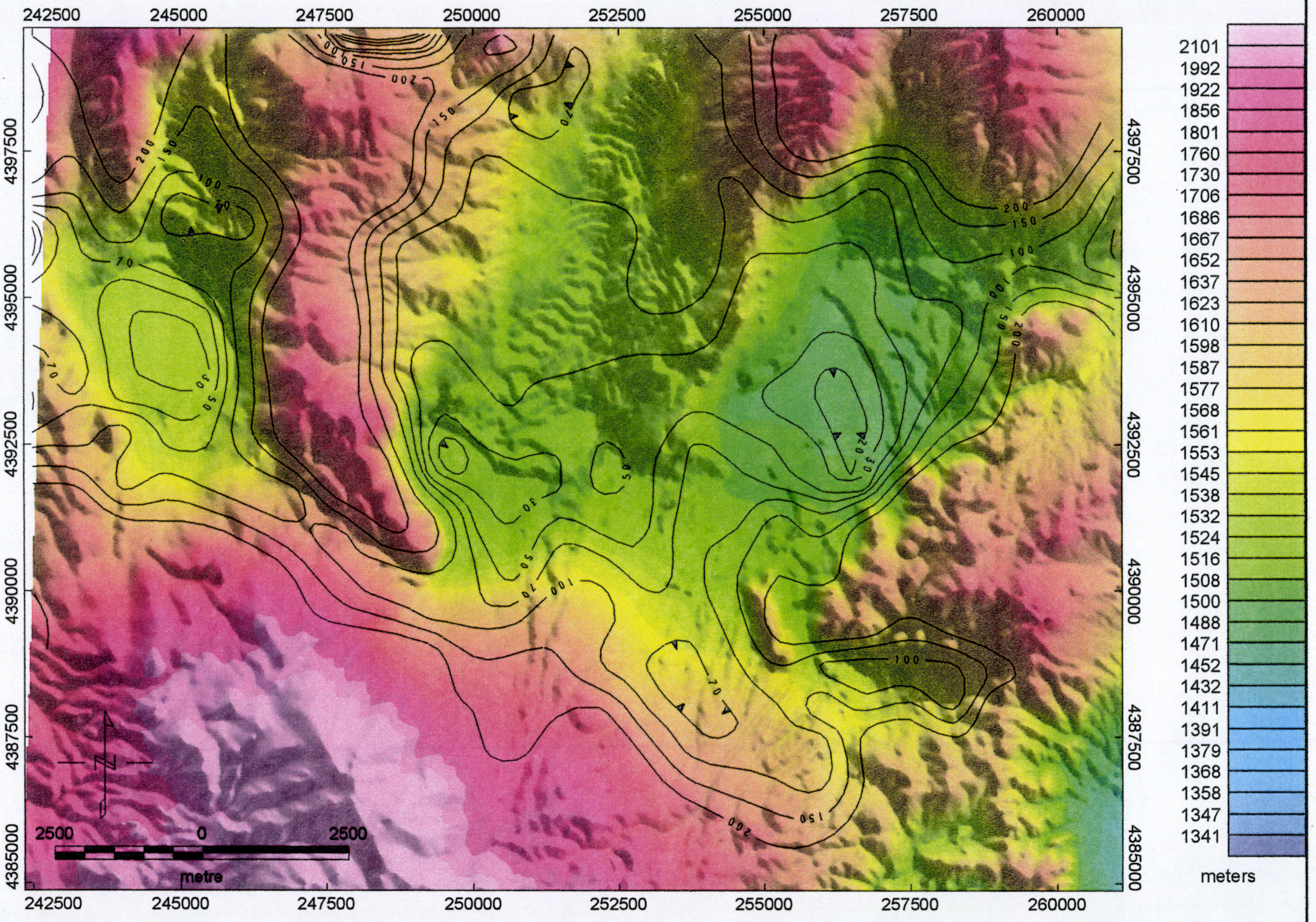


Figure 17c. Digital elevation map overlain with 900 Hz apparent resistivity.

Contour intervals are bracketed from 5 to 200 ohm.m.

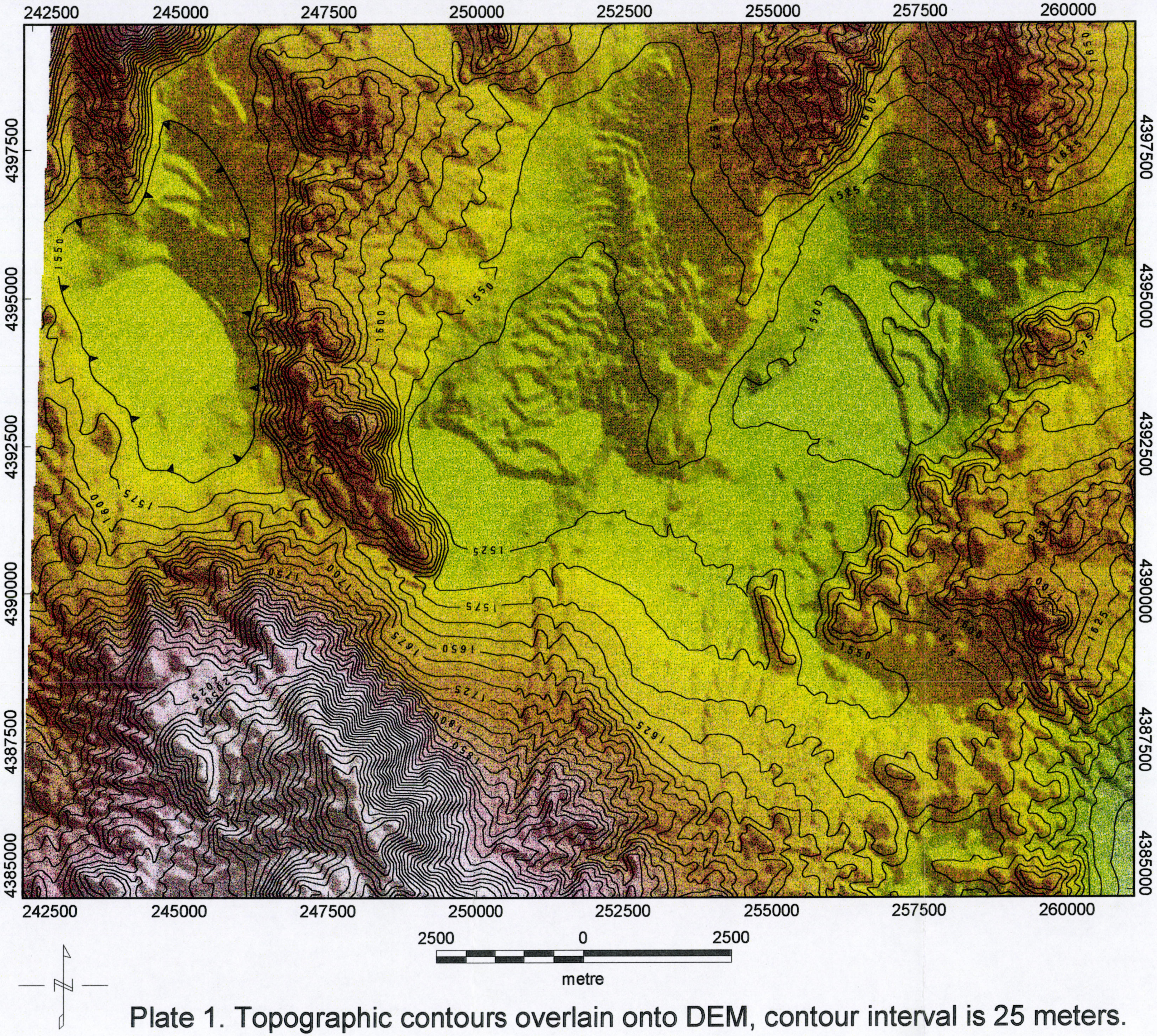

Plate 1. Topographic contours overlain onto DEM, contour interval is 25 meters.

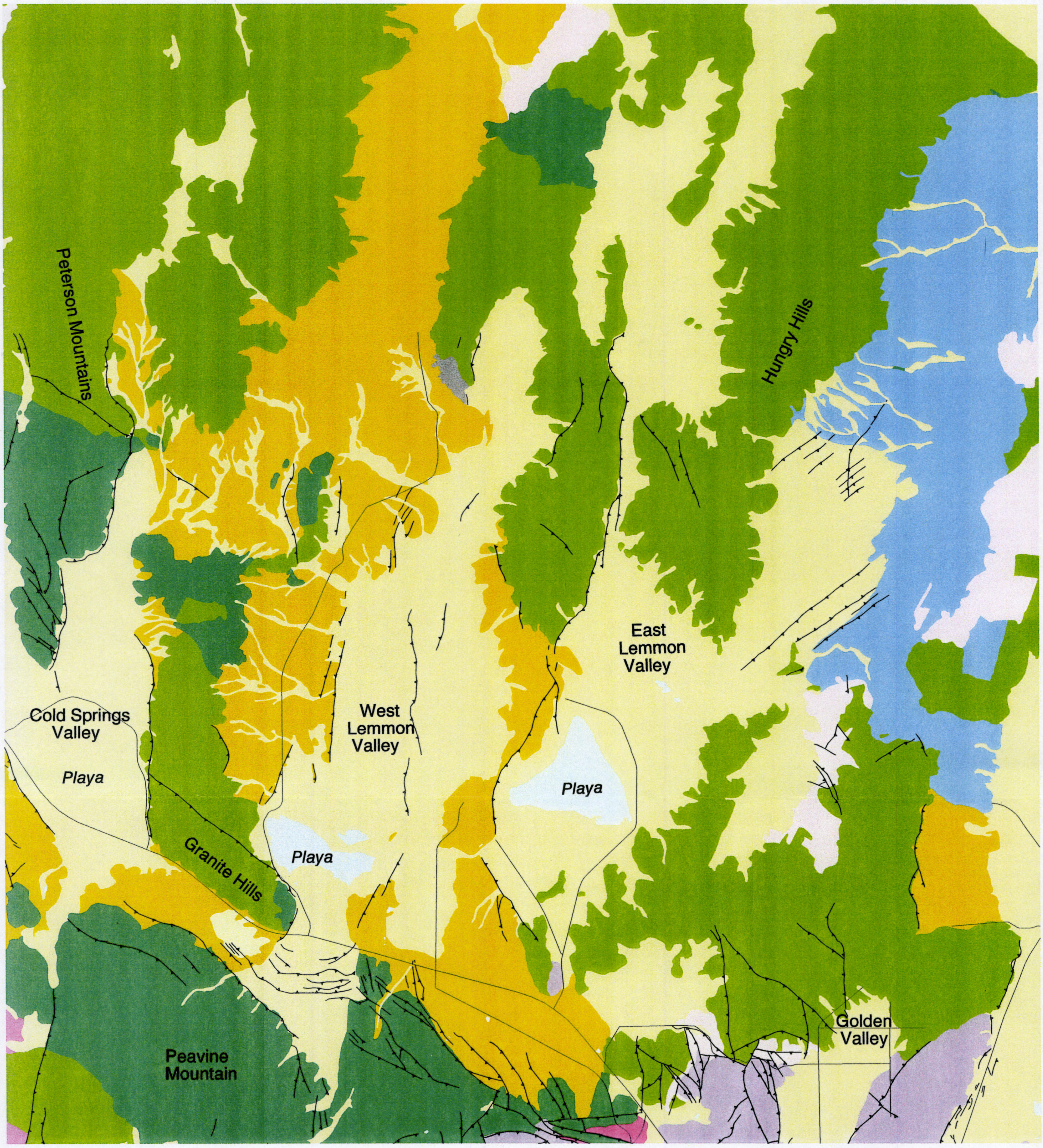


PLATE 2.

# Geologic Map

**QUATERNARY**

- UNDIFFERENTIATED QUATERNARY SEDIMENTS
- LANDSLIDE DEPOSITS
- ALLUVIAL FANS
- PLEISTOCENE BASALTS AND ANDESITES

**TERTIARY**

- PLIOCENE SEDIMENTARY ROCKS
- RHYOLITE PLUGS
- KATE PEAK FORMATION
- TERTIARY GRANITIC ROCKS
- ALTA FORMATION
- HARTFORD HILLS RHYOLITE

**MESOZOIC**

- CRETACEAOUS INTRUSIVE - GRANODIORITE
- PEAVINE SEQUENCE
- WATER BODIES
- Fault

SOURCE: WASHOE COUNTY DEPARTMENT OF WATER RESOURCES

DATE: JANUARY 2000



0 3500 7000

SCALE IN FEET

**Department of Water Resources**

**WASHOE COUNTY NEVADA**

Post Office Box 11130
Reno, Nevada 89520
(775) 954-4600

# APPENDIX

The appendix contains the potential fields modeling of twenty-one geologic cross sections of Lemmon and Cold Springs Valley oriented from west (left) to east (right). The first cross section is 20010 and is the most northern. The cross sections continue southward to 20210. See Figure 4 for the orientation of the cross sections.

Geologic Model of Line 20010 in Cold and Lemmon Valleys

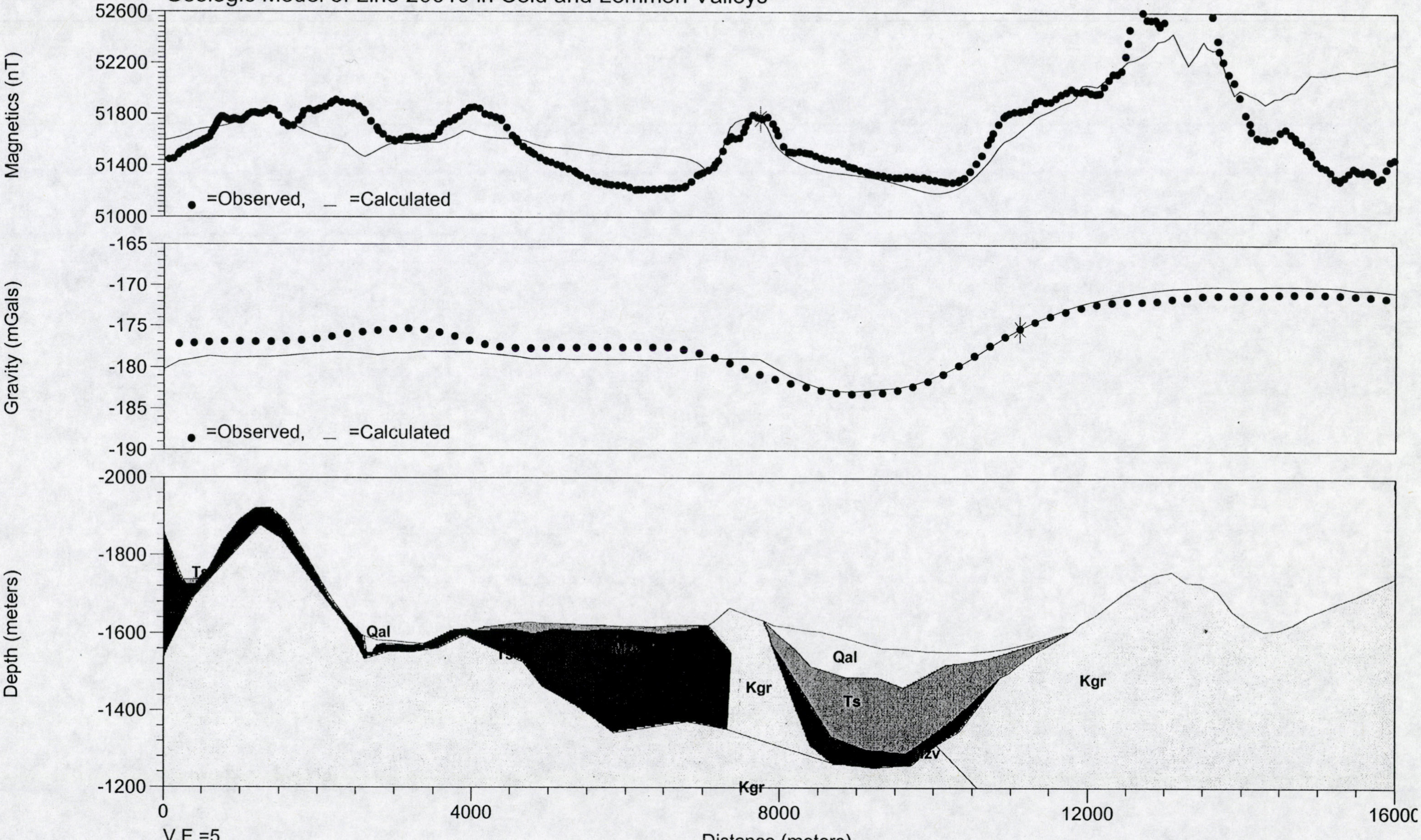


V.E.=5
Scale=69991

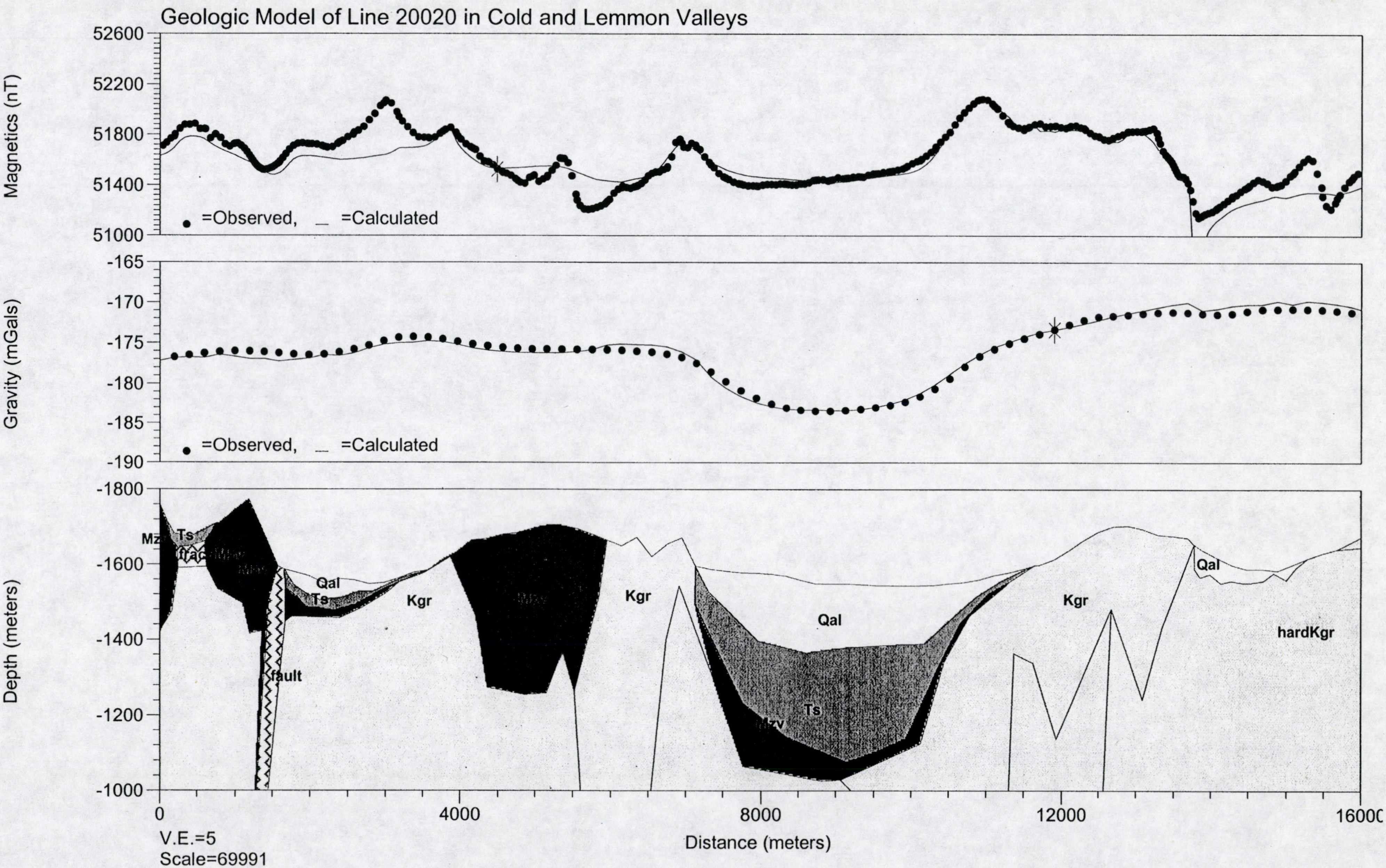

Geologic Model of Line 20020 in Cold and Lemmon Valleys
Magnetics (nT)
52600
52200
51800
51400
51000
● =Observed, _ =Calculated
Gravity (mGals)
-165
-170
-175
-180
-185
-190
● =Observed, _ =Calculated
Depth (meters)
-1800
-1600
-1400
-1200
-1000
Mzv
Ts
Qal
Ts
Kgr
fault
Kgr
Qal
Ts
Mzv
Kgr
Qal
hardKgr
0
4000
8000
12000
16000
V.E.=5
Scale=69991
Distance (meters)

Geologic Model of Line 20030 in Cold and Lemmon Valleys

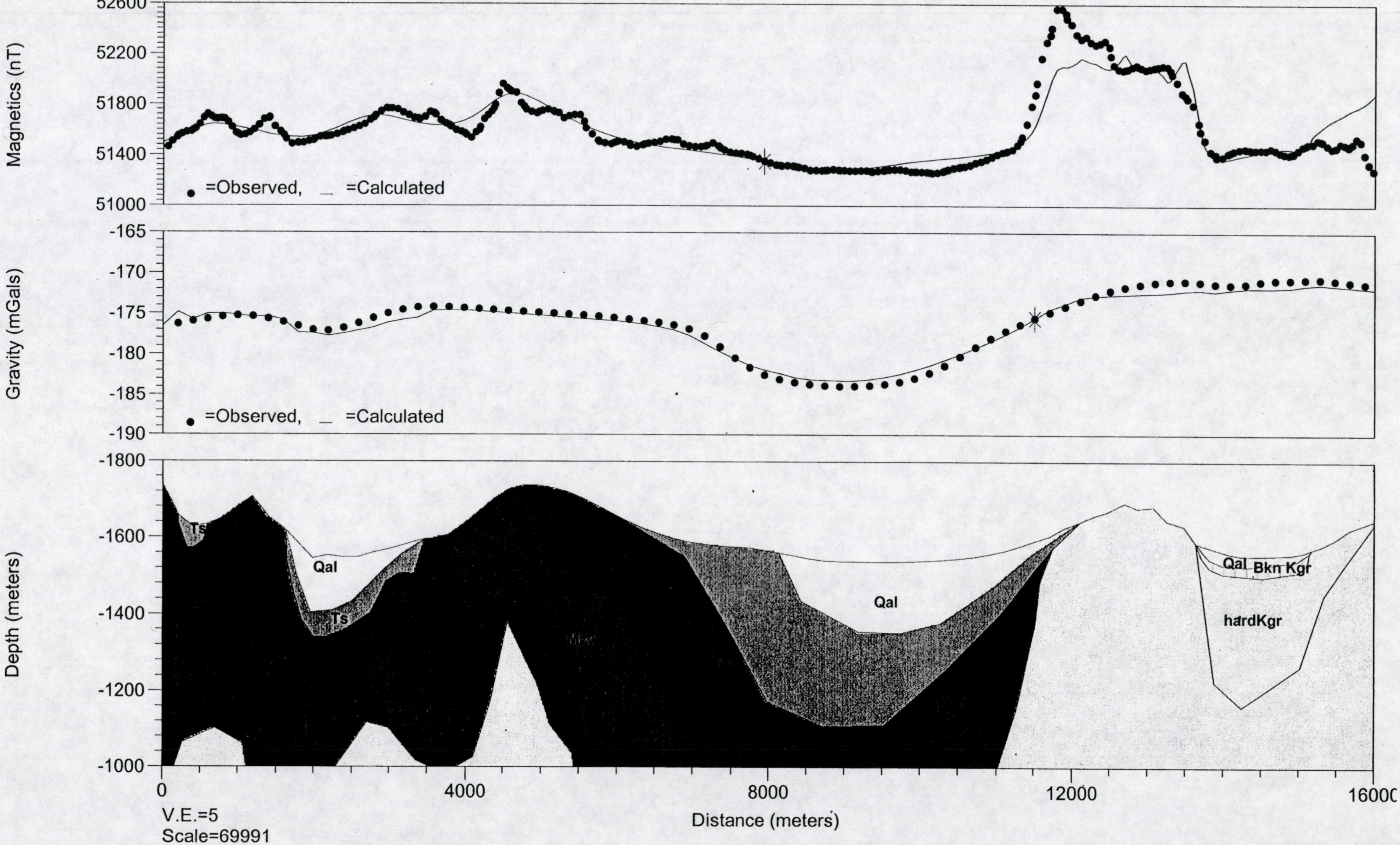

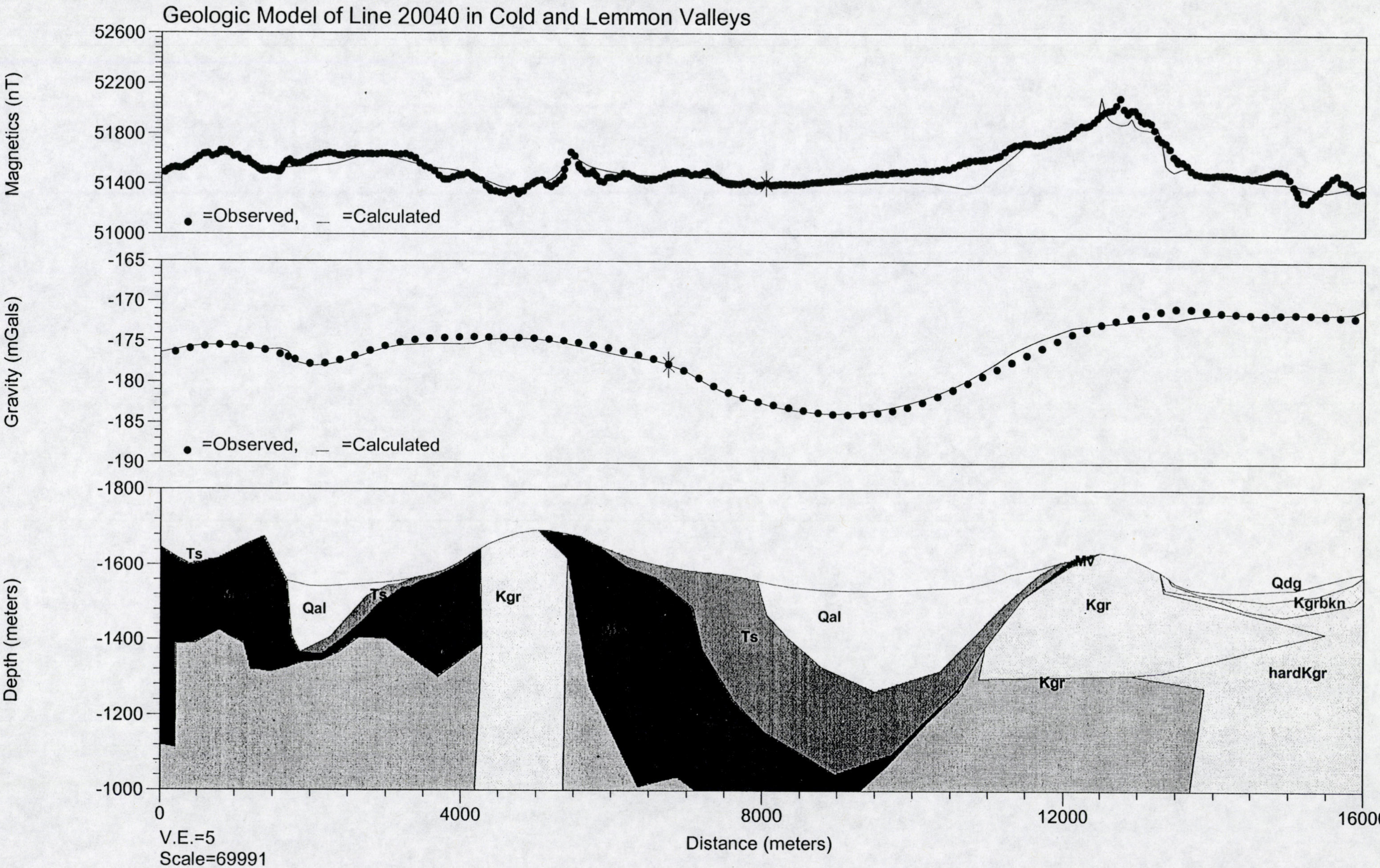
Geologic Model of Line 20040 in Cold and Lemmon Valleys
Magnetics (nT)
52600
52200
51800
51400
51000
=Observed, _ =Calculated
Gravity (mGals)
-165
-170
-175
-180
-185
-190
=Observed, _ =Calculated
Depth (meters)
-1800
-1600
-1400
-1200
-1000
Ts
Qal
Ts
Kgr
Ts
Qal
MV
Kgr
Kgr
Qdg
Kgrbkn
hardKgr
0
4000
8000
12000
V.E.=5
Scale=69991
Distance (meters)

Geologic Model of Line 20050 in Cold and Lemmon Valleys

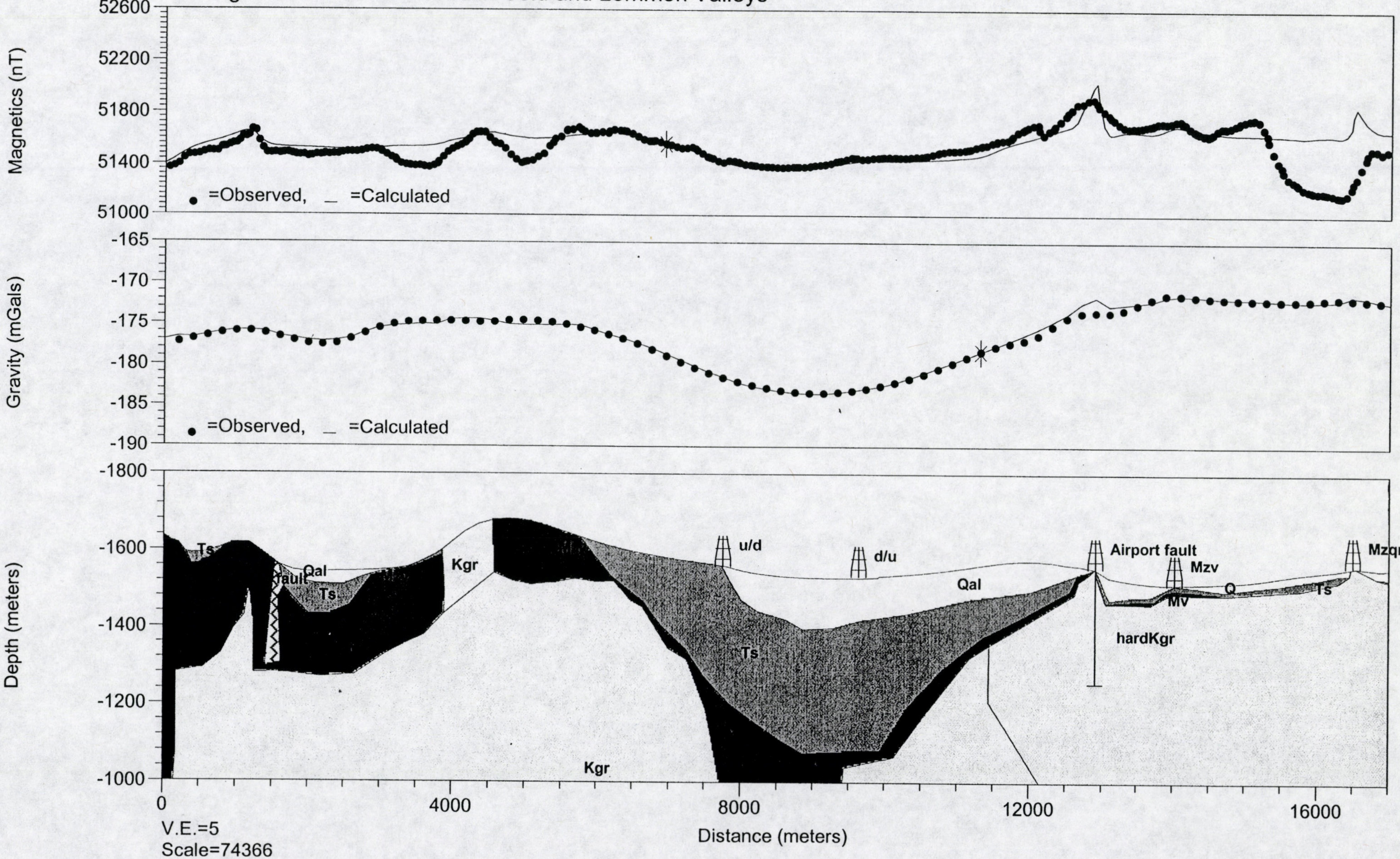

Geologic Model of Line 20060 in Cold and Lemmon Valleys

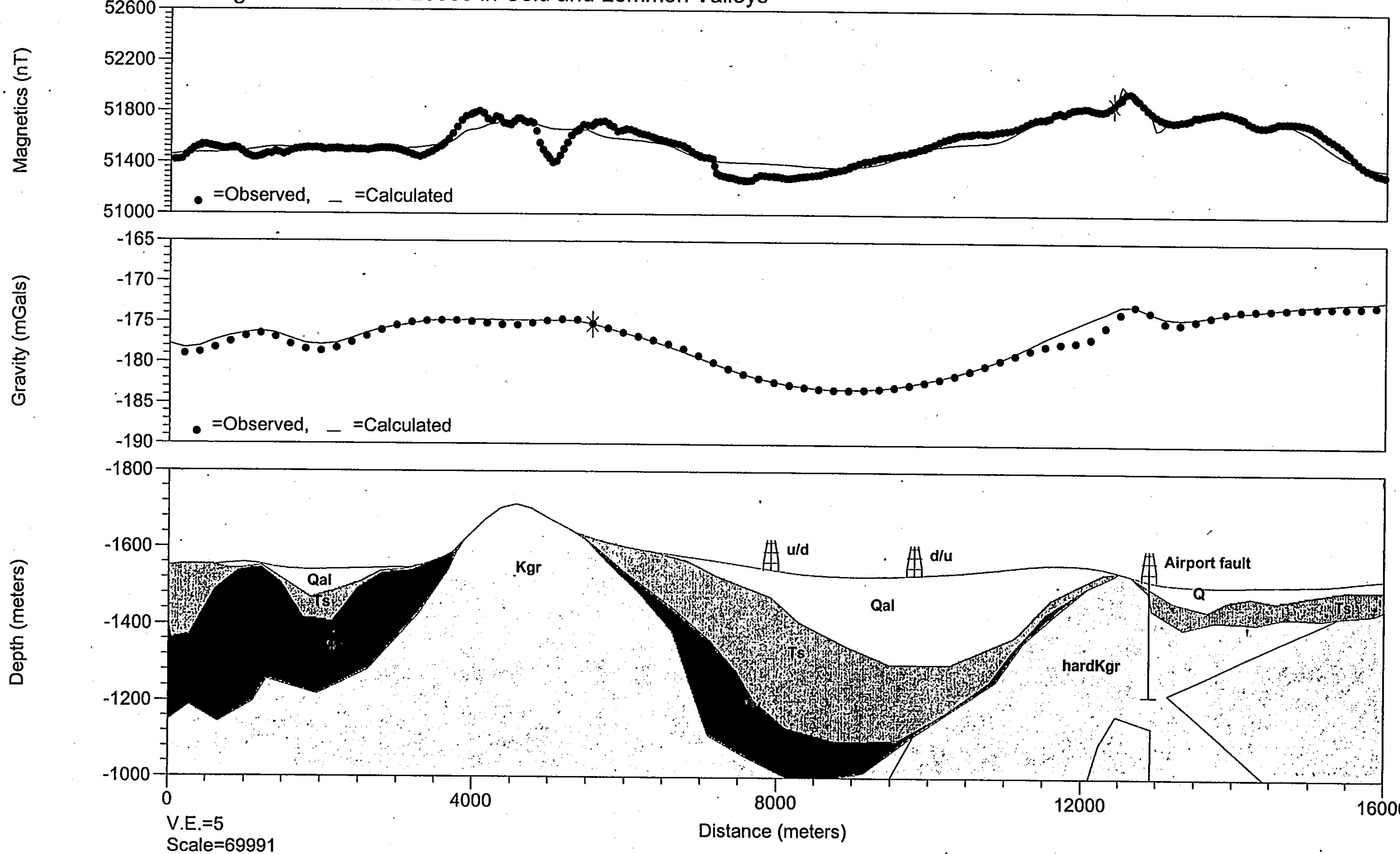

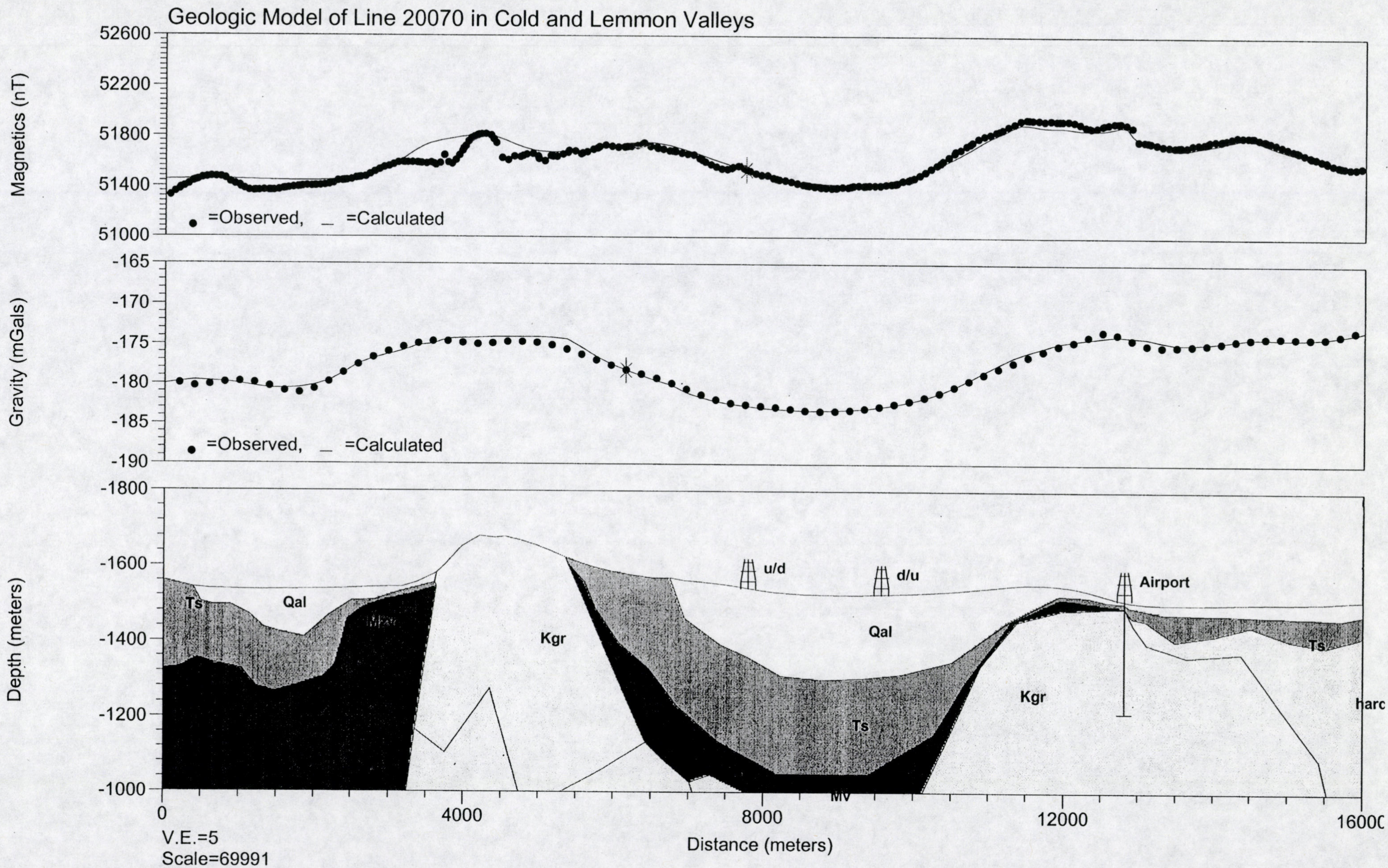
Geologic Model of Line 20070 in Cold and Lemmon Valleys
Magnetics (nT)
52600
52200
51800
51400
51000
=Observed, _ =Calculated
Gravity (mGals)
-165
-170
-175
-180
-185
-190
=Observed, _ =Calculated
Depth (meters)
-1800
-1600
-1400
-1200
-1000
Ts
Qal
Kgr
u/d
d/u
Qal
Ts
Mv
Airport
Kgr
Ts
harc
0
4000
8000
12000
16000
V.E.=5
Scale=69991
Distance (meters)

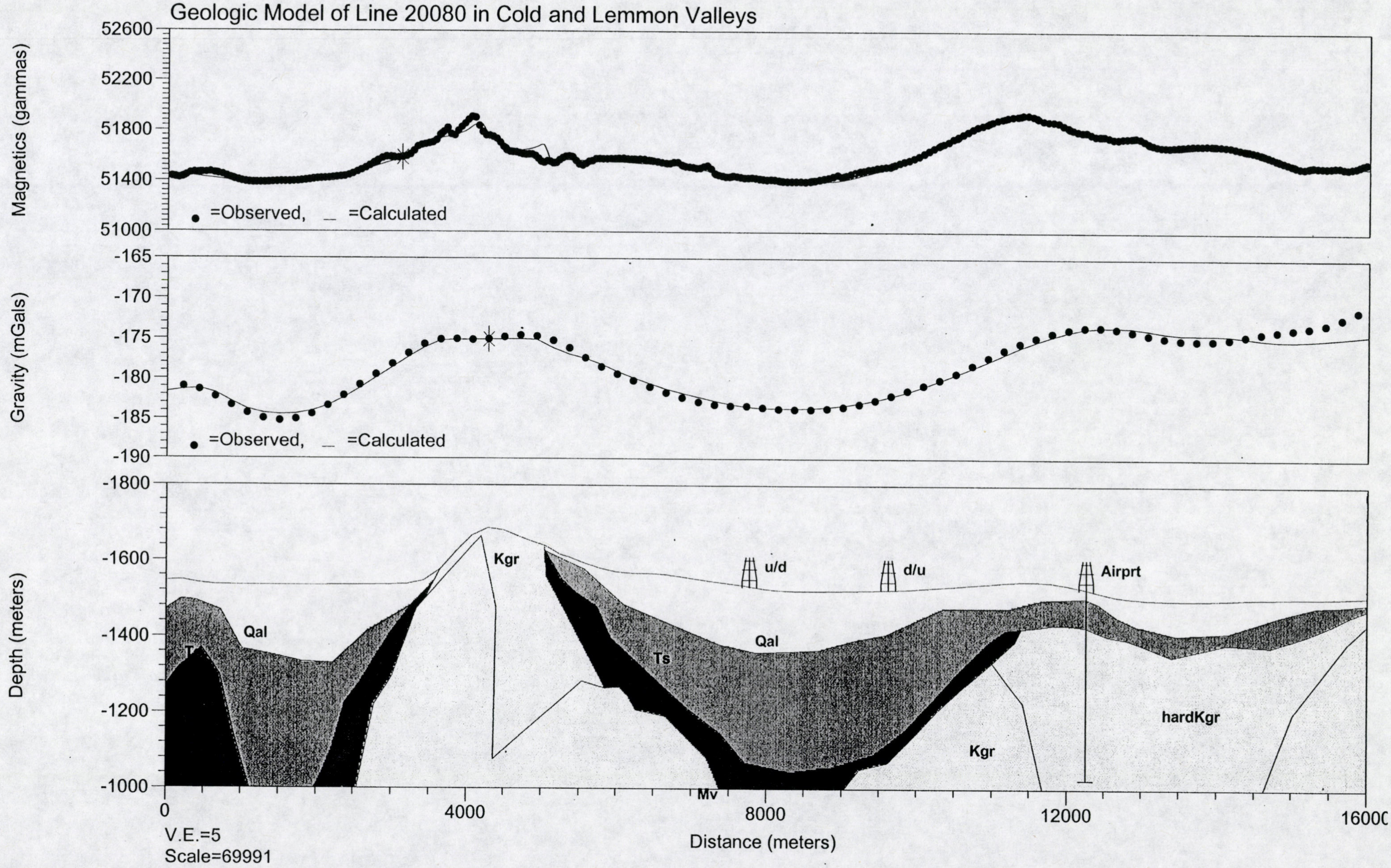
Geologic Model of Line 20080 in Cold and Lemmon Valleys
Magnetics (gammas)
52600
52200
51800
51400
51000
=Observed, _ =Calculated
Gravity (mGals)
-165
-170
-175
-180
-185
-190
=Observed, _ =Calculated
Depth (meters)
-1800
-1600
-1400
-1200
-1000
Qal
Ts
Kgr
u/d
d/u
Airprt
Qal
Ts
Mv
Kgr
hardKgr
0
4000
8000
12000
16000
V.E.=5
Scale=69991
Distance (meters)

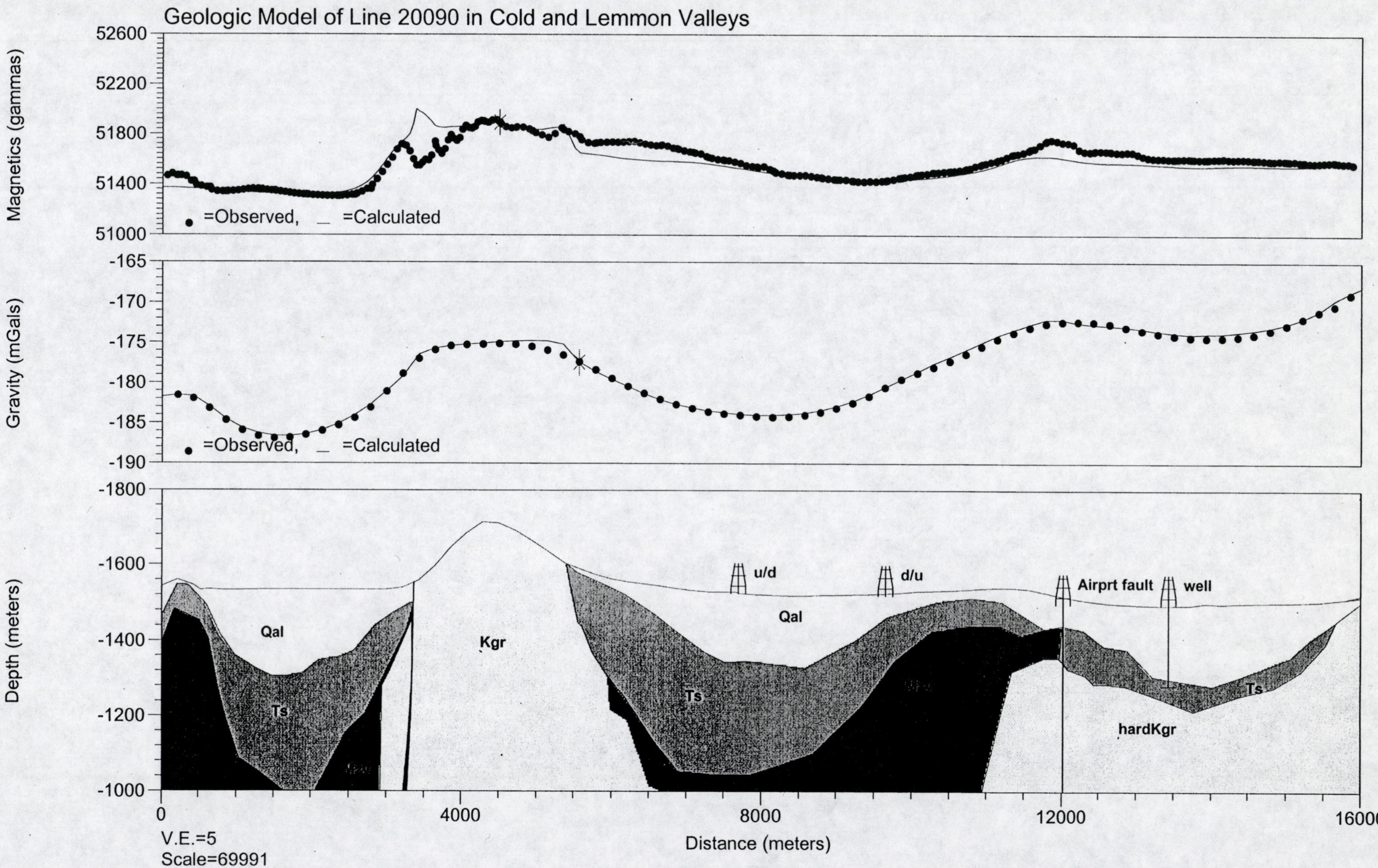
Geologic Model of Line 20090 in Cold and Lemmon Valleys
Magnetics (gammas)
52600
52200
51800
51400
51000
=Observed, _ =Calculated
Gravity (mGals)
-165
-170
-175
-180
-185
-190
=Observed, _ =Calculated
Depth (meters)
-1800
-1600
-1400
-1200
-1000
Qal
Ts
Kgr
u/d
d/u
Airprt fault
well
hardKgr
0
4000
8000
12000
1600C
V.E.=5
Scale=69991
Distance (meters)

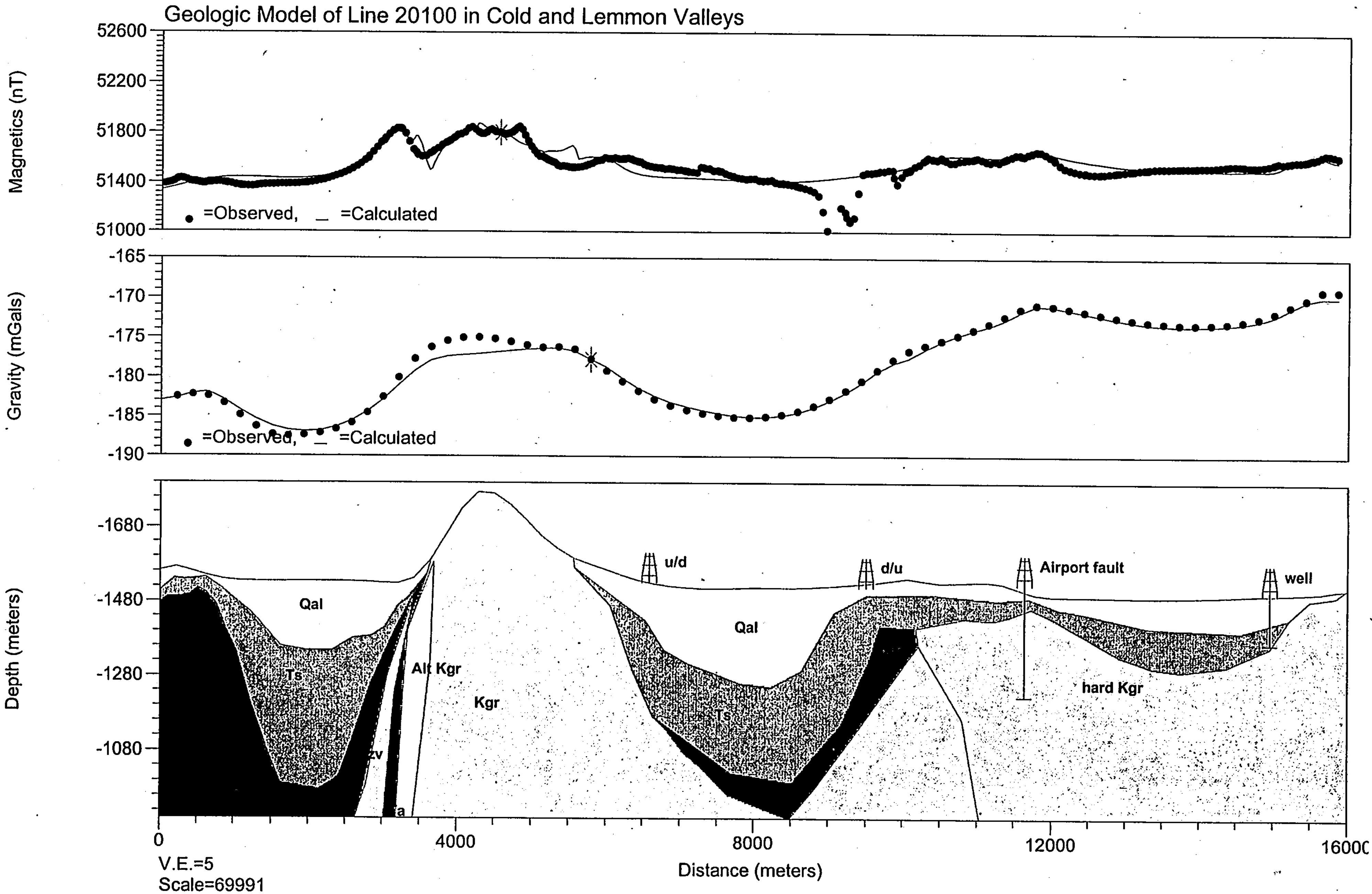
Geologic Model of Line 20100 in Cold and Lemmon Valleys
Magnetics (nT)
52600
52200
51800
51400
51000
● =Observed, _ =Calculated
Gravity (mGals)
-165
-170
-175
-180
-185
-190
● =Observed, _ =Calculated
Depth (meters)
-1680
-1480
-1280
-1080
Qal
Ts
zv
a
Alt Kgr
Kgr
u/d
d/u
Airport fault
well
hard Kgr
0
4000
8000
12000
16000
Distance (meters)
V.E.=5
Scale=69991

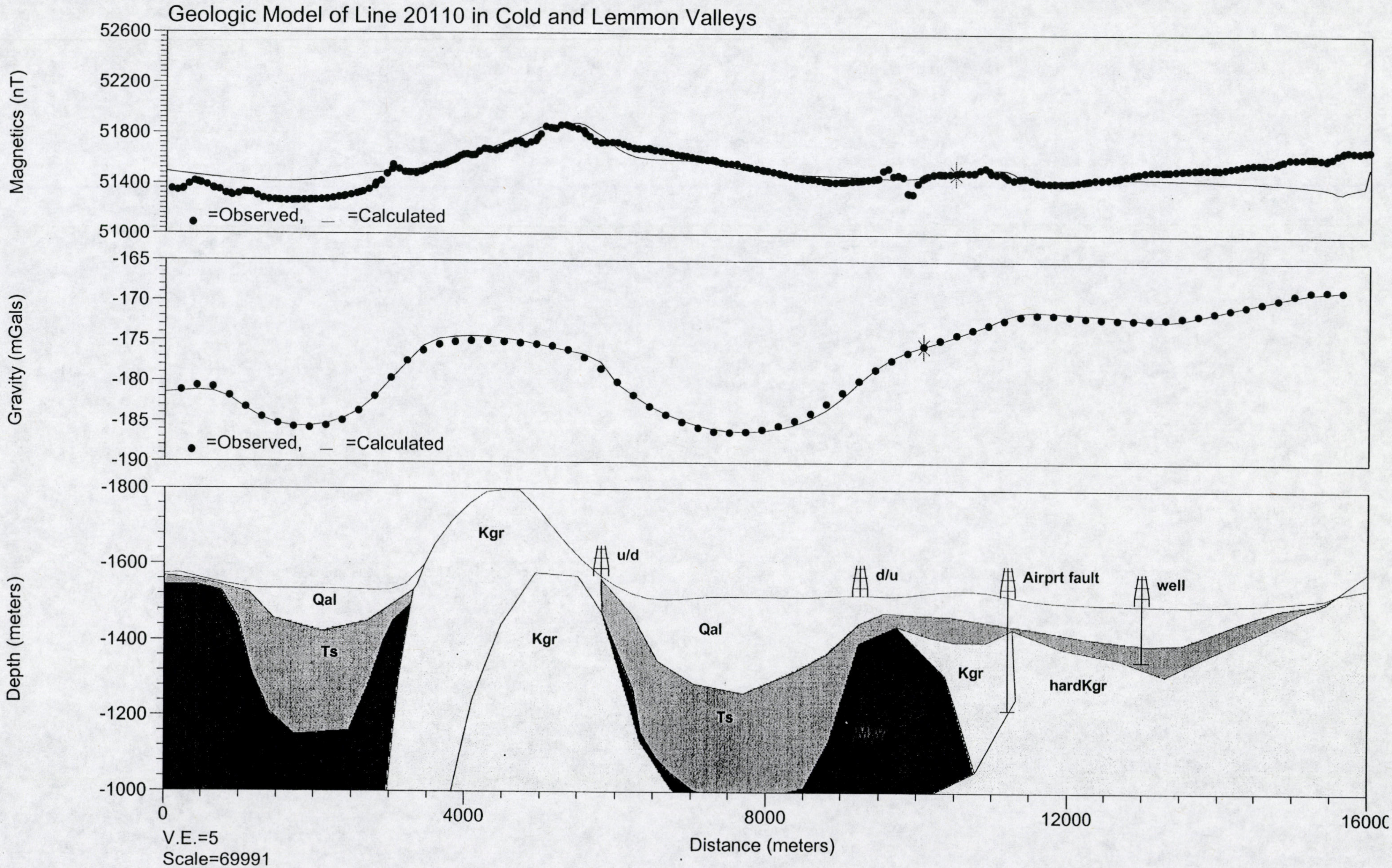
Geologic Model of Line 20110 in Cold and Lemmon Valleys
Magnetics (nT)
52600
52200
51800
51400
51000
=Observed, _ =Calculated
Gravity (mGals)
-165
-170
-175
-180
-185
-190
=Observed, _ =Calculated
Depth (meters)
-1800
-1600
-1400
-1200
-1000
Kgr
u/d
d/u
Airprt fault
well
Qal
Ts
Kgr
Qal
Ts
Kgr
hardKgr
0
4000
8000
12000
1600C
Distance (meters)
V.E.=5
Scale=69991

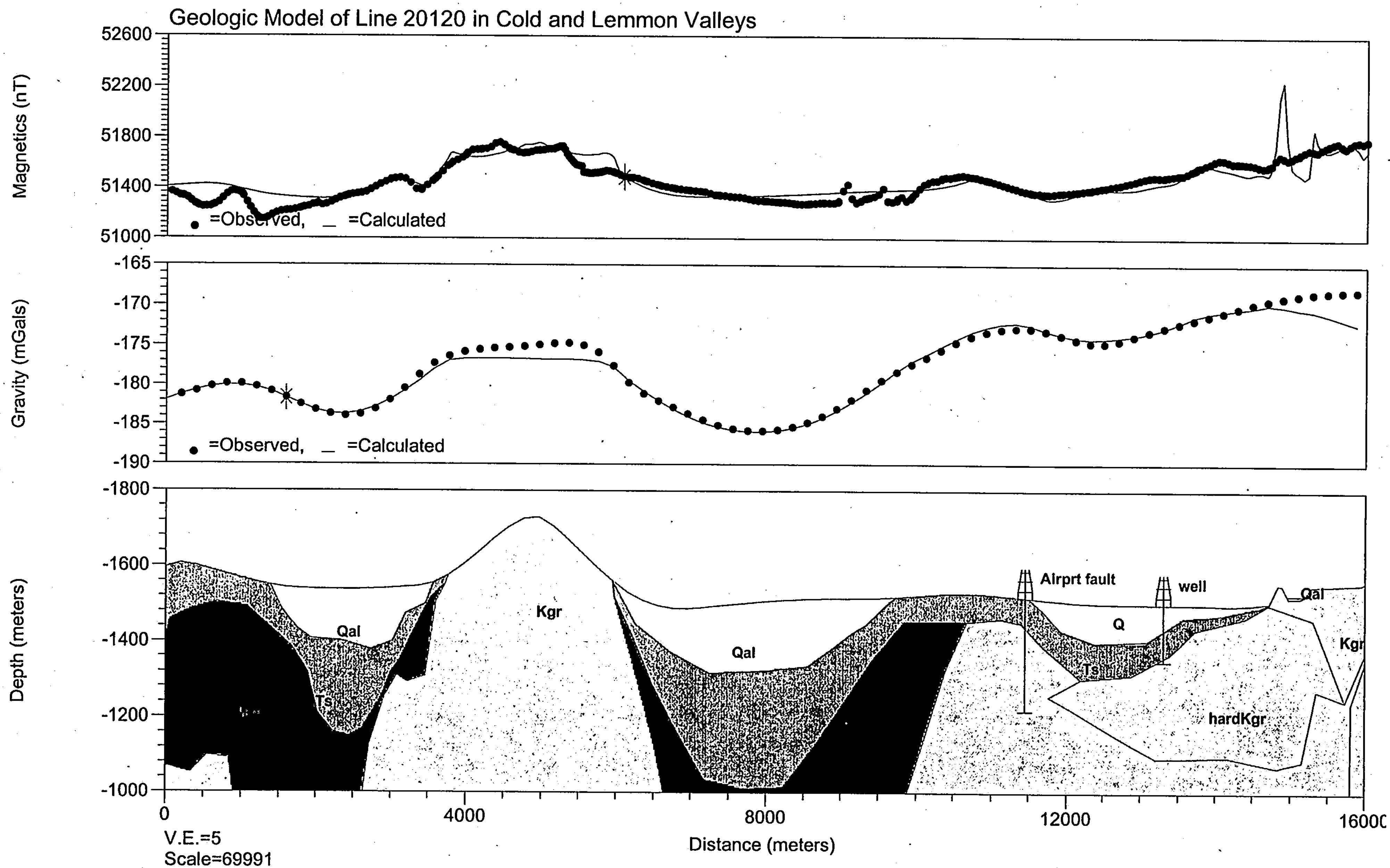

Geologic Model of Line 20120 in Cold and Lemmon Valleys
Magnetics (nT)
52600
52200
51800
51400
51000
● =Observed, _ =Calculated
Gravity (mGals)
-165
-170
-175
-180
-185
-190
● =Observed, _ =Calculated
Depth (meters)
-1800
-1600
-1400
-1200
-1000
Qal
Ts
Kgr
Qal
Airprt fault
well
Q
Ts
Qal
Kgr
hardKgr
0
4000
8000
12000
1600C
V.E.=5
Scale=69991
Distance (meters)

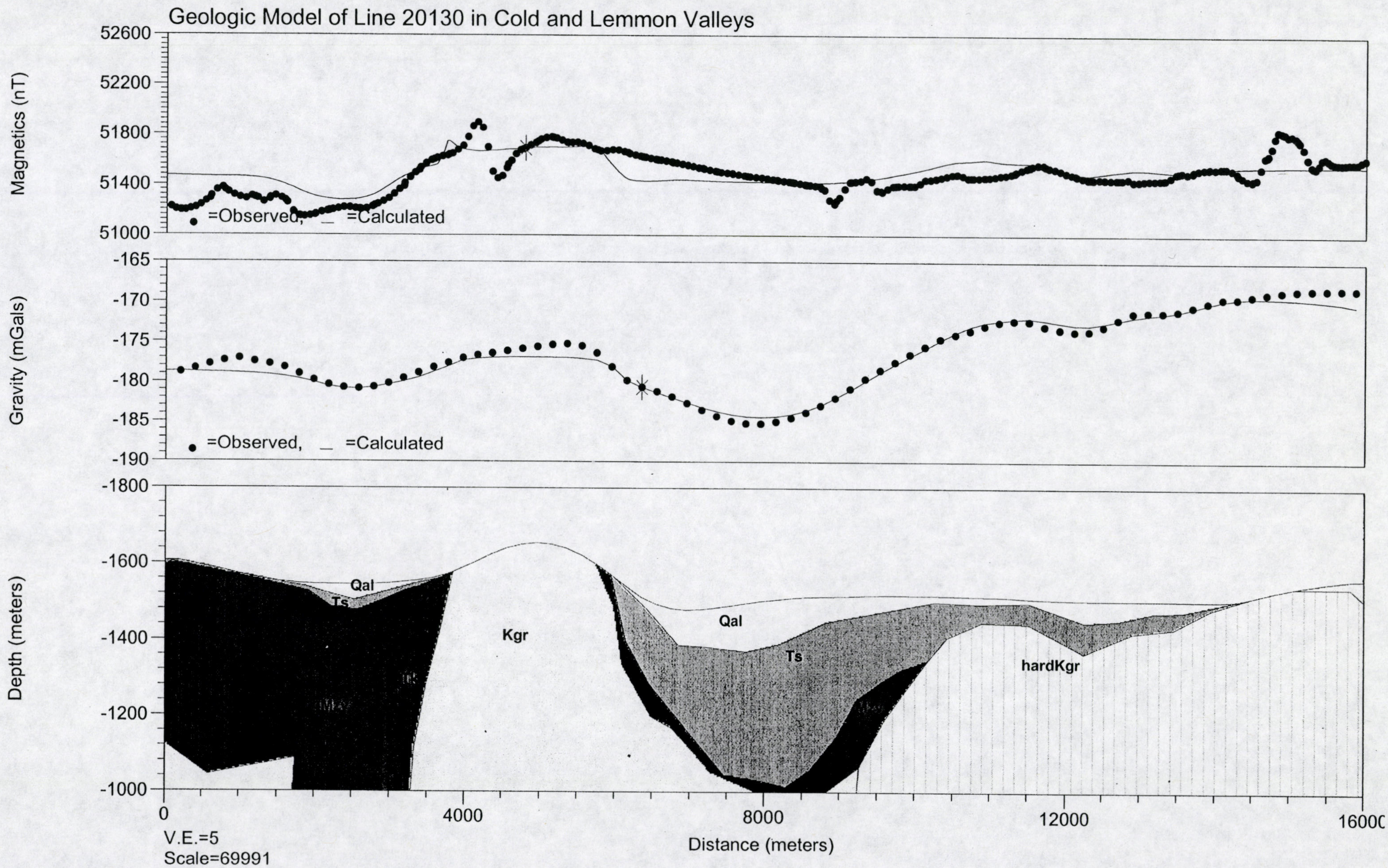
Geologic Model of Line 20130 in Cold and Lemmon Valleys
Magnetics (nT)
52600
52200
51800
51400
51000
=Observed, _ =Calculated
Gravity (mGals)
-165
-170
-175
-180
-185
-190
=Observed, _ =Calculated
Depth (meters)
-1800
-1600
-1400
-1200
-1000
Qal
Ts
Kgr
Qal
Ts
hardKgr
0
4000
8000
12000
16000
Distance (meters)
V.E.=5
Scale=69991

Geologic Model of Line 20140 in Cold and Lemmon Valleys

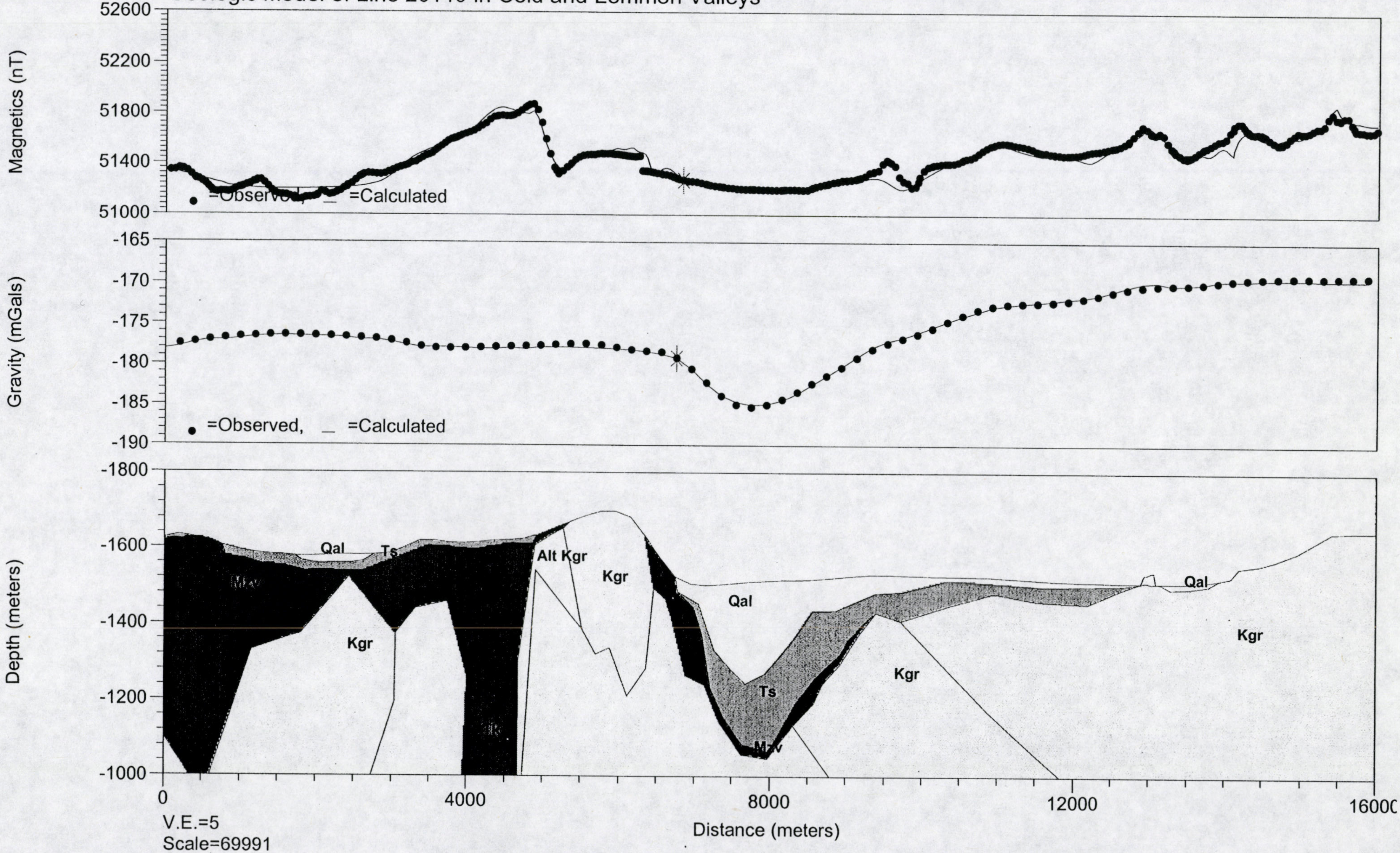

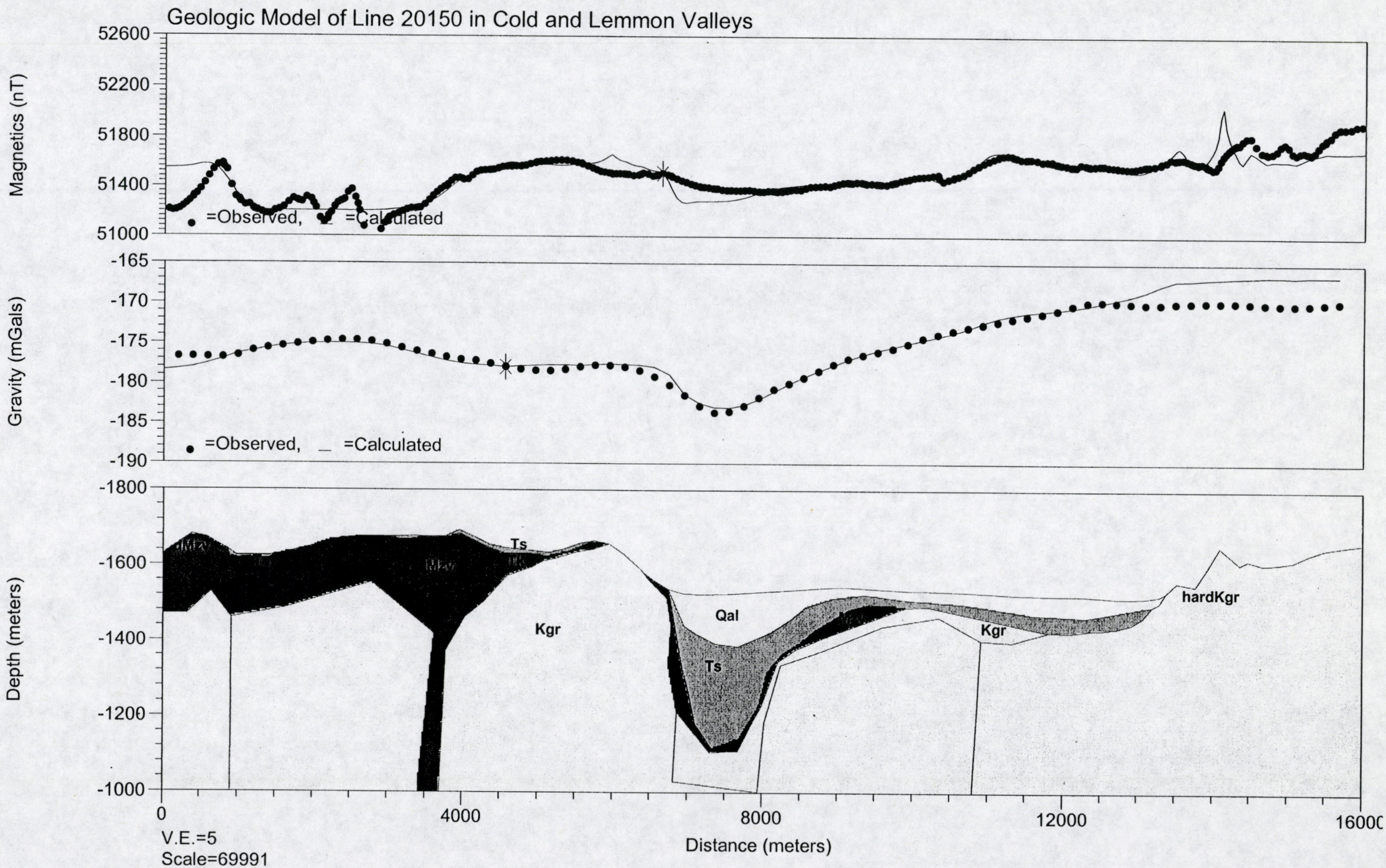
Geologic Model of Line 20150 in Cold and Lemmon Valleys
Magnetics (nT)
52600
52200
51800
51400
51000
● =Observed, _ =Calculated
Gravity (mGals)
-165
-170
-175
-180
-185
-190
● =Observed, _ =Calculated
Depth (meters)
-1800
-1600
-1400
-1200
-1000
Ts
Kgr
Qal
Ts
Kgr
hardKgr
0
4000
8000
12000
1600(
V.E.=5
Scale=69991
Distance (meters)

## Geologic Model of Line 20160 in Cold and Lemmon Valleys

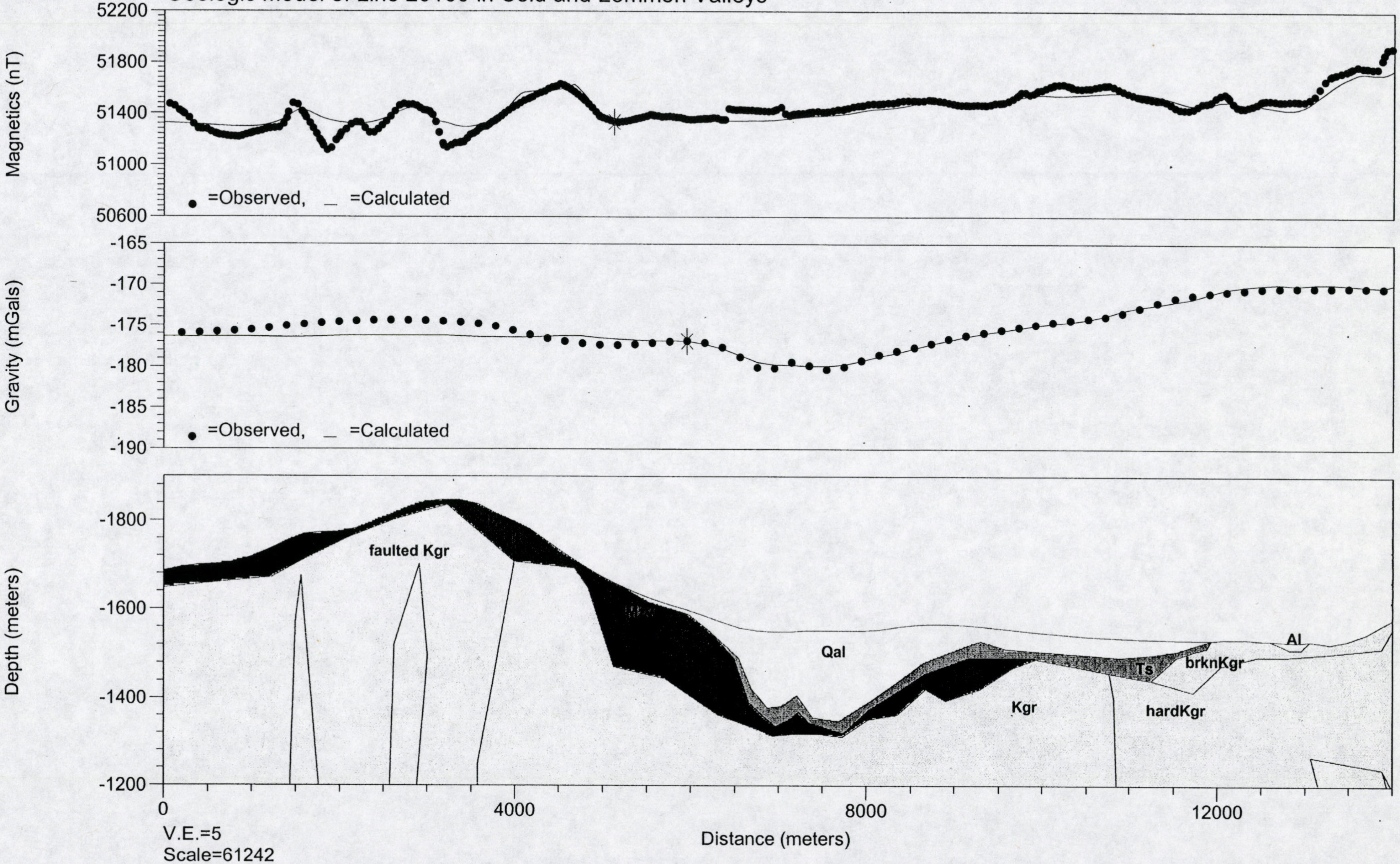

Geologic Model of Line 20170 in Cold and Lemmon Valleys

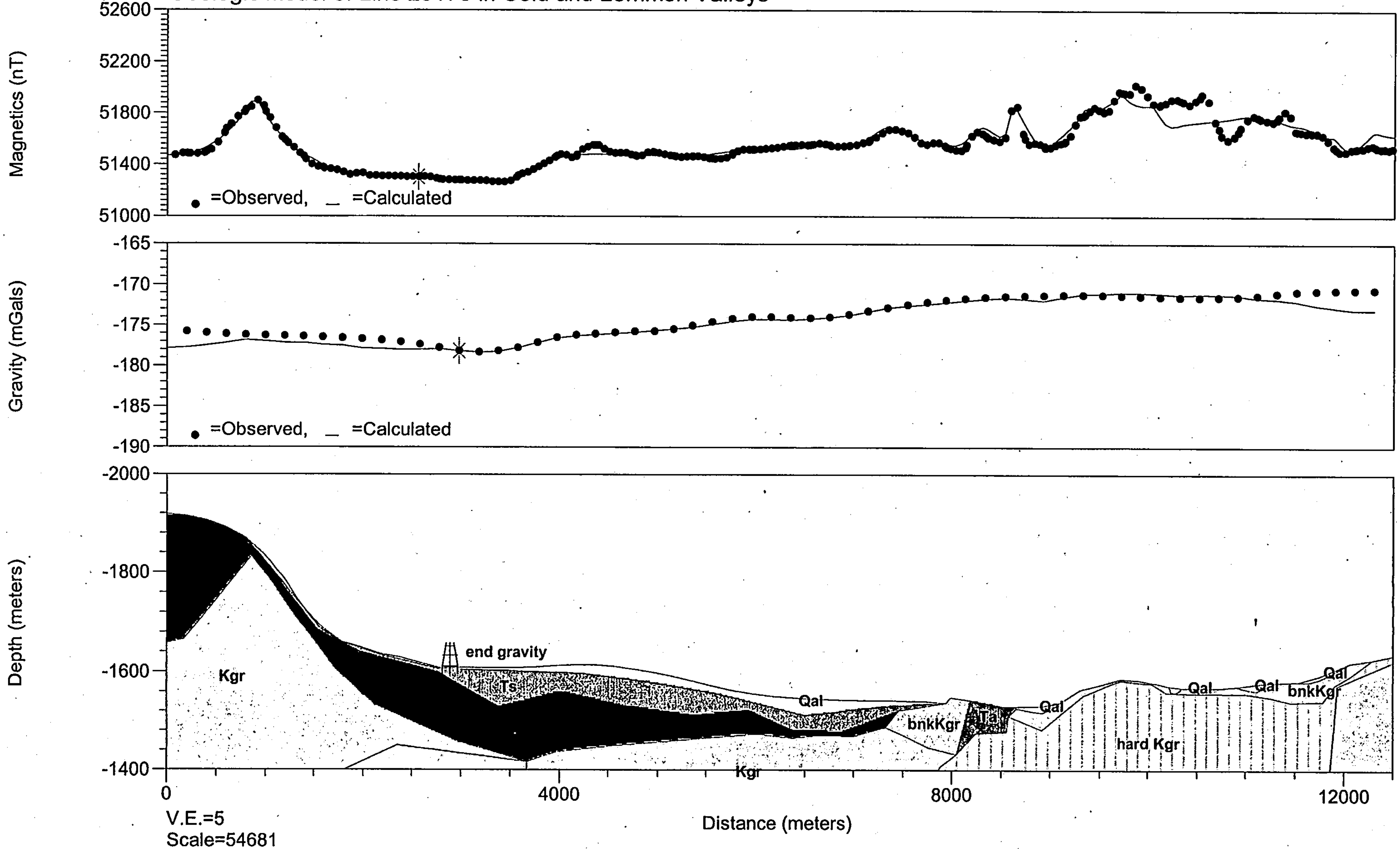

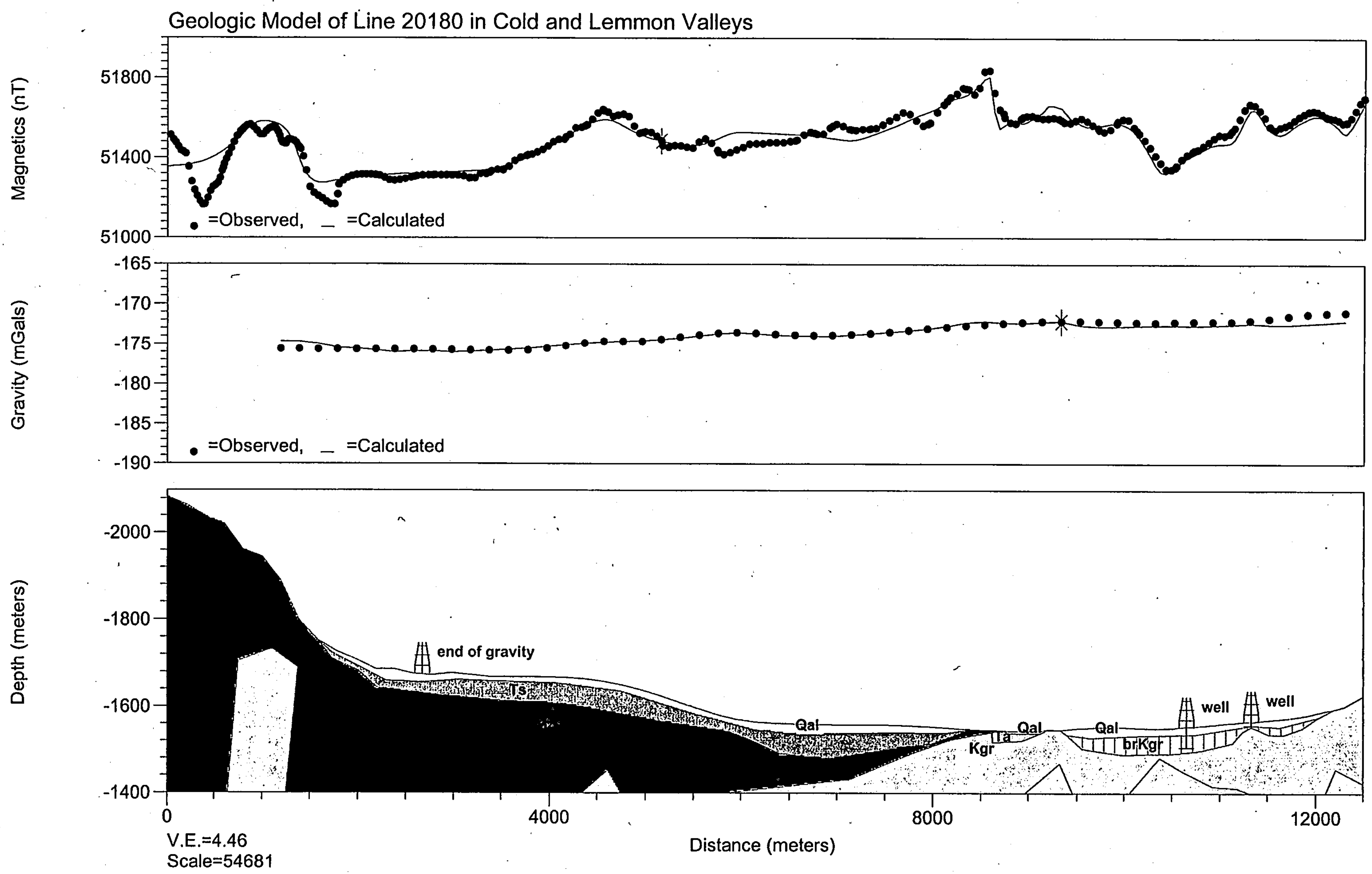
Geologic Model of Line 20180 in Cold and Lemmon Valleys
Magnetics (nT)
51800
51400
51000
=Observed, _ =Calculated
Gravity (mGals)
-165
-170
-175
-180
-185
-190
=Observed, _ =Calculated
Depth (meters)
-2000
-1800
-1600
-1400
end of gravity
Ts
Qal
Ta
Kgr
brKgr
well
well
0
4000
8000
12000
V.E.=4.46
Scale=54681
Distance (meters)

Geologic Model of Line 20190 in Cold and Lemmon Valleys

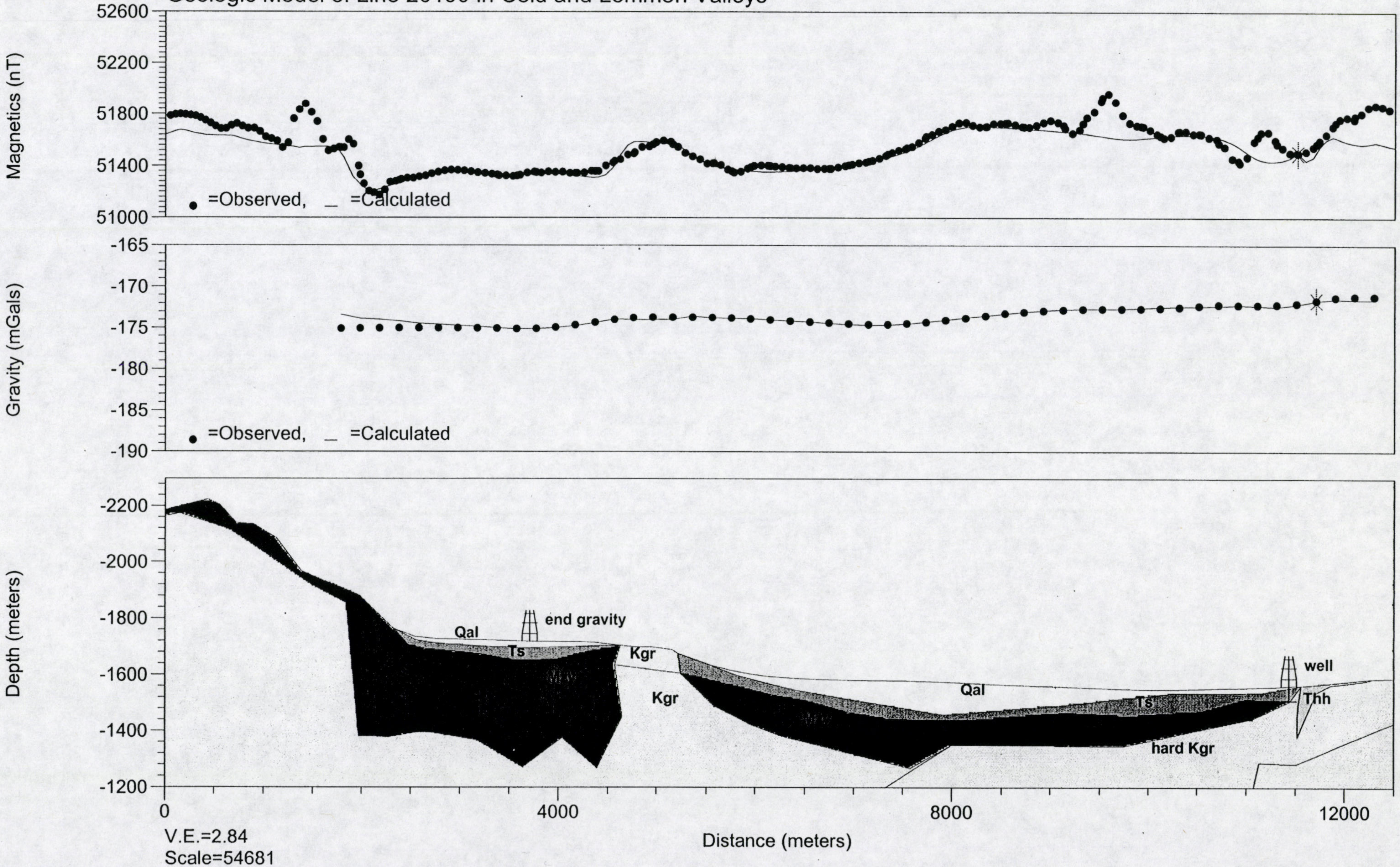

## Geologic Model of Line 20200 in Cold and Lemmon Valleys

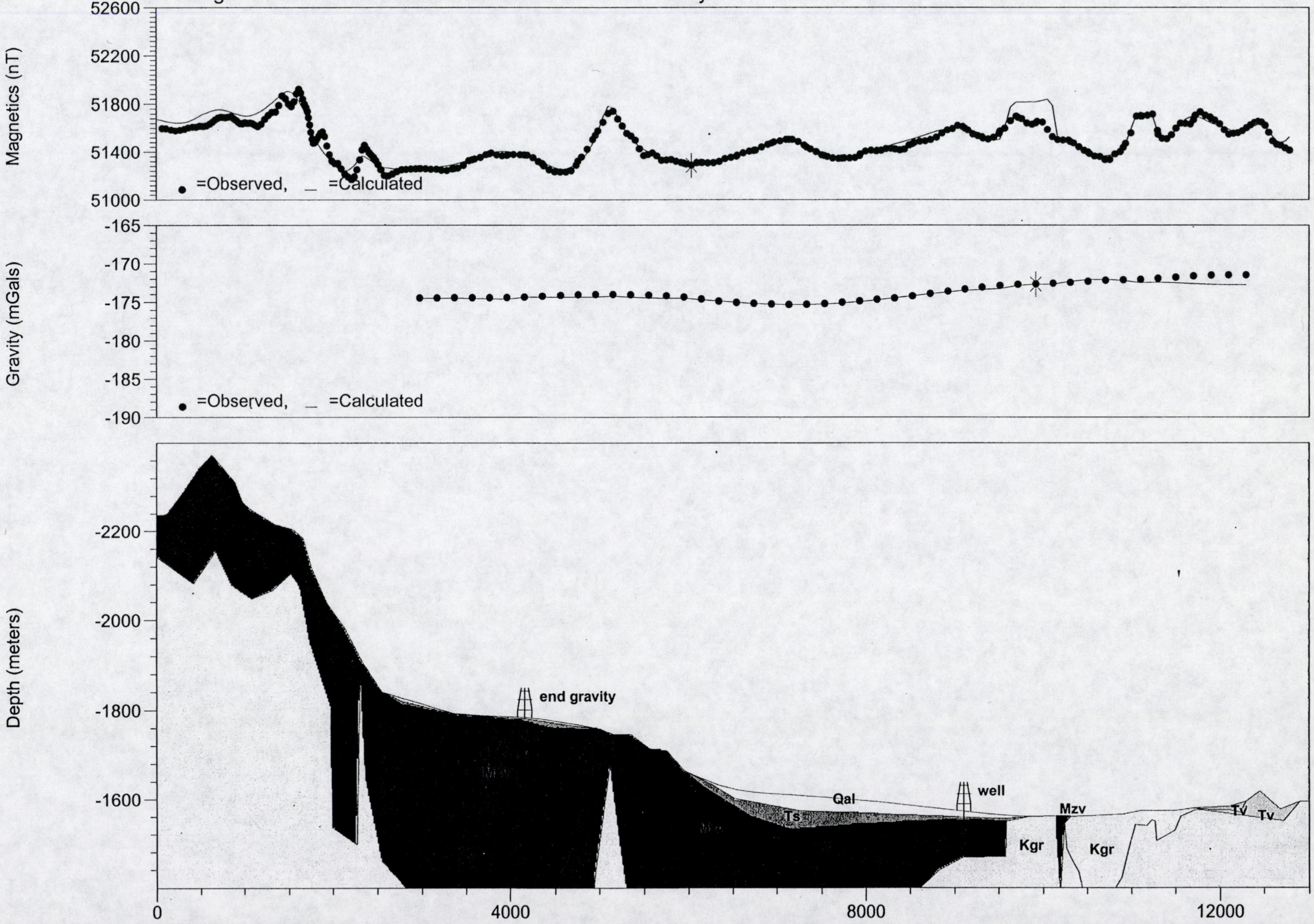

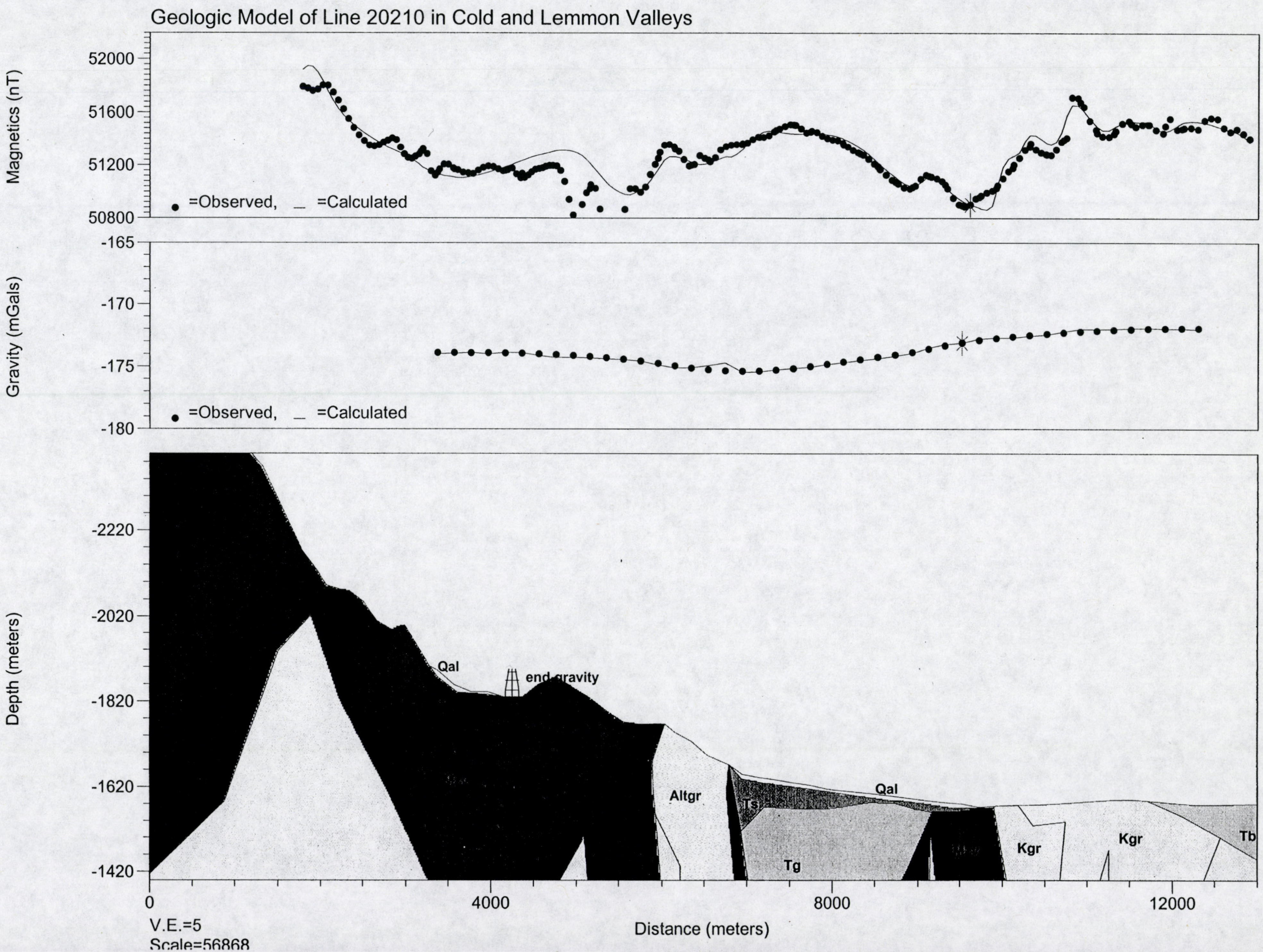

Geologic Model of Line 20210 in Cold and Lemmon Valleys
Magnetics (nT)
52000
51600
51200
50800
=Observed, _ =Calculated
Gravity (mGals)
-165
-170
-175
-180
=Observed, _ =Calculated
Depth (meters)
-2220
-2020
-1820
-1620
-1420
Qal
end gravity
Altgr
Ts
Qal
Tg
Kgr
Kgr
Tb
0
4000
8000
12000
V.E.=5
Scale=56868
Distance (meters)